University College of Southeast Norway
Faculty of Technology
Master's Thesis
Process, Energy and Environmental Technology
Spring 2016

Sanjay Shah

Methane from Syngas by Anaerobic Digestion.

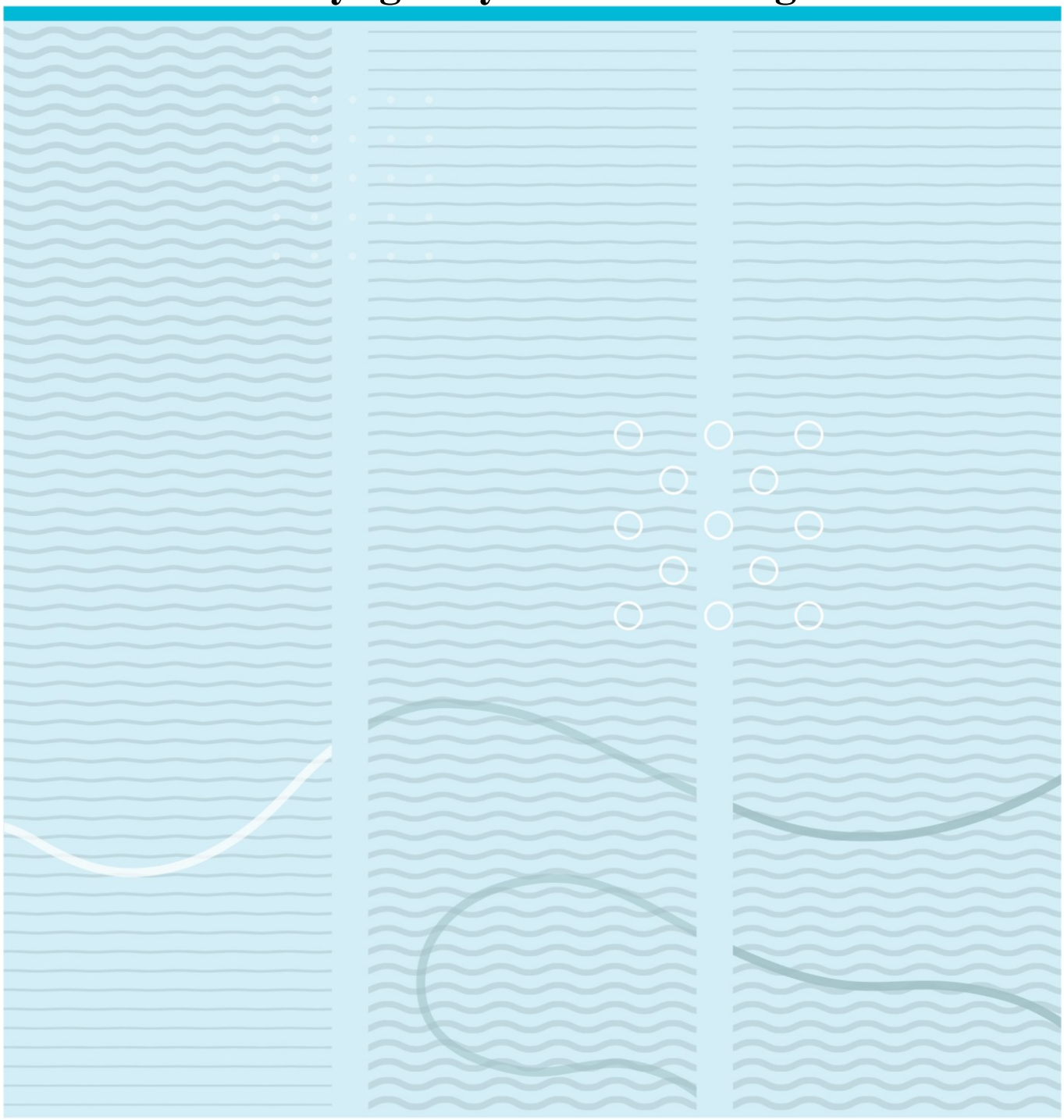

University College of Southeast Norway
Faculty of Technology
Department of Process, Energy and Environmental Technology

http://www.usn.no

Summary

University College of Southeast Norway

MASTER'S THESIS, COURSE CODE FMH606

Student: Sanjay Shah

Thesis Title: Methane from Syngas by Anaerobic Digestion.

Signature: . . . . . .

Number of pages: < 91 >

Keywords: Anaerobic Digestion, ADM1, Syngas degradation, CH_4 production

Supervisor:	Wenche Bergland	Sign. . .
2nd supervisor:	Rune Bakke	Sign. . . . .
3rd supervisor:	Britt Moldestad	Sign.: . . . . .
Censor:	Wolfram Franke	Sign.: . . . . .
External partner:	No	Sign.: . . . . .

Availability: <Open>

Archive approval (supervisor signature)**:** Sign.: . . . . . **Date :** . . .

Abstract:

Anaerobic digestion is a prominent green technology used for methane production from organic waste. Previous studies have shown that CH_4 in AD can be increased by adding inorganic electron donors such as H_2 and CO. These can be for example; produced as syngas from wood. If so, AD could be a method to convert the syngas into methane. The principal of this thesis work is to implement syngas into AD.

In this thesis, the principles were investigated by experimental work and modelling. The experiment did not give any useful result, but relevant experimental data was found in the literature.

Modelling involves implementing syngas degradation pathways into the ADM1 model. Simulation is carried out by choosing an experimental sludge treatment study by Batchstone[2], a published pilot scale case with experimental data where model parameters were used as the best case. The case was further modified by a diffusive link in AQUASIM software. Three different compositions; the first one is pure hydrogen, and two other compositions of syngas are 86% H_2, 7% CO and 7% CO_2, and 44.4 % H_2, 33.3 % CO and 22.2 % CO_2 respectively were used for simulation.

The CH_4 production rate can be increased up to 40% by adding H_2 and the threshold limit i.e. $\frac{Load\ of\ H_2}{Load\ of\ Feed}$ ratio is 0.35(kgCOD hydrogen.day-1 / (kgCOD feed.day-1) where the threshold corresponds to pH going above 8.5. The maximum CH_4 content in the produced biogas is around 94%. The addition of H2-rich syngas (composition of 86% H_2, 7% CO and 7% CO_2) shows more favorable condition than pure H_2. $\frac{Load\ of\ H_2}{Load\ of\ Feed}$ ratio is around 0.89 and CH_4 production rate can be increased up to 60%. The CH_4 content with H_2-rich syngas is around 81%. The third composition of syngas (44.4 % H_2, 33.3 % CO and 22.2 % CO_2) produce more biogas but CH_4 content obtained from simulation results is only around 49%.

Contents

Preface

This thesis concludes my Master of Science in Process Technology at the Faculty of Technology, University College of Southeast Norway (USN). The thesis was performed throughout my 4th semester, spring 2016, at the department of Process, Energy, and Environmental Technology, under the subject code FMH 606.

This thesis describes the study of the Anaerobic Digestion process by using syngas for methane production. The aim to evaluate syngas component effect and degradation pathways on AD reactor by using ADM1 model.

I would like to express my sincere gratitude to my supervisors Associate Professor Wenche Bergland, Professor Rune Bakke and Professor Britt Margrethe Emilie Moldestad for their excellent guidance and kind support throughout the thesis period, and also for their kind helps during the two-year master study at Porsgrunn (Norway). Thank you very much for a great experience. Moreover, I would like to thank Eshetu Janka Wakjera for providing me assistance and suggestion during this study. Also, I would like to thank Lab. Chief H.H.Haugen for assisting me in lab and Carlos.Dinamarca-Røed for helping me to use gas chromatography.

Finally, I want to present my thanks to all the faculties of Technology at USN. Last two years have been quite an experience for me, and you have all made it a memorable time in my life.

Porsgrunn, 03.06.2016

Sanjay Shah

List of figures

List of table

Abbreviations

AD	Anaerobic Digestion
COD	Chemical Oxygen Demand
ADM1	Anaerobic Digestion Model No. 1
VFA	Volatile Fatty Acid
LCFA	Long Chain Fatty Acid
WGS	Water Gas Shift
GWP	Global Warming Potential
HRT	Hydraulic Retention Time
CODH	Carbon Dehydrogenase
GC	Gas Chromatography
IC	Inorganic Carbon
CO_2	Carbondioxide
CO	Carbon monoxide
H_2	Hydrogen
CH_4	Methane
NH_3	Ammonia
H_2O	Water
CH_3COOH	Acetate
ΔG^o	Gibbs-free energy
Y	yield
K_m	Specific uptake of substrate
μ_m	Specific growth rates
g	gram
KG	Kilo Gram
m^3	Cubic meter
ml	millilitre
L	Litre

1 Introduction

Modern society is on the verge of high consumption of energy from fossil fuels (coal, oil, and natural gas). The massive utilization of fossil fuels is unsustainable and results in the emission of harmful greenhouse gases to the atmosphere. The fossil fuels reserve is limited and cannot encounter the growing global energy demand in near future. So, the alternative source of energy from renewable and eco-friendly sources are an urgent need. The exploration of alternative energy and fuels has inspired the researchers to put more focus on the renewable and sustainable resources rather than relying on the conventional source of fuel production[3]. Several green technology was developed in last decades, and some of them are even commercialized. Biomass is renewable and abundant, and its accumulation releases harmful greenhouse gases that have an adverse impact on the global environment. At the same time, municipal solid waste and agricultural wastes generation are rapid. 1.3 tons of solid waste is generated from world every year, and it is expected to be double in 2025[4]. More than half of this solid waste is organic and can be reduced to a renewable energy source in the form of biogas (has been developed)[5]. Biogas consists of mixtures of gases mainly methane (CH_4) and carbon dioxide (CO_2)[6].

The concept of Waste to energy from different kind of biomass waste and wet organic waste like manure for biogas generation by Anaerobic Digestion (AD) is prominent green technology since it reduces greenhouse gases and odors. The Norwegian government has put forward a goal where 30% of manure waste must be treated by AD within 2020[7]. Manure is the largest source of methane production by AD which accounts to produce nearly 40% in Norway[8]. Anaerobic digestion (AD) is a biochemical process, where anaerobes reduce organic pollutant in the absence of oxygen to produce biogas. The produced biogas consists of (55-75) % methane and (25-45) % carbon dioxide[9].

There is various kind of waste used to generate methane. For readily degradable material like food waste, AD process has been employed. But however, for woody biomass which contains complex compound like lignin and cellulose cannot be degraded by AD process[10]. So to circumvent these disadvantages, a new two-stage process is proposed where the first step is to produce syngas by gasification and further this syngas is fed to the AD reactor for methane production. Gasification is a thermochemical process where biomass waste converted into a mixture of gases called syngas that contains H_2, CO, and

CO_2[11]. The acetogens can utilize syngas in the AD process and act as biocatalyst which consumes syngas and produces CH_4 and CO_2. So, methane production from syngas is a combination of gasification (conversion of biomass to syngas) and fermentation (bio-methanation of syngas in AD reactor) as shown in figure 1.1. This thesis was a study on methane production from syngas.

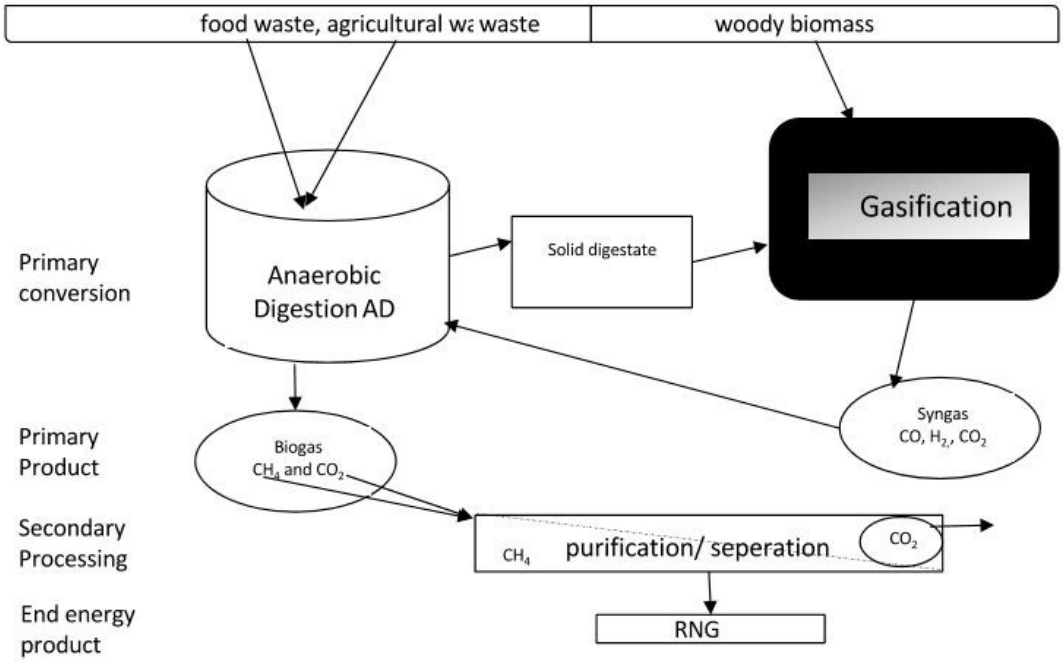

Figure 1-1: A waste-processing biorefinery concept is integrating anaerobic digestion and gasification towards the production of renewable natural gas[12].

A major challenge during syngas degradation is the gas- liquid mass transfer rate (kLa). Due to the low solubility of CO and H_2, kLa limits the syngas degradation in AD process[13]. Another main problem is the H_2 if present in excess amount can cause the rise of pH[14] and ultimately failure of Reactor. The ADM1 model is the best model for AD process developed by IWA in 2002 [2], but the implementation of syngas into ADM1 model is also a challenge.

The aim of this thesis was to evaluate and suggest syngas composition and degradation pathways in AD reactor which include:

- Experimental evaluation of syngas component effects on the AD reactor performance with different quality of syngas (mainly hydrogen) to be used in AD reactor.

- Evaluation of syngas microbial degradation pathways and kinetics, and implementation of the syngas degradation in ADM1 model and simulate this model using AQUASIM software.
- Optimization of the overall energy production by evaluating both the AD reactor performance and the syngas production process. But due to time restriction, this task is not included in this thesis.

2 Theory

2.1 Biogas Production by Anaerobic Digestion process

Biogas is a very promising source of renewable energy and consists of mixtures of gases mainly methane (CH_4) and carbon dioxide (CO_2) with traces of hydrogen sulphide (H_2S), oxygen (O_2) and Hydrocarbons[15]. Its production does not require high capital investment and operating cost with the major benefit of occupying fewer areas for the landfill.[16]. The market of global biogas upgrading is growing rapidly, and it is estimated to reach up to $338.5 million by the year 2016 with the compounded annual growth rate of 22 % [17]. The central element of biogas is methane which is odorless and colorless at ambient condition, and it has tetrahedral structure. Due to methane's abundance and high energy density makes it very attractive fuel in comparison with other fuels [18], as mentioned in Table 1.

Table 2-1: energy content of various fuels[18].

Fuel	Energy content (MJ/Kg)
Methane	55-55.7
Natural gas	38-53.3
Diesel	48.1
Ethanol	23.4 – 30
Charcoal	30
Wood	6-17

Methane is considered to remain a very potent greenhouse gases and has the GWP of 25 over 100 years [19]. If properly utilize, biogas can also be seen as a valuable source of renewable energy which can be used for cooking or heating as a fuel, upgrading to natural gas quality (biomethane) or can be utilized directly for electricity production[20]. There are several techniques which are being used for biogas upgrading like water washing, polyglycolic adsorption, pressure swing adsorption and chemical treatment [21]. The methods mentioned above are performed outside of the anaerobic reactor for biogas upgrading which requires extra investment for external means like pumps, compressor, membrane, etc.[20]. So to avoid this additional cost, the alternative and efficient way to

upgrade methane production from waste is to add syngas directly into Anaerobic Digestion process. This process is a technologically simple and effective method for treatment of organic waste along with a greater environmental and economic advantages[22].

Anaerobic digestion (AD) is a biochemical process, where microbial activity comes underplay and reduce organic pollutant in the deficiency of oxygen to produce biogas. The produced biogas consists of (55-70) % methane and (25-45) % carbon dioxide[9]. This process is considered to be as established green technology for the generation of methane-rich biogas production from biomass waste and wastewater[23].

2.2 Biochemical process of Anaerobic Digestion.

Anaerobic digestion is a complex process where reduction of organic waste takes place through some biochemical reactions under anoxic conditions[24].The microbiological process, where microorganisms grow and drive energy for the metabolism of organic waste in oxygen-free condition to produce methane, occurs in four steps [9], which is described below and shown in figure 2.1.

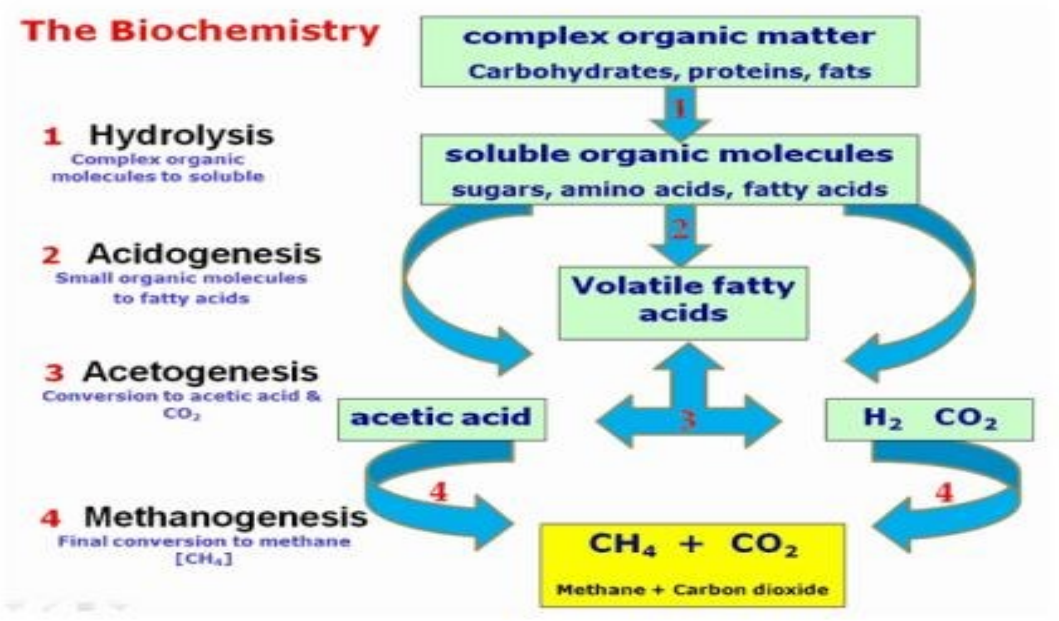

Figure 2-1: systematic representation of the primary conversion process in anaerobic digestion for biogas production[25].

1. Hydrolysis: The first step of AD where non-soluble biopolymer and complex organic matter such as lipids, polysaccharides, fats, proteins, nucleic acids, etc. gets converted into simple soluble organic compounds by the help of hydrolytic enzymes produced by hydrolytic microorganism[26].

$$lipids \xrightarrow{lipase} fattyacids, glycerol \quad \text{(R2-1)}$$

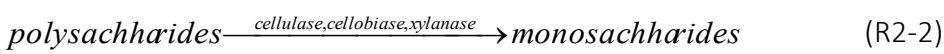

$$polysachharides \xrightarrow{cellulase,cellobiase,xylanase} monosachharides \quad \text{(R2-2)}$$

$$proteins \xrightarrow{protease} a\,\mathrm{min}oacids \quad \text{(R2-3)}$$

2. Acidogenesis: The produced monomers which are the product of hydrolysis are being degraded by different facultative and obligatory acidogenic bacteria and transform the soluble organic compound to VFA (volatile Fatty Acid) and CO_2[27].
3. Acetogenesis: The third step of anaerobic digestion process where the product formed during acidogenesis step cannot be converted directly into methane by methanogen bacteria. VFA oxidized into methanogenic substrate like Acetate and Hydrogen [26]. The production of H_2 increases the partial pressure of hydrogen and inhibits the metabolism of acetogenic bacteria. So it is crucial that the microorganism responsible for anaerobic oxidation reactions must collaborate with the other group which consumes hydrogen within the system. Methanogens consume the hydrogen and make the partial pressure low for oxidation reactions. Therefore, methanogenesis and acetogenesis run parallel to produce methane which explains the symbiotic relationship between two groups of the organism[28].
4. Methanogenesis: This step is considered to be a critical step and slowest biochemical process where acetate, carbon dioxide plus hydrogen are converted into methane gas by methanogenic bacteria[6].

   70% of methane are produced from acetate by acetoclastic methanogenesis while 30% from hydrogen and carbon dioxide by hydrogenotrophic methanogenesis[26].

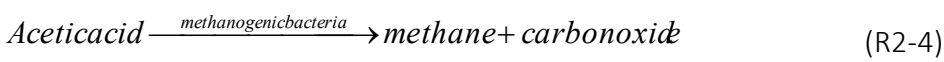

$$Aceticacid \xrightarrow{methanogenicbacteria} methane + carbonoxide \quad \text{(R2-4)}$$

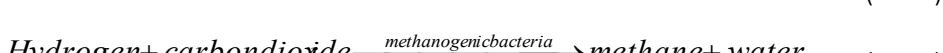

$$Hydrogen + carbondioxide \xrightarrow{methanogenicbacteria} methane + water \quad \text{(R2-5)}$$

Since it is a biological process, some environmental factors like temperature, pH, alkalinity C/N ratio, hydraulic retention time (HRT) and toxicity has a strong influence. Neutral pH is necessary for biogas production, and the favourable range is given for methanogens to grow between the pH ranges of (6.5-7.5). Also, the alkalinity should be present in high amount since it causes an adverse effect on biogas production. Similarly, the temperature is another critical parameter since it plays a vital role in the production of biogas. Most of the acetogens and methanogens grow under the mesophilic condition, but however thermophilic condition seems to be more favourable for methanogens [6]. C/N ratio mainly depends on upon the substrate used. Too many variations in C/N ratio may affect the production process. It is seen that microorganism consumes 25-30 times more Carbon than Nitrogen, so microbes need 30:1 C/N ratio[29]. Methanogens grow slowly and a reported doubling time is around 5-16 days. So HRT should be at least 15 days[27].

Two parameters are used to determine the organic content of aqueous waste i.e. Biochemical Oxygen Demand (BOD) and Chemical Oxygen Demand (COD). COD represented the organic compound present in the aqueous waste stream and used to predict the potential for sustainable biogas production. It is equivalent to the amount of oxygen consumed by the strong chemical oxidizing agent to oxidize the organic compound in acidic medium and is consider as the best among the two most important parameters used to determine the total organic load[30].

Volatile Fatty Acids (VFAs) are known as important transitional compounds produced from the microbial action in the metabolic pathway of methane fermentation process, and its higher concentration develops some microbial stress which results in a decrease of pH and eventually causes digester failure[31].

2.3 Modelling of Anaerobic Digestion Process

The International Water Association (IWA), an anaerobic digestion modelling task group[32] prepared the generalized mathematical model (ADM1) for anaerobic digestion processes. ADM1 is a structured model that describes the biochemical and physicochemical processes that are responsible for methane production. The biochemical reactions are the core of this model which includes disintegration of complex organic material to carbohydrates, proteins, and lipids. The products of decay are then

hydrolyzed into sugars, amino acids and long-chain fatty acids (LCFAs). Carbohydrate and protein undergo fermentation and produces molecular hydrogen and volatile organic acids (acidogenesis). Then, LFCA is broken down to acetate and hydrogen (acetogenesis). The last step is the split of acetate ions into methane and carbon dioxide (acetoclastic methanogenesis). The hydrogenotrophic methanogenesis step also produces methane when hydrogen reduces carbon dioxide[33]. Each step can be inhibited, and inhibition is due to pH, hydrogen and or by NH_3. Inhibition is a factor which is multiplied by reaction rate. If it is below one, then it shows inhibition.

Similarly, the physiochemical process is a non-biological process, and three types of kinetics rates which occur in Anaerobic Digestion process are[2]:

1. Liquid-liquid mass transfer process (i.e. ion association/ dissociation: rapid)
2. Liquid-gas exchange(i.e. liquid-gas mass transfer: rapid/medium)
3. Liquid-solid transformation process(i.e. precipitation and solubilization of ions: medium/slow)

In ADM 1 model, only first two processes are addressed, and liquid-solid transfer process is not included because of its robust in implementation in the process. Figure 2.2 shows the overview of processes that is discussed in the ADM1 model[2].

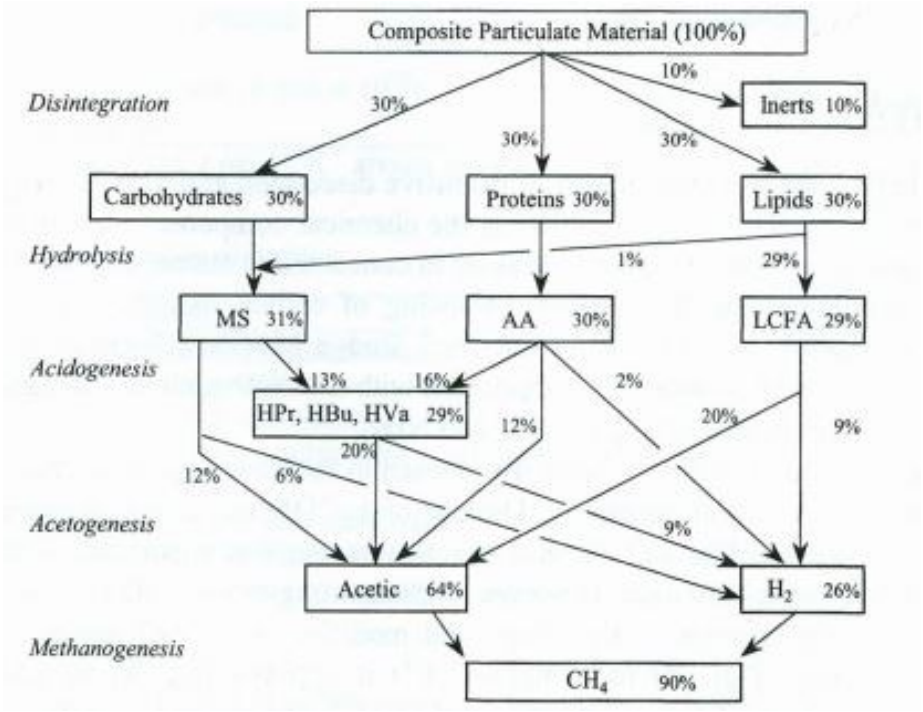

Figure 2-2: systematic representation of anaerobic digestion process described in ADM1 model[2].

2.4 Biomass gasification and syngas production

2.4.1 Biomass as feedstock for energy production

The demand for biomass-based energy is increasing. Biomass is one of the most abundant energy sources for biofuel production since it contains mainly carbon, oxygen, and hydrogen and it is generated biologically by nature. According to "Lynn and Osburn", the world's biomass production is estimated to be more than 146 billion metric tons/year[34]. Biomass contains lignocelluloses which are the biggest pool of carbohydrate (55-65) %[35]. Lignocellulosic biomass generally consists of (35-50) % cellulose, (22-32) % hemicellulose followed by (15-25) % lignin[17]. These Lignocellulosic biomass doesn't easily get degraded by a microorganism, which gets accumulated in nature and causes methane emission into the atmosphere. The difficulty in degradation is because of the complex nature of lignocellulose compounds (Strong bond between the lignin, cellulose, and hemicellulose). Cellulose is a polysaccharide that aligns in a linear chain or row. These chains forms bigger rows in parallel with each other and synthesize a crystalline structure which provides strength to lignocellulosic biomass[36]. Cellulose is a polymer of hexose

blocks like glucose, while hemicellulose is from xylose (pentose block). During fermentation of glucose and xylose, hexoses become easier to digest by the microorganism rather than pentose. Lignin is another complex organic polymer which has very high energy content. It is made up of non-sugar molecules, which helps to hold the biomass molecule together. Further, lignin compound can be burned at a higher temperature for energy production or turned into high strength carbon fibres[17].

2.4.2 Biomass gasification

Waste like lignocellulosic biomass can be utilised to generate power by gasification, which is one of the established and excellent technology for solid waste treatment in many countries. The main advantage of gasification is that it converts a variety of waste feedstock into valuable biofuels and reduce the emission of methane from landfills[37].
Gasification is a thermochemical process which converts biomass at high temperature (500-1500)˚C and pressure (1-80 atm) into a mixture of combustible and non-combustible gases called as synthetic gas or producer gas[13]. Gasification is either air based or steam based. Steam based gasification produce synthesis gas with high hydrogen content[11]. An example of biomass gasification from steam with and without selective transport of CO_2 are shown in Figures 2.3 and 2.4[38].

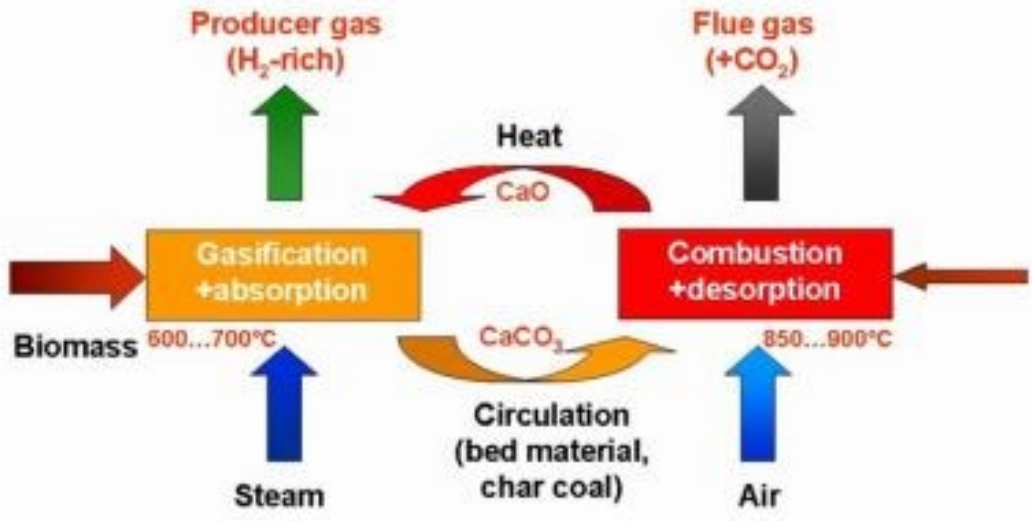

Figure 2-3: biomass gasification with the selective transport of Co_2[38].

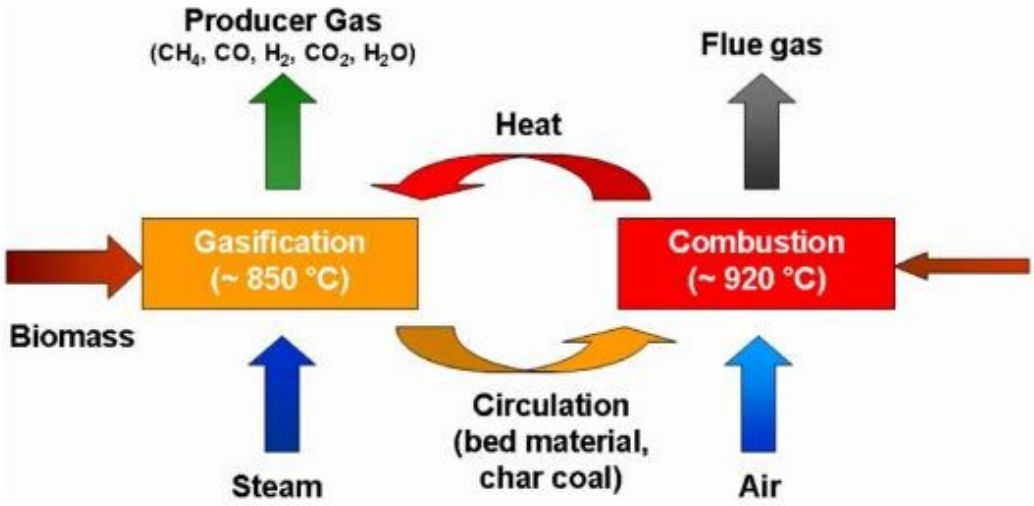

Figure 2-4: biomass gasification without selective transport of Co_2[38].

2.4.3 Syngas

The mixture obtained from the gasification process is called synthesis gas or syngas. The syngas composition consists of carbon monoxide (CO), carbon dioxide (CO_2) and hydrogen (H_2) as a major component. Along with few minor components which include methane (CH_4), water vapour (H_2O), light hydrocarbons like ethane (C_2H_6), ethylene (C_2H_4), and some volatile impurities[13]. Its composition mainly depends on upon gasification temperature and gasification agent[11]. Syngas can be directly utilised by power industries to generate electricity, or it can also be upgraded into methane with the help of chemical catalyst as suggested in Fischer- Tropsch process. This process includes Water-gas-shift (WGS) which increases the H_2/CO ratio and then nickel is use as a catalyst for methanation process (Sabatier) which converts CO & CO_2 into methane and water as shown in below equations[13].

$$nCO + (2n+1)H_2 \rightarrow C_nH_{(2n+2)} + nH_2O \text{ (Fischer-Tropsch Equation)} \quad \text{(R2-6)}$$

$$CO_2 + 4H_2 \rightarrow CH_4 + 2H_2O \text{ (Sabatier Equation)} \quad \text{(R2-7)}$$

Also, syngas can be used to produce methanol and ammonia as shown in figure 2.5.

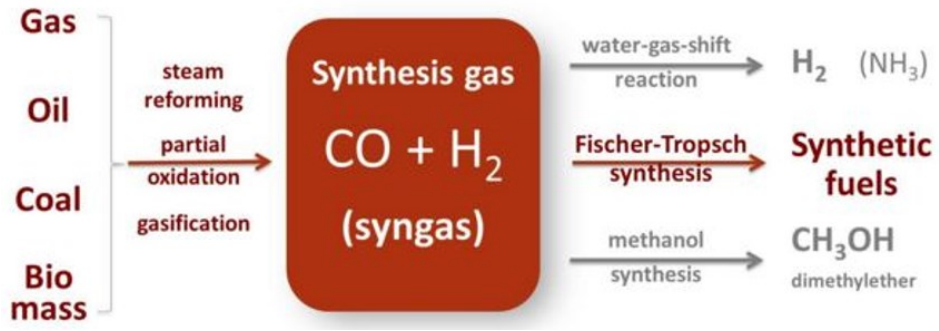

Figure 2-5: Synthesis gas production and conversion routes in various products[39].

2.4.4 Syngas Production-Thermochemical Process

The more efficient way for energy recovery from feedstock is the thermochemical process, in which syngas is produced as an intermediate between pyrolysis and gasification. Pyrolysis is the thermal conversion of biomass which is conducted at a high temperature at about (100-600) ˚C in the absence of oxygen. As a result, the product of pyrolysis consists of solid charcoal, coke, liquid (tars), hydrogen and methane. The composition of pyrolysis product depends mainly on temperature and residence time, higher the temperature and longer the residence time yields more gases while shorter residence time and moderate temperature yields more liquids[11]. During gasification, the produced coke shows some reaction with oxygen and water at higher temperature. The following extreme reactions occurring during gasification are summarised in equations R2 (8-10)[40].

$$C + \frac{1}{2}O_2 \leftrightarrow CO \quad \text{(R2-8)}$$

$$C + O_2 \leftrightarrow CO_2 \quad \text{(R2-9)}$$

$$C + H_2O \leftrightarrow CO + H_2 \quad \text{(R2-10)}$$

The first reaction (R2-8) shows the partial oxidation of carbon into CO (carbon monoxide) and the second reaction is the complete oxidation of carbon molecule into carbon dioxide (CO_2) that takes place during gasification. The third result is water gas shift (WGS) reaction. During WGS reaction, CO oxidation provides the required energy by the transferring of an electron from CO to H_2O as mentioned in following reactions[41].

$$H + 2e^- \rightarrow H_2 \quad \text{(R2-11)}$$

$$CO + H_2O \leftrightarrow CO_2 + H_2 \quad \text{(R2-12)}$$

$$CO + 3H_2 \leftrightarrow CH_4 + H_2O \quad \text{(R2-13)}$$

The equation R2-11 is an electrochemical equation, where carbon monoxide dehydrogenase (CODH) provides the electron and proton. In equation R2-12, an enzyme catalyst known as hydrogenase make available energy for cell growth[42]. The last reaction shows methane formation during gasification. The less amount of energy (4.46Kcal/mol) is generated during anaerobic pathways of WGS reaction where microbial cell growth is much slower than aerobic reaction, which produces 61.6Kcal/mol.

Gasification process deals with the number of complex chemical reactions. The primary method includes biomass drying (which decompose biomass at 100 ˚C -200 ˚C), pyrolysis followed by oxidation and reduction. During oxidation, Carbon molecule is oxidised to carbon dioxide and hydrogen is converted into water, the reaction is exothermic. However, the reduction is made under anaerobic conditions[43]. After that, the syngas is purified. The gasification process is done in gasifiers, and two different types of gasifiers which are most common in use are fluidised bed and fixed bed gasifiers[44]. The fluidised bed is used for large scale gasification process and is considered to be more cost-effective.

2.5 Syngas degradation and microbial pathways in AD

Methane gas is generated from syngas by two different methods. The first method is anaerobic digestion process, where various types of microorganisms are used as a biocatalyst to ferment the syngas. The second way of up gradation of methane from syngas is with the chemical as a catalyst, which was first proposed by Fisher and Tropsch in 1925 in Germany[13]. A variety of products can be generated from anaerobic or biological digestion process such as methane, ethanol, butanol butyric acid, and acetic acid[45]. The combination of gasification and anaerobic digestion is considered to be one of the most promising technology which has many advantages over the first generation for biofuel production process[46].

2.5.1 Microbiology and biochemical process of syngas in AD

During the anaerobic digestion process, the microorganism responsible for methane formation as a catabolic end product belongs to the kingdom of *Euryarchaeota*. These Archea-group microbes called methanogens produce energy for themselves during process and convert acetate, carbon dioxide, and hydrogen to methane[47]. During syngas degradation, a group of bacteria collectively known as acetogens is capable of fermenting

syngas (i.e.CO, CO_2 and H_2) into fuels via reductive acetyl-CoA pathways also recognised as carbon monoxide pathways[48]. In the Acetyl-CoA pathways, carbon monoxide dehydrogenase enzyme is the key enzyme which converts CO to CO_2[49].

Three different group of microorganisms are usually found in the anaerobic digestion process. They are acetogenic bacteria (acetogens [1]), sulphate reducing bacteria, and methanogenic bacteria (methanogens [2])[50]. The acetogens generate acetate and hydrogen, methanogens consume this hydrogen and produce methane. Both acetogens and methanogens show a symbiotic relationship with each other[28]. Sulphate reducing bacteria reduces sulphate to hydrogen sulphate providing a more favourable condition for methanogens[50].

Methanogens are either strict anaerobes which degrade complex proteins or facultative anaerobes that digest pure organic compounds. Most of the microbes can grow under mesophilic condition (i.e. temperature range between 30 - 35 ^{o}C) and also, they can grow well under the thermophilic environment (i.e. temperature range between 50 - 55 ^{o}C). More than 50 different kinds of methanogens are discovered so far which comes underplay during the anaerobic process and converts CO from syngas into methane[51]. Some of them are listed in below table 2.

[1] Obligatory anaerobes responsible for acetate formation.
[2] Obligatory methane forming anaerobic archaebacterai.

Table 2-2: Methanogens that converts methane.

Microorganisms	Reference
Methanobacterium thermoautotrophicum	*[52]*
Methanothermobacter wolfeii	*[53]*
Methanosarcinabarkeri	*[54]*
Metnanobacteriumformicicum	*[55]*
Methanosaracinaacetivorans C2A	*[56]*
Methanobrevibacter arboriphilicus	*[57]*
Methanocaldococcus jannaschii	*[13]*
Methanopyrus kandleri	*[30]*
Methanosaeta thermophila	*[58]*

2.5.2 CO-degradation and catabolic pathways in AD

Some microorganisms are responsible for the degradation of carbon monoxide into methane. CO degradation is either by direct reaction or by indirect reaction[13]. Immediate reactions are:

$4CO + 2H_2O \rightarrow CH_4 + 3CO_2$ ($\Delta G^{\circ'}$ = -53 KJ/mol CO) (R2-14)

$CO + 3H_2 \rightarrow CH_4 + H_2O$ ($\Delta G^{\circ'}$ = -150 KJ/mol CO) (R2-15)

The first reaction shows slow growth while the second reaction shows faster growth and thermodynamically more feasible. Both these reactions depend on hydrogen concentration inside the reactor. When H_2 is sufficient, the second reaction should prevail, and the first reaction should occur once H_2 starts to decrease.

Possible indirect reactions are:

$CO + H_2O \rightarrow H_2 + CO_2$ ($\Delta G^{\circ'}$ = -20 KJ/mol CO) (R2-16)

$4CO + 2H_2O \rightarrow CH_4 + 3CO_2$ (R2-17)

$2CO + 2H_2 \rightarrow CH_3COOH$ ($\Delta G^{\circ'}$ = -67 KJ/mol CO) (R2-18)

$4CO + 2H_2O \rightarrow CH_3COOH + 2CO_2$ ($\Delta G^{\circ'}$ = -44 KJ/mol CO) (R2-19)

$CO + 2H_2 \rightarrow CH_3OH$ ($\Delta G^{\circ'}$ = -39 KJ/mol CO) (R2-20)

$CH_3OH \rightarrow 3/4CH_4 + 1/4CO_2 + 1/2H_2O$ (R2-21)

$CO + H_2O \rightarrow HCOOH$ (R2-22)

The reaction (R2-16) is a WGS reaction and equation (R2-17) is obtained by either carboxydotrophic methanogenesis, or the methanogenic reduction of CO_2. The equations (R2-18) and (R2-19) are CO-homoacetogenisis and acetogenesis respectively, which is followed by acetoclastic methanogenesis or methanol production (R2-20). This methanol further converted into methane by methylotrophic methanogenesis (R2-21), or oxidation of CO to formic acid (R2-22), which is reduced into methane[13].

Under mesophilic condition, CO first gets converted mainly into acetate and then further It gets reduced into methane. CO conversion pathways depend on the partial pressure. Partial pressure (P_{co}) lower than 0.3 atm is more favourable for methanogenic activity under mesophilic condition. Further increase in CO leads to inhibition for methanogenesis, but, however, the hydrogenotrophic methanogenesis is enhanced more at high CO[12] as shown in figure 2.6.

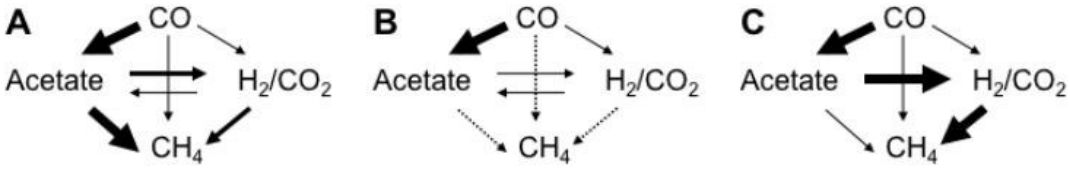

Figure 2-6: Different catabolic pathways for CO conversion into methane.[12]

Three different potential pathways at different partial pressures are shown in below figure. A represents the paths at low CO ($P_{co<}$ 0.5 atm), B shows at higher CO ($P_{co>}$1 atm) and last C, after acclimation, which is 100% CO. Four different widths of the arrow are used to indicate the possible conversion routes. Thick arrows indicate (60-70) % conversion followed by intermediate pointer (20-40) % and the thin arrow accounts for (5-20) %. The dotted line shows blockage.i.e. no conversion of CH4 by CO is possible[12].

2.5.3 Effect of H_2 and CO addition for biogas production/upgrading

Hydrogen is used to upgrade the methane production directly into the reactor to increase the hydrogenotrophic methanogenesis. It has some positive effect only in methanogenesis, but no any effect on the acetogenesis is observed[20]. Methanogenesis process enhanced by the addition of hydrogen where hydrogenotrophic microorganisms bind the H_2 with CO_2 and converts them into methane[15].

$4H_2 + CO_2 \rightarrow CH_4 + 2H_2O$ ($\Delta G^{\circ'}$ = -130 KJ/mol) (R2-23)

Hydrogen addition for the biogas upgrading has many advantages and also some negative impact as well. The advantages are:

- More than 90% of hydrogen gets converted into methane which increases the heating value of biogas, and can be added to the natural gas grid as a renewable energy source[15].
- Hydrogen consumes CO_2 in the biogas reactor ensuring biogas with a lower content of CO_2 which in turn decreases the upgrading cost. Also, some left or unconverted hydrogen would increase the combustion properties of biogas[14].

The disadvantages are:

- The addition of hydrogen can affect the anaerobic digestion process by increasing the pH of the reactor. Therefore, particular attention is required, and one way to control the pH is Co-digestion of manure by acidic substrate[15].
- If Hydrogen is added directly to the reactor's headspace, the biggest problem is the hydrogen consumption rate which depends on the partial pressure of H_2 and mixing intensity. Increase in the partial pressure can lead to the VFA (propionate and butyrate) inhibition. VFA inhibition can also occur at higher mixing intensity (300 rpm)[14].

Some challenges were observed in the biogas reactor during bioconversion of Carbon monoxide. Due to its high affinity towards metal-containing enzymes, it has been considered as the highly toxic for several microorganisms[59].

In 2013, Irini Angelidaki and Gang Luo published the article given in [1]. The work is the experimental study of CO Biomethanation and Anaerobic digestion from sewage sludge treatment. The experiment shows that CO depends on partial pressure and retention time. At low partial pressure, i.e. between 0.25 and 1 atm, CO shows inhibition only to methanogens under thermophilic condition. But at high pressure, i.e. 1.58 atm, it shows no inhibition inside the Hollow Fibre Membrane due to low solubility in the liquid. At 0.2d of gas retention time, total consumption of CO was reached as shown in figure 2.7.

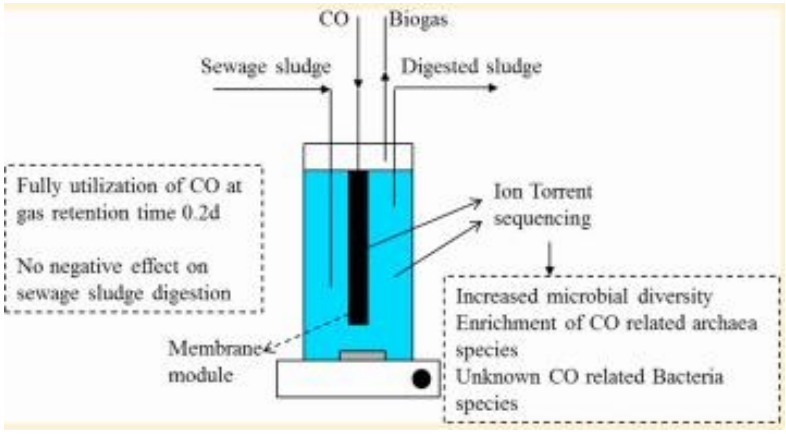

Figure 2-7: biogas production by CO conversion in Anaerobic Digestion[1].

3 Methods

3.1 Experiment

Two parallel fed-batch reactor A and B (600 Ml laboratory glass bottles) were established for the Anaerobic Digestion process. Each reactor contains 500 ml of working volume and 100 ml of headspace. Both reactors were filled up by the mixture of three solutions; 200 mL of granular sludge, 200 mL of effluent, and 100 mL of pig manure. To investigate the conversion efficiency of hydrogen gas to methane by AD process, reactor A was further connected with 1 L of a glass bottle. Hydrogen gas was introduced inside the glass bottle with the help of 20 ml syringe. The silicon tube of small diameter was dipped inside the reactor A and linked with a hollow metallic rod which was combined with syngas bottle. Both reactors were well insulated and conducted under mesophilic condition; 35˚ C. The produced biogas was collected in the gas bags and periodically analyzed in the gas chromatography (GC).

3.1.1 Reactor design

3.1.1.1 Reactor setup

Two identical 600 mL of the glass laboratory bottle were chosen for reactor A, and B. Both reactors were equipped with plastic caps which has three vents, one inlet, and two outlets. Further, these holes have opening and closing lid mounted at the top. A transparent plastic tube was inserted into the different openings of the reactor. All these three inlet/outlets were equipped for various purposes. The first channel was constructed to introduce feed inside the reactor. Similarly, the second outlet is to take effluent out of the reactor, and the third opening is connected with the gas bags for produced biogas collection. Both reactors are well insulated and sealed with a white solution called as patrix silicone. All the outlet pipe are assembled with a plastic valve which can be operated manually as shown in figure 3.1.

Furthermore, the Reactor A was assembled with 1 L Glass bottle, where hydrogen gas was introduced with the help of a syringe. A 1 L bottle was chosen in order to control the pressure inside the bottle since at higher pressure hydrogen might diffuse into the atmosphere. The bottle was sealed with the thick rubber cap, and a thin hollow metal rod

of 20 cm was penetrated inside the bottle at one end and connected to the Reactor A at the other end. The metal rod was further dipped into the reactor's headspace and at the end of this metal rod, a silicon tube of 2.79 mm diameter was connected and fixed to the bottom of the reactor. The closing valve closes the silicon tube at the end of tube and magnet (of a certain weight) is attached to prevent it from coming out of the liquid volume. The primary benefit of the hollow metallic rod is to avoid the syngas diffusion into the atmosphere since hydrogen gas is very light gas. The function of chosen silicon tube is for better diffusion of hydrogen gas, directly by the tubes into the reactor. The experimental setup is shown in figure 3.1.

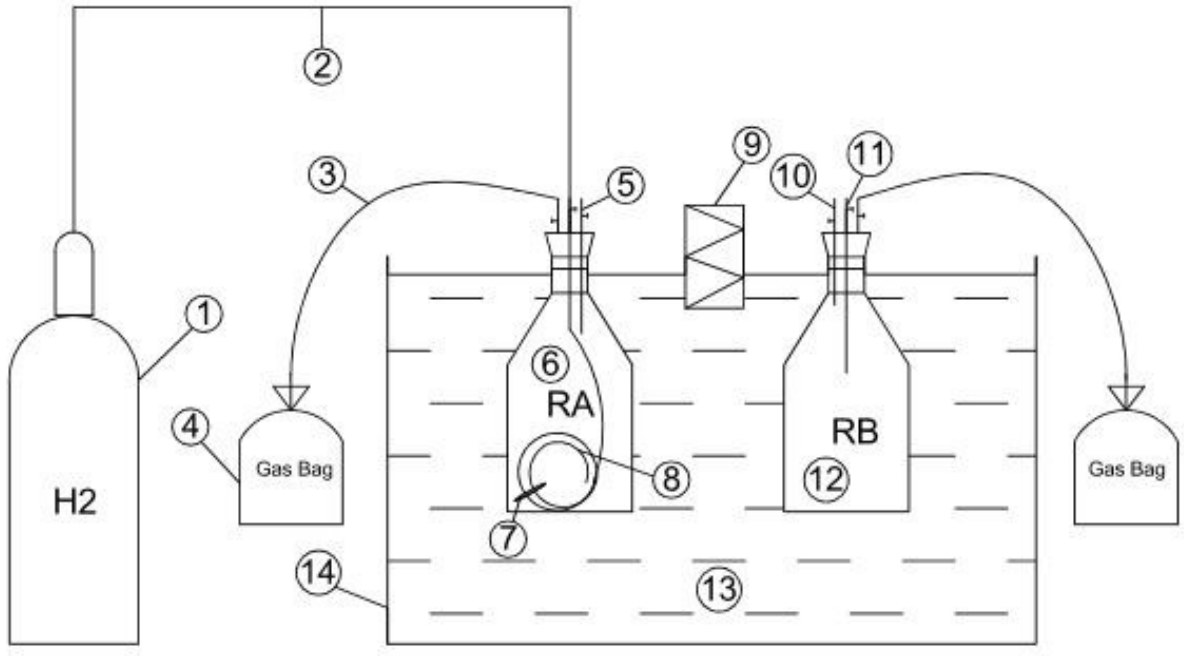

Figure 3-1: Schematic of Experimental setup. (1) Gas cylinder (2) hollow metallic rod (3) gas sample outlet (4) gas collection bag (5) feed inlet and outlet (6) anaerobic digester with H_2 (7) magnet of certain weight (8) silicon tube (9) digital electrical heater (10) effluent outlet of reactor B (11) feed inlet of reactor B (12) anaerobic digester without syngas (13) water at 35˚C (14) rectangular water beaker.

Initially, Water bubble test was performed to check the leakage and both reactors are flushed with nitrogen to make anaerobic condition while the big bottle was flushed with hydrogen gas. The nitrogen cylinder was maintained at control pressure, and gas was sent directly into the both reactors through the openings for about 10 minutes. Nitrogen gas was carried into the reactor through one opening and simultaneously it was allowed to

leave the reactor from another opening, regulated by the manual valve. Similarly, the hydrogen bottle was flushed with hydrogen gas where 100 mL of hydrogen gas was used for flushing the bottle, and it was performed by the help of syringe needles. Two long syringe needle were taken, both were penetrated through the rubber cap of the bottle and 20 ml of hydrogen gas was injected from one needle by the help of a syringe and simultaneously it leaves the bottle from another needle. The same procedure is repeated for five times (20 mL each time).

3.1.2 Reactor Operation

3.1.2.1 Preparation of anaerobic culture

Preparation of anaerobic culture (inoculum) was done before the start of the experiment. An anaerobic culture used is granular sludge. 300 ml of granular sludge was collected and 100 ml of pig manure was added into it and leave it for one week period for incubation at room temperature. After one week of incubation, the inoculum was diluted with the effluent from sludge bed AD treatment of the same feed. The dilution was done several times and the primary purpose to dilute the mixture with effluent is to balance free ammonia concentration into equal amount of granular sludge since ammonium is inhibition of some bacterial growth.

3.1.2.2 Start-up of the reactor

Fed-batch experiment was conducted. The temperature inside the both reactor was controlled at 35˚ C by hot water. The reactors are placed inside the rectangular vessel of 30 L volume provided with the digital electrical heater as shown in figure 3.1.
During operation phase of the reactor, initially the temperature was controlled at room temperature, and it was increased by one ˚ C to every day until it reached up to 35 ˚ C.

3.1.2.3 Feeding to the Reactor

Substrate or feed was added into the reactor through the inlet, and a particular volume of bulk liquid (effluent) was taken out (by syringe) from the outlet of the reactor. The feeding was done twice in a week. Each time 100 mL of feed was added, and 100 mL of effluent was taken out from the both reactor. The hydraulic retention time (HRT) of feed was calculated by:

$$HRT = \frac{Volume(mL)}{Load(mL/day)} = \frac{500}{200/7} = \frac{3500}{200} = 17{,}5day$$

20 mL of hydrogen gas was injected every day into the Reactor A. 10 mL of hydrogen gas was added twice a day, once in the morning and other at the evening.

3.1.3 Analytical methods

The pH, Total and soluble COD, VFA of effluent and added feed was then measured in the laboratory. The volume of biogas produced was measured, and the gas chromatography analyzed the composition.

3.1.3.1 pH measurement

The pH of the effluent and feed are measured by a pH meter (Beckman 390).The ph measurement was carried out twice in every week. An electrode was immersed into the sample to perform the pH measurement, and value was displayed after 30-60 seconds depending upon the sample.

3.1.3.2 COD measurement

The COD analysis was carried out according to US standard 5220D (APHA, 1995)[60]. For COD_t determination, the samples were homogenized first into homogenizer for 5 minutes and then oxidized with a hot sulphuric solution of potassium dichromate, with silver sulfate as a catalyst. The sample is then heated at 148^0C for about 2 hours in MT 00114 THERMOREACTOR TR620, and the final value is noted down after displayed in the photometer. Similarly for COD_S measurement the samples were centrifuged at 10,000 rpm for 30 minutes and then filtered (0.45 µm)[60].

3.1.3.3 VFA analysis

The samples were prepared for VFA's measurement in the laboratory and measured by gas chromatography (Hewlett Packard 6890) with a flame ionization detector with a capillary column (FFAP 30 m, film 0.5 µm, and inner diameter 0.250 mm). The oven was programmed to go from 100° C, hold for 1 min, at 200° C at a rate of 15° C/minute, and then to 230° C at a rate of 100° C/minute. Helium gas was used as carrier gas at 23 ml/minute. The temperatures of detector and injector were set to 250° C and 200° C, respectively[60].

3.1.3.4 Biogas composition analysis.

The amount of biogas were collected in the gas bag. Gas composition (CH_4, CO_2, and H_2) were analyzed by multiple gas analyzer chromatograph (GC system, the SRI Model 8610C, Bad Honnef, Germany). The carrier gas was argon and temperature was kept constant at 40° C.

3.2 Modelling and simulation

Ordinary ADM1 model was chosen, and simulation of this model was performed in the AQUASIM software. The selected case is the simulation of an experimental sludge treatment study of AD for wastewater treatment by Batchstone[2]. This ADM1 model is based only on biochemical process. The addition of syngas is not included, so the ADM1 model was modified by a diffusive link. All the syngas is now transported through this diffusive link. Hydrogen gas diffuses to the reactor from membrane while CO and CO_2 are sent to reactor from feed by the ratio between components in the syngas. Some changes are made where new biochemical and physiochemical parameters are added, and processes are modified[61].

3.2.1 Addition of new compartment in AQUASIM

The new compartment was added in AQUASIM software. The name of the new compartment is a membrane. Here the pressure of hydrogen is set through the inflow of a given amount. From here the H_2 diffuses to the reactor through a diffusive link by using Henry's constant for hydrogen[61].

3.2.2 New link in AQUASIM

New link "gas_from_membrane" was added for diffusion of hydrogen from the membrane compartment to the reactor compartment as explained in figure 3.2[61].

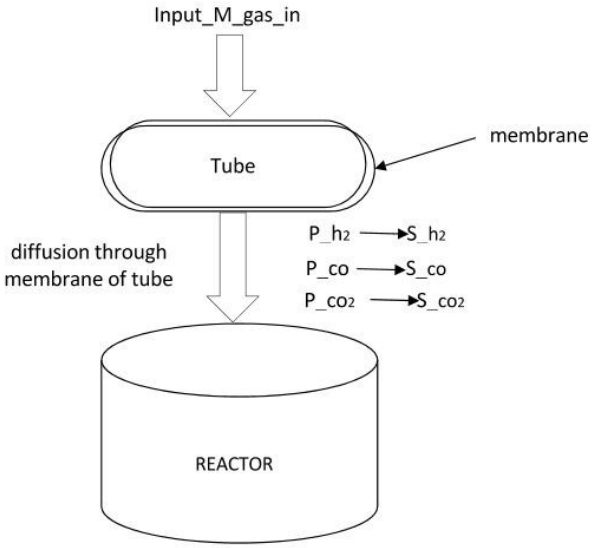

Figure 3-2: flow diagram of syngas diffusion through the membrane of the tube to the reactor.

Some new variables are added and changed model parameters are listed in Table 3. In the model, S_co and S_co_2 are added to the reactor through the water inflow. The main aim is to get the right ratio of hydrogen for slowest diffusion. Also, S_co is added to the existing diffusive link between the reactor and the headspace. S_co in both reactor and headspace is activated before the simulation starts.

Table 3-1: changed biochemical and physiochemical parameters used for the new model.

S.NO.	Variables	Description	Units
1.	inputM_gas_in	The flow of syngas into the tube membrane to maintain some membrane pressure. It is the amount of H_2 going into the membrane to keep up the H_2 pressure. Therefore, it is affecting the diffusion of H_2 through the membrane.	m3/d
2.	inputM_p_h2_in	Partial pressure of h2 in membrane.	Bar
3.	inputM_p_Co_in	Partial pressure of Co in membrane.	Bar
4.	inputM_p_CO2_in	Partial pressure of CO2 in membrane.	Bar

5.	km_co_ac	Maximum uptake rate for Co degrading organisms.	kg COD S.kg COD X.d-1
6.	X_co_ac	Co degrading organisms. Units:	kg COD.m-3
7	Ks_co_ac	half saturation constant for co degradation (same as for h2)	kg COD.m-3
8.	I_ph_co_ac	pH inhibition of Co to acetate degrading organisms	-
9.	I_h2_co_ac	hydrogen inhibition for Co.	-
10.	kdec_x_co_ac	decay rate for Co degrading organisms	d-1
11.	Y_co_ac	The yield of biomass on the uptake of Co to acetate.	kg COD.kg COD-1
12.	S_co	Total carbon-monoxide.	kg COD.m-3
13.	S_co2	Total carbon-dioxide.	kg COD.m-3
14.	S_co2_mem, S_co2_reac	Carbon-dioxide in membrane and reactor.	kg COD.m-3
15.	S_co_mem, S_co_reac	Carbon-monoxide in membrane and reactor	kg COD.m-3
16.	C_co	Carbon content of Co	mole.g COD-1
17.	KH_co	Non-dimensional henry's law constant for co with temperature correction (calculated from original KH in M.bar-1)	Mliq.Mgas-1
18.	KLa_in	Apparent mass-flux coefficient for syngas into reactor	m3d-1
19.	kLa_in	Volume-specific gas-liquid transfer coefficient (1-20) h^{-1};[13]	d-1
20.	p_co	Partial pressure of Co. S_co/16*R*T	Bar
21.	p_co_adjust	Partial pressure of co adjusted. p_co/P_headspace*100	%
22.	methaneflow1	Methane flows out of reactor	m3/d

23.	exp_gasflow_methane	Real list variable. Calculated from batchstone experimental values.	-
24.	S_h2_mem	Elemental hydrogen in membrane.	kg COD.m-3
25.	S_h2_reac	Elemental hydrogen in reactor.	kg COD.m-3

Similarly, two new processes are added into the model. One is the uptake of carbon monoxide to acetate and second is decay rate of carbon monoxide organisms. The rate equation and stoichiometry coefficient are given in Table 4.

Table 3-2: uptake rate and decay rate of Co in the model.

Dynamic process	Rate equation	Stoichiometry coefficient
uptake_co_ac	km_co_ac*X_co_ac*S_co/(Ks_co_ac+S_co)*I_ph_co_ac*I_h2_co_ac*I_NH_limit	km_co_ac*X_co_ac*S_co/(Ks_co_ac+S_co)*I_ph_co_ac*I_h2_co_ac*I_NH_limi
decay_co_ac	X_co_ac*kdec_x_co_ac	X_co_ac*kdec_x_co_ac

3.2.3 Estimation of k_m and Y for CO.

In anaerobic process CO converts into acetate. Acetogens utilize the CO and yields acetate, energy, cell material and CO_2. The stoichiometry reaction of CO utilization is given by [50] is:

$$6.8CO \rightarrow CH_3COOH + 3.5CO_2 + 0.4biomassC + 0.9unrecoveredC \qquad \text{(R3-1)}$$

This unrecovered C is further splitting into acetate, CO_2, for simplicity. The above reaction R3-1 is based on a carbon basis. This equation can be converted into mole and gCOD.g^{-1} by following steps of calculation:

$$6.8CO \rightarrow 1.15CH_3COOH + 4.1CO_2 + 0.4biomassC \qquad \text{(R3-2)}$$

The reaction R3-2 is the final equation after splitting of unrecovered C. this equation is further converted into mole basis.

$$6.8CO \rightarrow 1.15CH_3COOH + 4.1CO_2 + 0.08biomass \qquad \text{(R3-4)}$$

The equation R3-4 is on mole basis where 0.08-mole biomass is obtained by dividing 0.4 with 5. The equation is further reduced to gram basis by multiplying with molecular weight.

$$6.8*28\frac{g}{mole}CO \rightarrow 1.15*60\frac{g}{mole}CH_3COOH + 4.1*44\frac{g}{mole}CO_2 + 0.08biomass \quad \text{(R3-5)}$$

Further to convert the above equation into gCOD.g^{-1}, The COD values are taken from "Advanced course in environmental biotechnology, TU Delft". The different value for a different compound is shown in Table 5.

Table 3-3: Mass and COD value of chemical compounds.

Compound name	Mass of compound (g.mole^{-1})	COD-value per mass of compound (gCOD.g^{-1})	Reference
CO	28	0.5714	[62]
Acetate	60	1.0667	
CO_2	44	0	

For biomass, 160 gCOD.mole^{-1} is used for calculation[2].

Now after calculation, the final equation in gCOD.g^{-1} is

$$108.8CO \rightarrow 73.6CH_3COOH + 0CO_2 + 12.8biomass \quad \text{(R3-6)}$$

Now biomass yield per mole of CO is achieved by:

$$= \frac{12,8}{108,8} = 0,12\,\text{gCODbiomass.g}^{-1}\,\text{CODCO}$$

The relation between maximum uptake rate of substrate (k_m) and maximum specific growth rate (μ_m) per day of organism is:

$$k_m = \frac{\mu_m}{Y}$$

Where Y is a yield of biomass and μ_m of the organism can be calculated from doubling times under growth condition[63].

μ_m = ln2/doubling times

The reported doubling times for acetogenesis bacteria which shows the fastest growth on CO is 0. 125^{-1} day· [50]

So,

$$\mu_m = \frac{\ln 2}{0,125} = 5.54$$

Now,

$$k_m = \frac{5.54}{0{,}12} = 46.20$$

So from the calculation, km_co_ac is equal to 46.20 and Y_co_ac is equal to 0.12 is used in the model.

3.2.4 Simulated reactor operation

This is a file provided by Batchstone, which includes both experimental work and simulated work. The volume of reactor used is 28 m^3. The feed load is shown in figure 3.3. The load of feed is increased at steps, after day16 and day37. The increment in the load balance the H_2/CO_2 ratio and increase the reactor's performance.

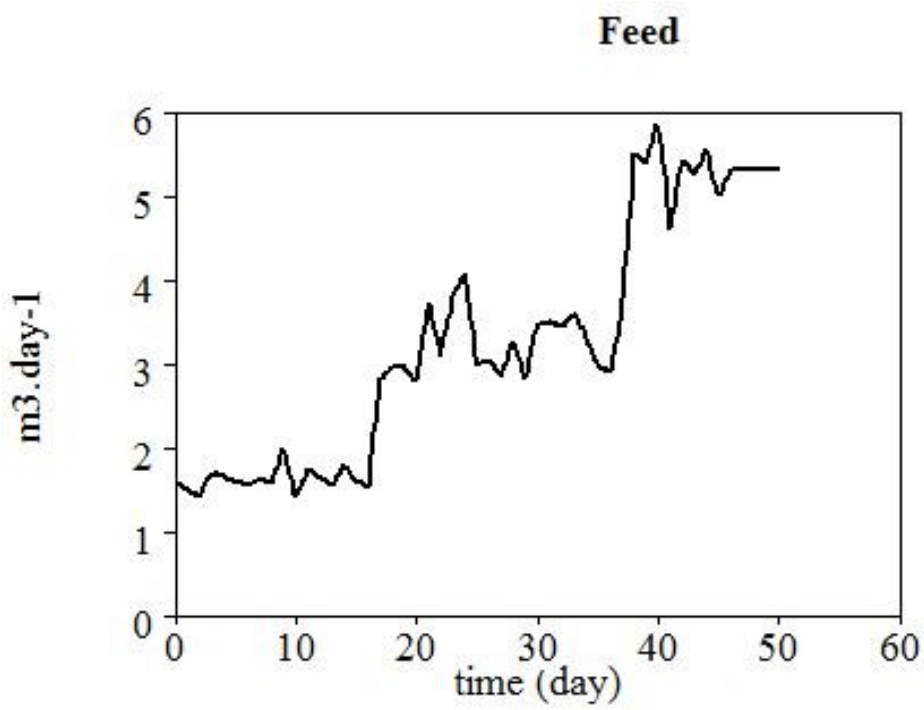

Figure 3-3: Feed to the reactor.

4 Results

Experimental results and simulation results are described in this chapter.

4.1 Experimental results

The experiment work was conducted for 50 days. The main aim of this experiment is to observe the syngas component effect on AD process. To achieve this goal, the biogas production rate from reactor A (with hydrogen addition) and reactor B (without hydrogen) is monitored. The results from the 50-day experiment are presented from figure 4.1 to 4.8.

The test was carried out at room temperature at the beginning, and the temperature was increased slowly and reached to the mesophilic range. So during temperature increase biogas production was not monitored therefore only after day 30 the result is published. Figure 4.1 and figure 4.2 is the biogas production rate and methane production rate after day 30 under mesophilic condition. RA represent the produced biogas from reactor A, and RB is from reactor B. from the figure it is clear that the addition of hydrogen doesn't show any difference between two reactors. Both RA and RB produce in equal amount. Biogas composition (CH_4 and CO_2) % is presented in figure 4.3 and 4.4 respectively. Both reactors show same performance.

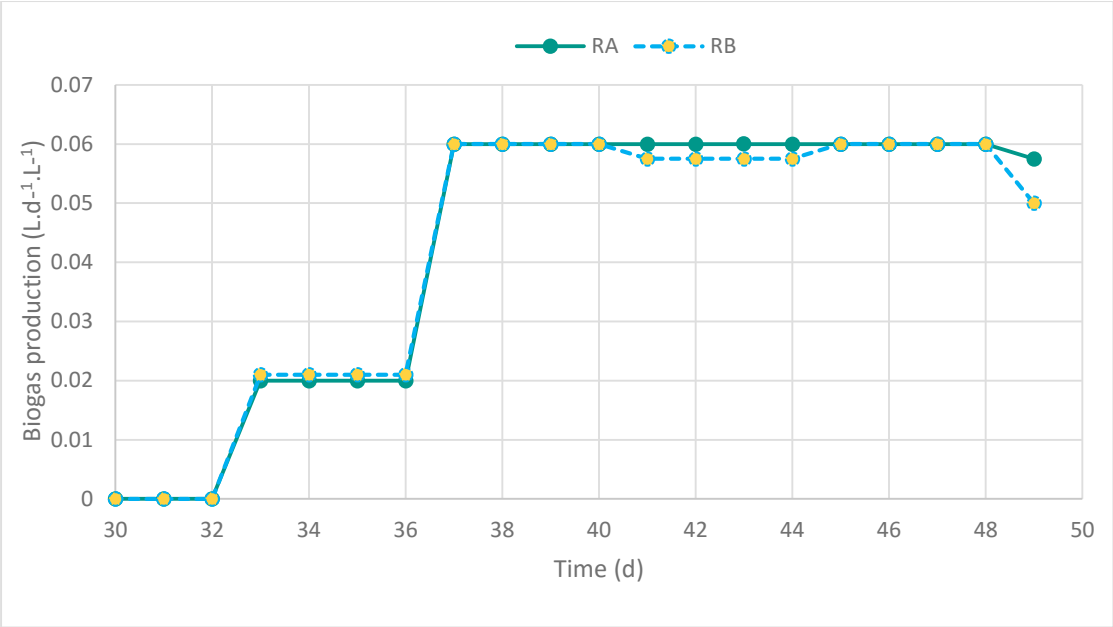

Figure 4-1: Biogas production rate in 50 experimental days of both reactors RA and RB.

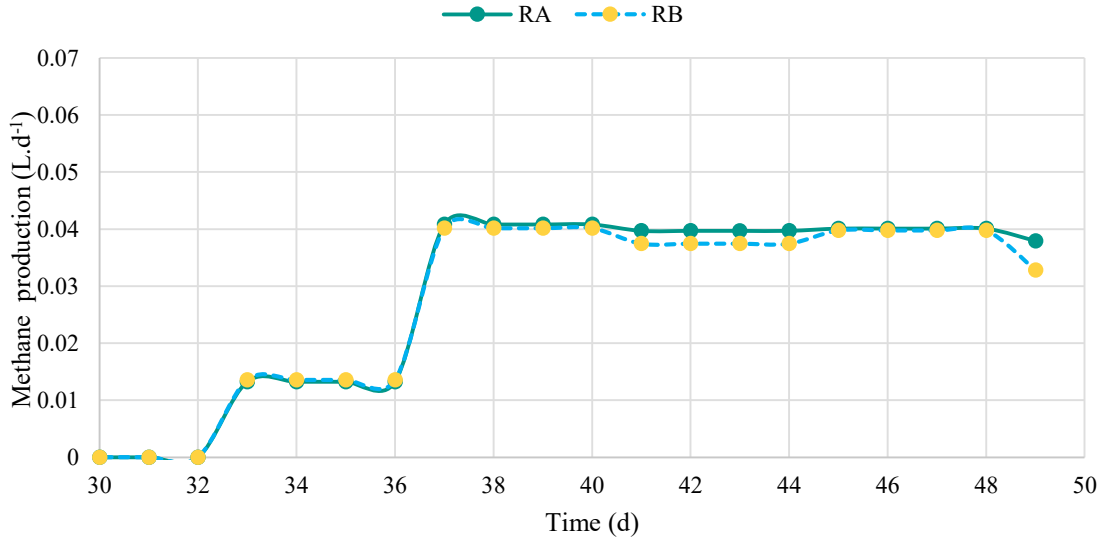

Figure 4-2: Biogas production rate in 50 experimental days of both reactors RA and RB.

.

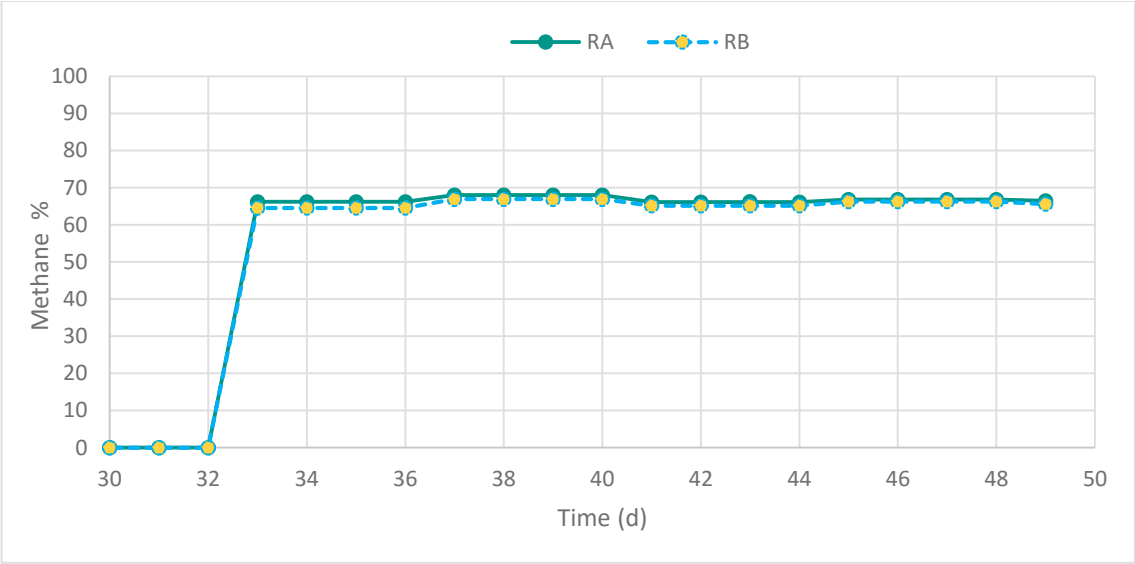

Figure 4-3: percentage of methane in 50 experimental days of both reactors RA and RB.

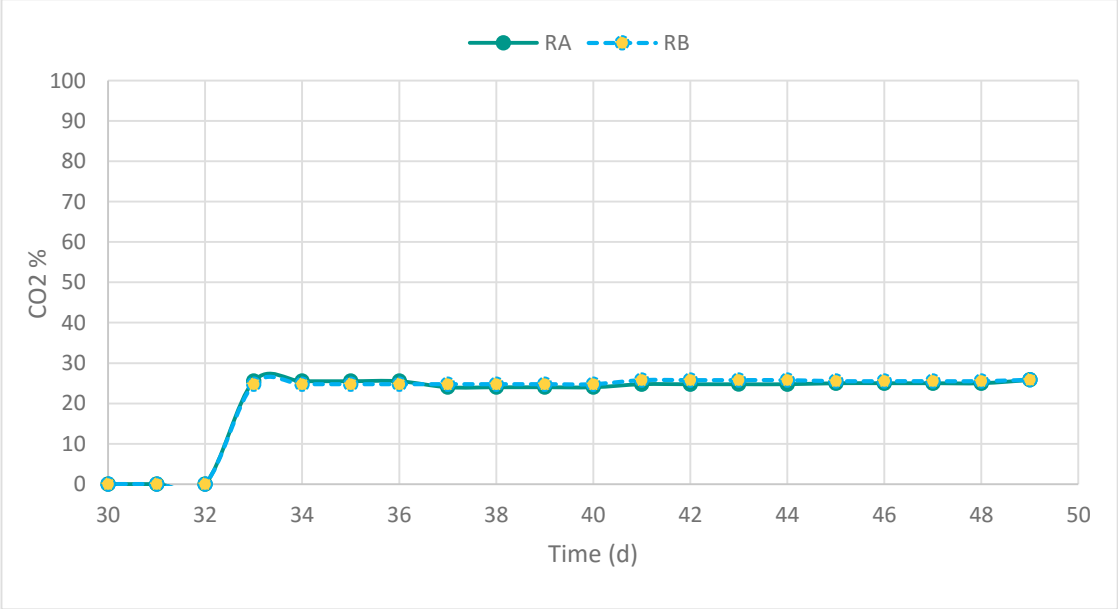

Figure 4-4: percentage of CO_2 in 50 experimental days of both reactors RA and RB.

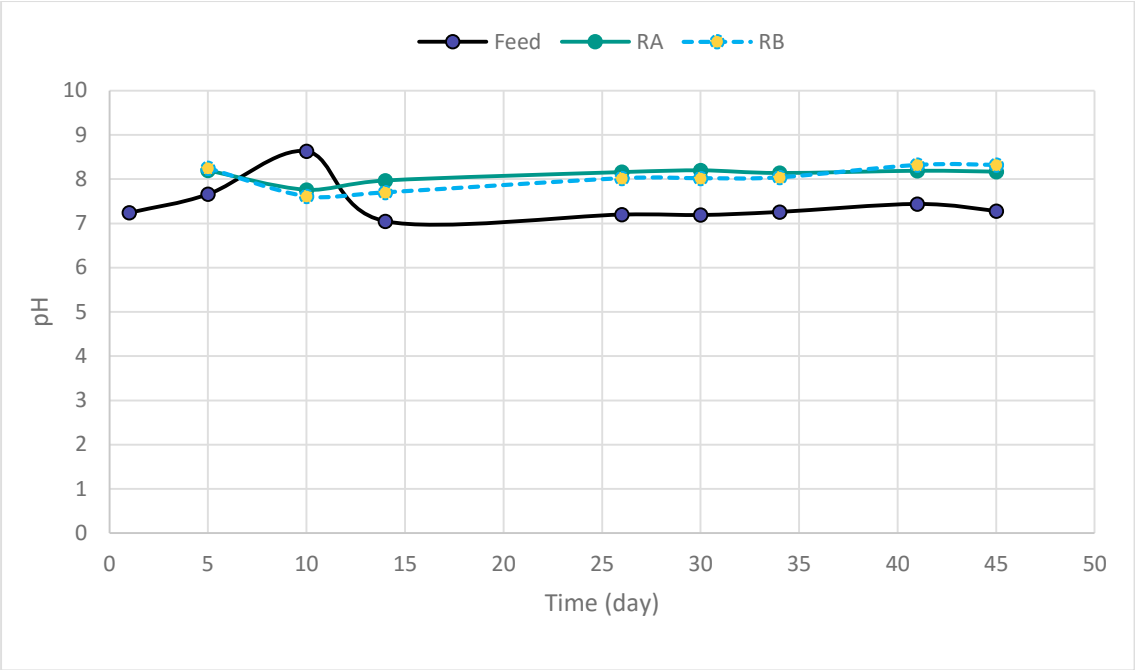

Figure 4-5: the pH value of bulk liquid of feed and effluent of RA and RB.

Figure 4.5 shows that the pH from both reactors is constant throughout the experiment.

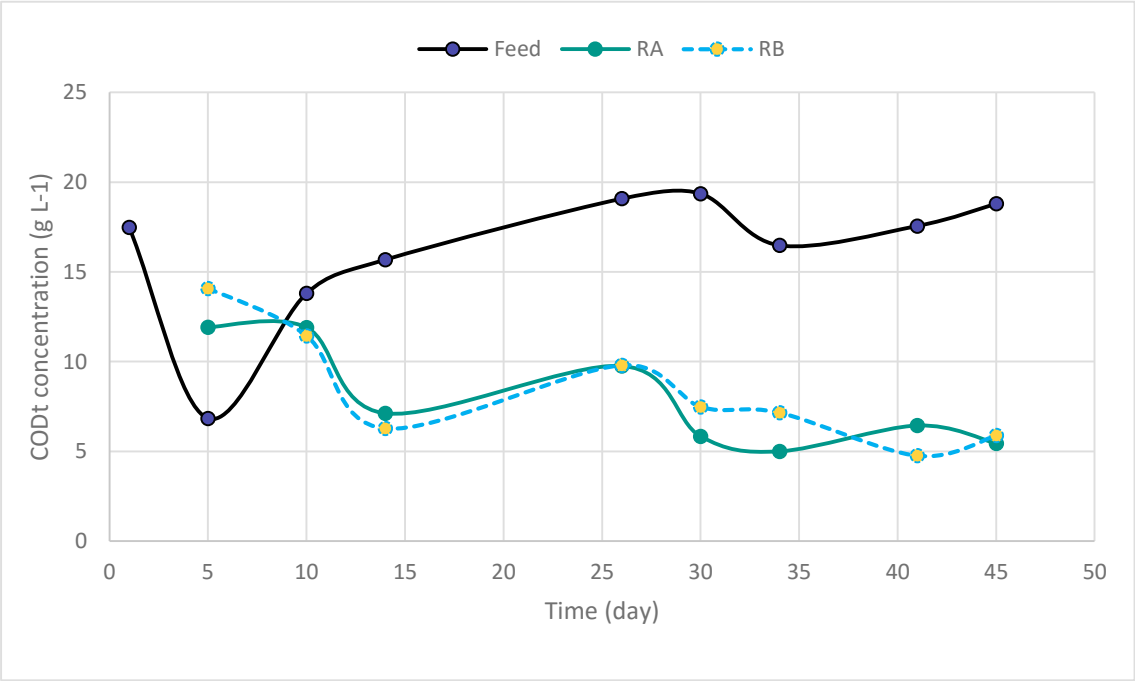

Figure 4-6: Total COD of combined feed and effluent of both reactors RA and RB respectively.

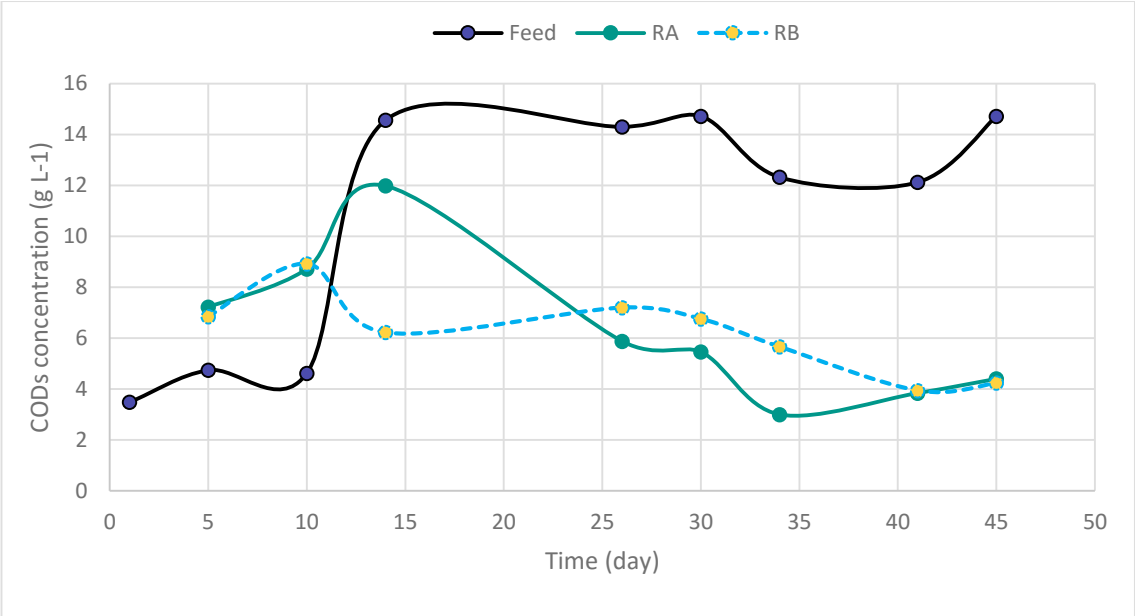

Figure 4-7: soluble COD of combined feed and effluent of both reactors RA and RB respectively.

Figure 4.6 and figure 4.7 represents the total COD and soluble COD concentration. Both the total COD and soluble COD of feed is increases with time while COD of RA and RB decreases with respect to time.

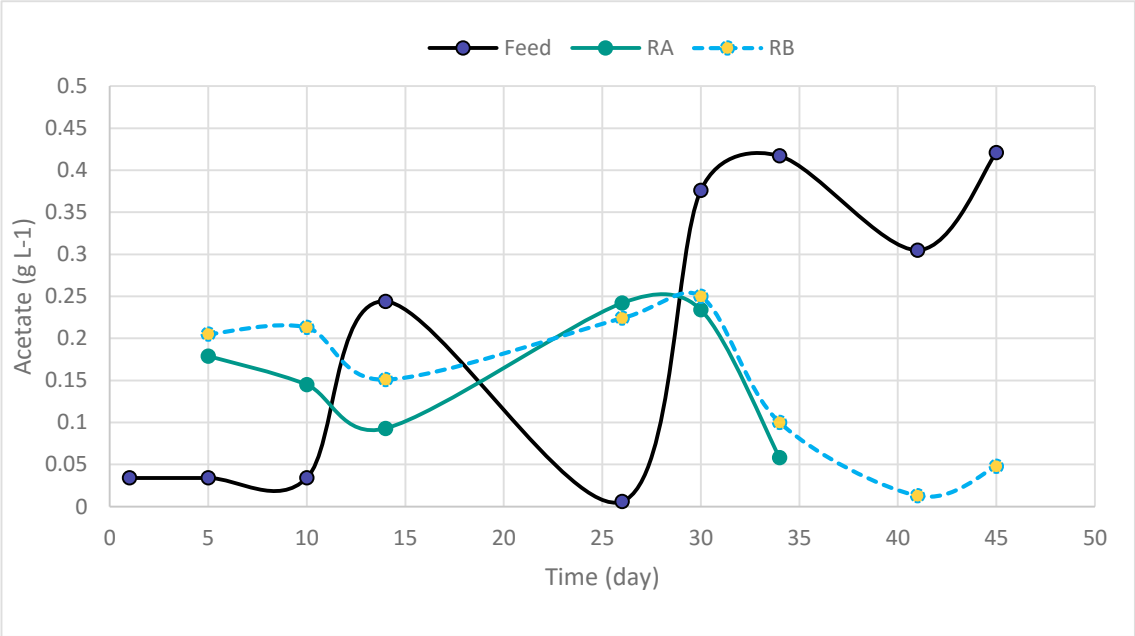

Figure 4-8: Acetate concentration of feed and effluent of both reactors, RA and RB respectively.

Figure 4.8 is the acetate consumption rate of both reactors. Both RA and RB shows value in the almost similar range.

4.1.1 Limitation on H_2 load for the reactor A

This shows how much H_2 is added to the reactor for not to get the failure of AD process. This can be described by the ratio load of H_2 to the reactor and load of feed.

20 ml of hydrogen was added per day to the reactor A.

$$Load\ of\ H_2 = 20\frac{ml\ H_2}{day} = \frac{20}{1000}\frac{L\ H_2}{day} = 0.02\frac{L\ H_2}{day}$$

At room temperature, one mole of gas contains 24 litre.

Now,

$$Load\ of\ H_2 = \frac{0.02}{24}\frac{mol\ H_2}{day} = 0.00083\frac{mol\ H_2}{day} = 0.00083 * 2\frac{\text{gram}}{mole.}$$

$$= 0{,}0016\frac{\text{gram}}{day} = 0{,}0016\frac{\text{gram}}{day} * 8\frac{\text{gramCOD}}{gram} = 0.013\frac{\text{gramCOD}}{day}$$

Now,

Load of feed can be calculated as:

200 ml of feed was added to the reactor per week. So,

$$\frac{200\ ml}{7\ day} = 28.5\frac{ml}{day}$$

Now,

$$load\ of\ Feed = 28.5\frac{ml}{day} = 0{,}0285\frac{L}{day} = 0{,}0285\frac{L}{day} * 5.68\frac{gram\ COD}{L}$$

$$= 0{,}16188\frac{gram\ COD}{day}$$

Now,

$$\frac{Load\ of\ H_2}{Load\ of\ Feed} = \frac{0.013}{0{,}16188} = 0.08$$

4.2 Simulation results

Three different compositions of syngas were simulated at three different gas-liquid mass transfer rates (kLa) in AQUASIM software. The gas input to the membrane is maintained at 25m^3day^{-1}.Altogether there are ten various cases were simulated. Among them, case 1(original shown in all figures) was the already simulated results by Batchstone while rest 9 cases are simulated and its overview is presented in Table 6.

Table 4-1: an overview of different cases of syngas composition for simulation in AQUASIM.

Run	Syngas composition (%)	Input (m^3day^{-1})	kLa values(day^{-1})
Case 2	Pure H_2 (100%)	25	24
Case 3	Pure H_2 (100%)	25	240
Case 4	Pure H_2 (100%)	25	480
Case 5	86% H_2, 7% CO & 7% CO_2	25	24
Case 6	86% H_2, 7% CO & 7% CO_2	25	240
Case 7	86% H_2, 7% CO & 7% CO_2	25	480
Case 8	44.4% H_2, 33.3% CO & 22.2% CO_2	25	24
Case 9	44.4% H_2, 33.3% CO & 22.2% CO_2	25	240
Case 10	44.4% H_2, 33.3% CO & 22.2% CO_2	25	480

4.2.1 Simulation results with pure hydrogen

The simulated final results with hydrogen at three different kLa values is illustrated in below figures from 4.9 to 4.23.

The simulation results for three different cases are shown in figure 4.9. In this figure, biogas production rate is explained for 50 days of reactor's operation. The black dotted line is the experimental results which are around 47 $m^3.day^{-1}$. The original is a simulation result without hydrogen. Case 2, case 3, and case 4 are the results obtained after addition of hydrogen at three different kLa values. At the beginning, all three cases produce biogas between ranges of (15-20) $m^3.day^{-1}$.

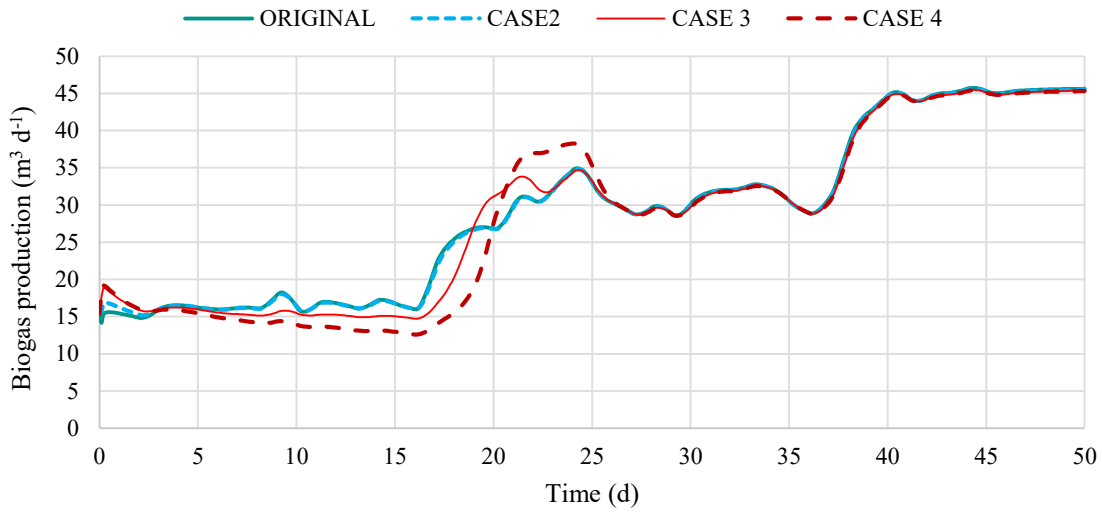

Figure 4-9: Biogas production at various kLa with pure hydrogen. Case 2(kLa 24), Case 3(kLa 240) and Case 4(kLa 480).

After 16 days, biogas production rate is rapid and reaches 37 $m^3.day^{-1}$. And finally, it shows the similar trend up to 35 days and again after that production rate increases and reaches above 45 $m^3.day^{-1}$. From figure (4.9), it is clear that all three cases including original produce biogas almost in similar range. Between (20-25) days, case 4 production rate is quite higher than the other cases.

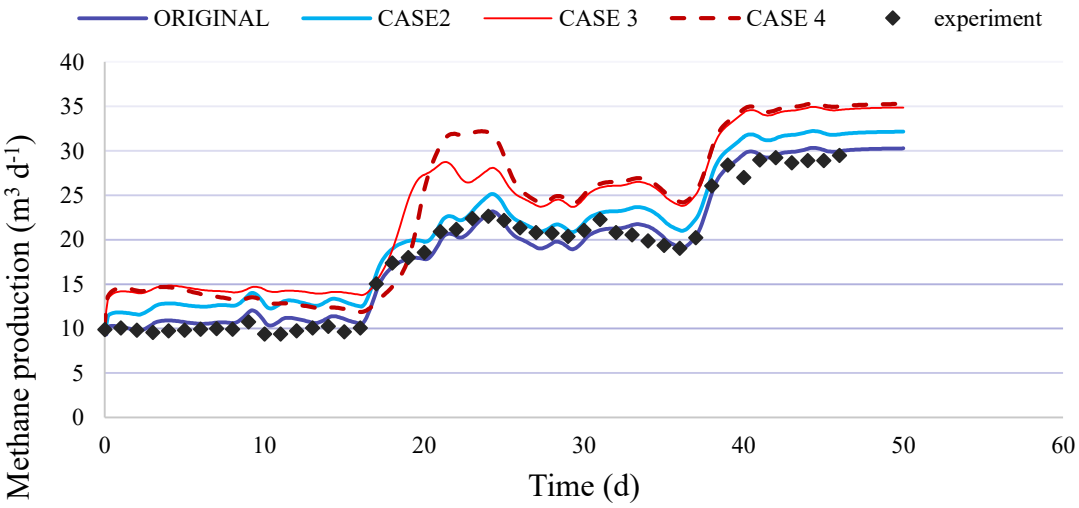

Figure 4-10: Methane gas production rate at different kLa with pure hydrogen. Case 2(kLa 24), Case 3(kLa 240) and Case 4(kLa 480).

The methane production rate with different kLa values is shown in figure 4.10. The impact of kLa is clearly illustrated for various cases in above figure. Methane production rate increases with increasing kLa values. Case 4 produces more methane per day followed by case 3 and case 2.

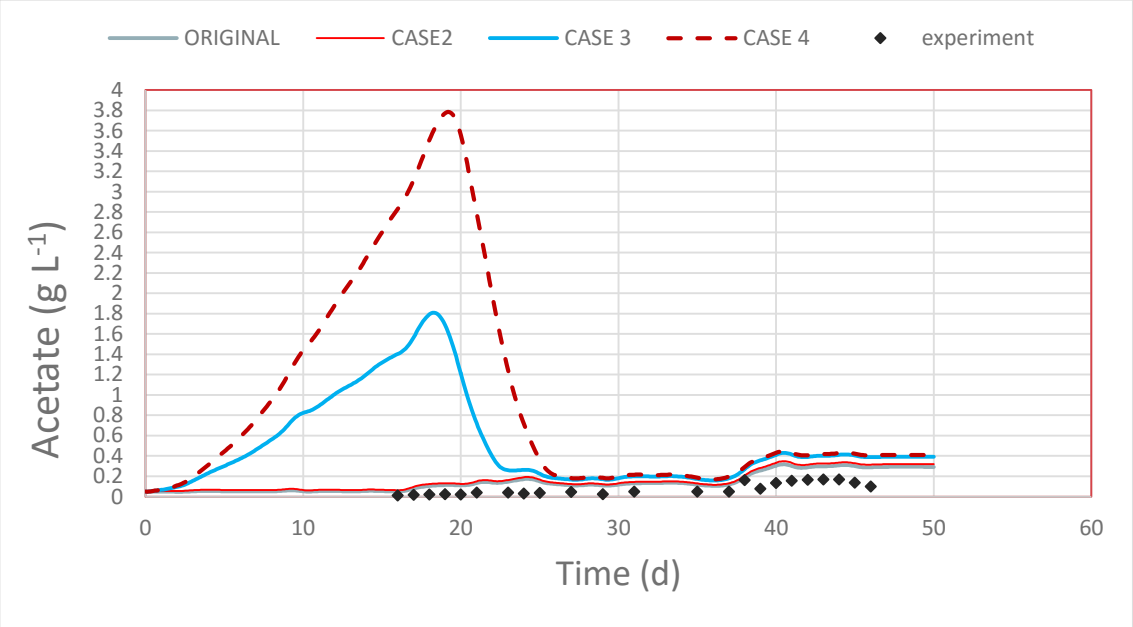

Figure 4-11: Acetate consumption rate for pure hydrogen with different kLa. Case 2(kLa 24), Case 3(kLa 240) and Case 4(kLa 480).

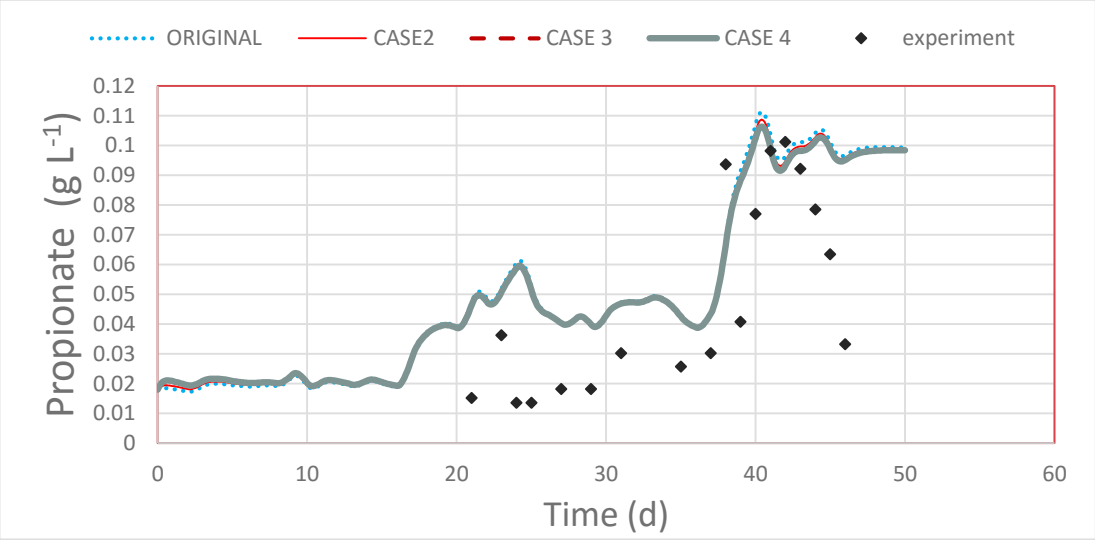

Figure 4-12: Propionate consumption rate with pure hydrogen at different kLa. Case 2(kLa 24), Case 3(kLa 240) and Case 4(kLa 480).

The acetate concentration is very higher at kLa 480 day^{-1} which reach up to 3.8 $g.L^{-1}$ followed by the case 2 at 240 day^{-1} as shown in figure 4.11. At low kLa values, case 1 shows the same trend as original and almost very near with the experimental concentration.

Figure 4.12 represents the propionate consumption rate in the reactor. For each case, the concentration is similar to original value as shown in above figure.

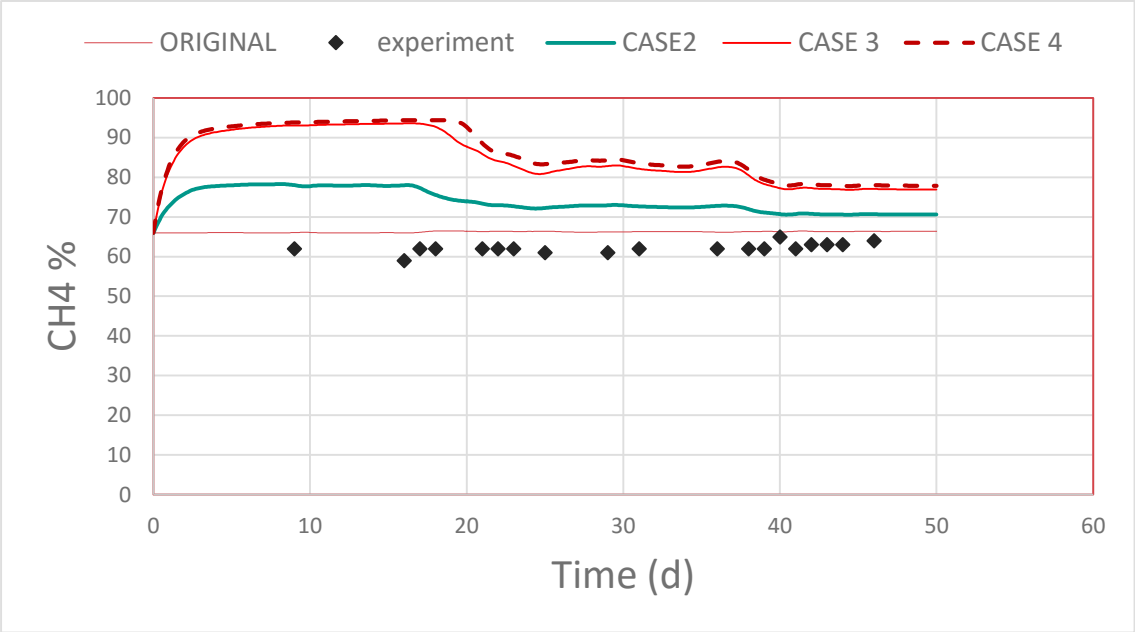

Figure 4-13: percentage of methane in headspace at different kLa. Case 2(kLa 24), Case 3(kLa 240) and Case 4(kLa 480).

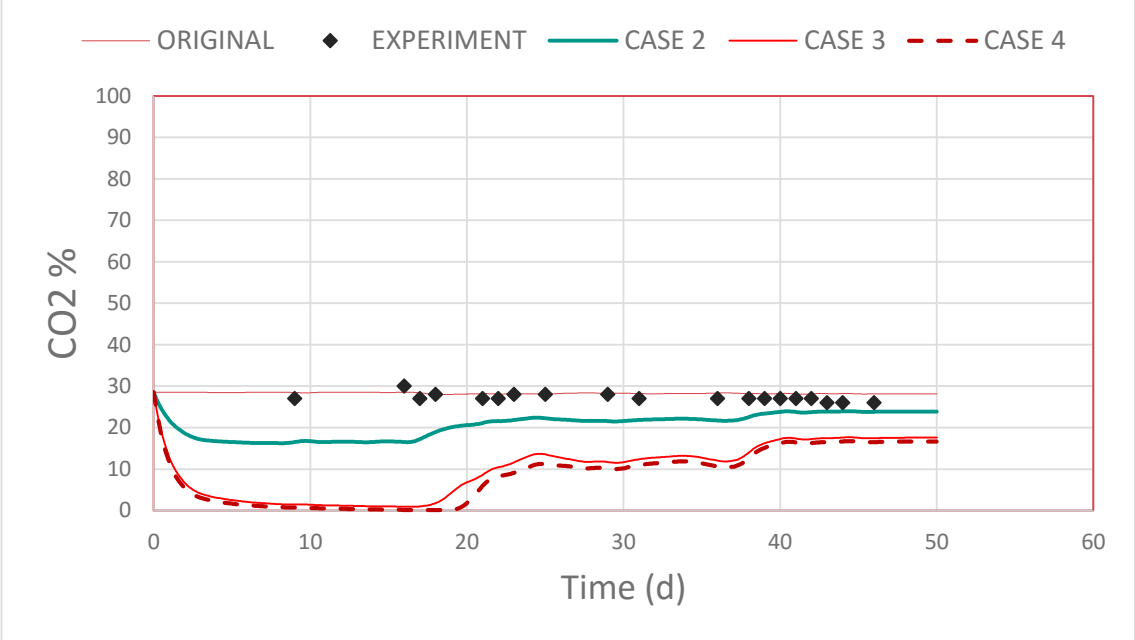

Figure 4-14: percentage of CO_2 in headspace at different kLa. Case 2(kLa 24), Case 3(kLa 240) and Case 4(kLa 480).

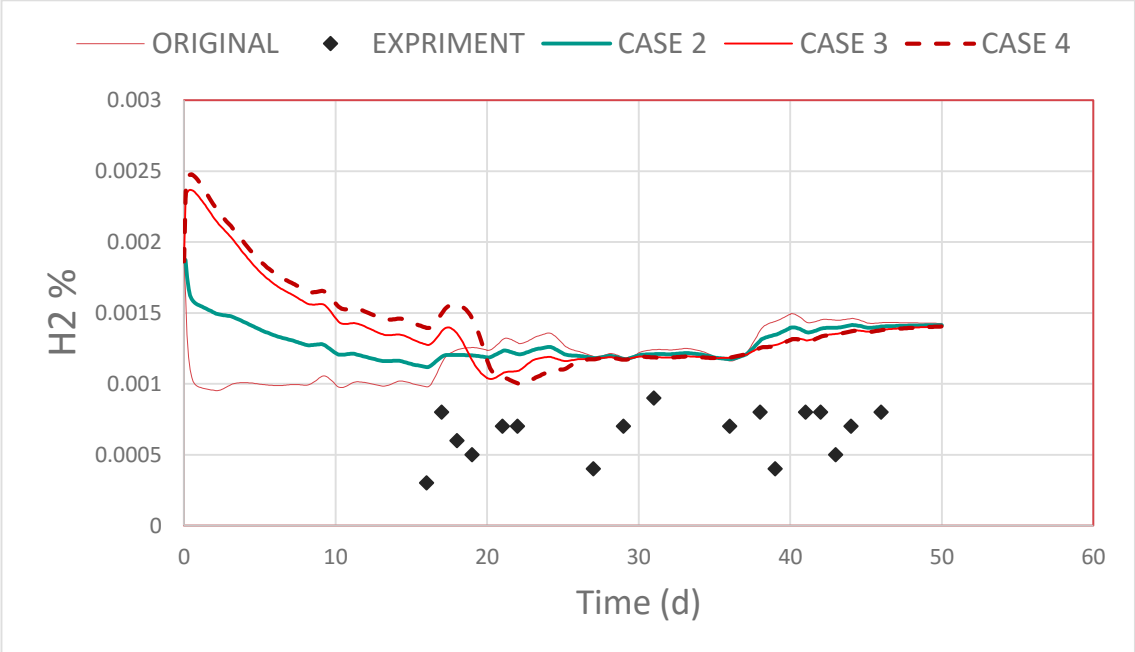

Figure 4-15: percentage of hydrogen in headspace at different kLa. Case 2(kLa 24), Case 3(kLa 240) and Case 4(kLa 480).

Figure 4.13 shows the detected percentage of methane in produced biogas. First, 20 days the methane concentration is high and at kLa value of 480 it reaches around 94 %. After 20 days it starts to decrease and follow the usual trend. This figure clearly tells that the addition of hydrogen enhances the methane concentration. The percentage of methane in reactor's headspace is increasing with increase in kLa which means diffusion of hydrogen through the membrane is better with higher kLa values as shown in figure 4.13. Case 4 shows a higher percentage than case 3 and followed by case 2.

On the other hand, carbon dioxide (CO_2) concentration detected followed the similar behaviour but in opposite way as present in figure 4.14. With the increment in kLa values, the CO_2 decreases. The percentage of CO_2 drops more in case 4 which is then followed by case 3 and case 2 respectively.

The percentage of hydrogen in biogas composition is illustrated in figure 4.15. The hydrogen is higher up to day16 but after day16 its concentration starts to decrease. Again case 4 reflects higher percentage than case 3 followed by case 2.

Figure 4.16 represents the pH value inside the reactor. The pH values of the original simulation are similar to the experimental values which are between 7-7.5. However, the addition of hydrogen causes a rise in pH. Case 4 and case 3 represents higher diffusion rate of hydrogen into the reactor. The pH of the bulk liquid inside reactor becomes higher with high kLa values and reaches the maximum level of pH above 8.5 as shown in figure 4.16. First, 16 days pH increases in a rapid way up to 8.7 and after that, it falls back quickly and stabilises to normal pH values. Also from the figure it is clear that case 4 reaches at maximum than case 3 followed by case 2.

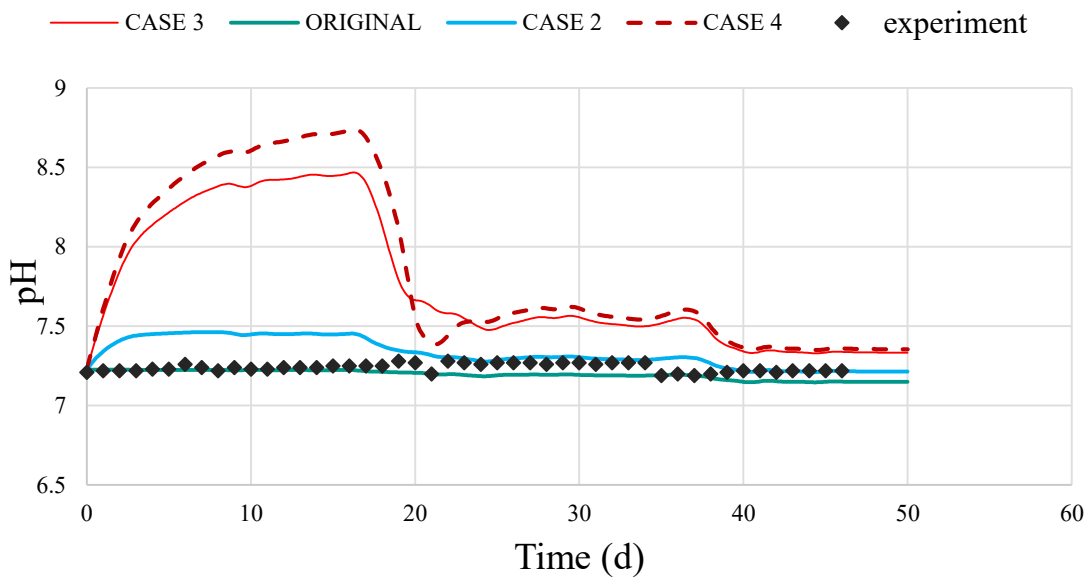

Figure 4-16: pH of bulk reactor volume with pure hydrogen at different kLa. Case 2(kLa 24), Case 3(kLa 240) and Case 4(kLa 480).

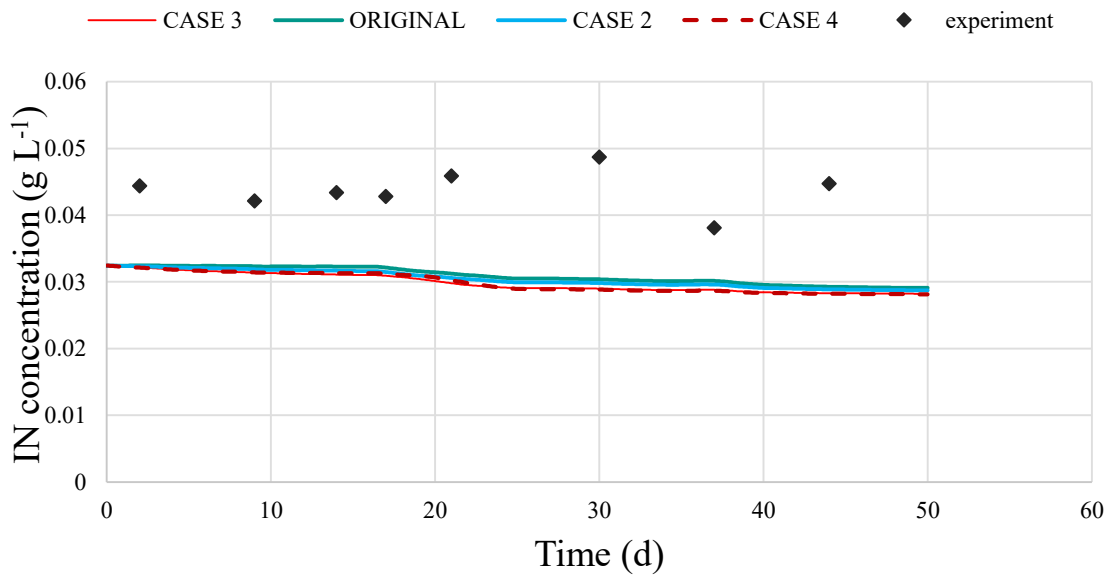

Figure 4-17: Total nitrogen concentration for three different cases with pure hydrogen. Case 2(kLa 24), Case 3(kLa 240) and Case 4(kLa 480).

The total nitrogen concentration is almost equal to the original values which are in the range between (0.02-0.03) g.L-1 as shown in figure 4.17. The graph also tells us that nitrogen concentration inside the reactor does not change much with the addition of hydrogen.

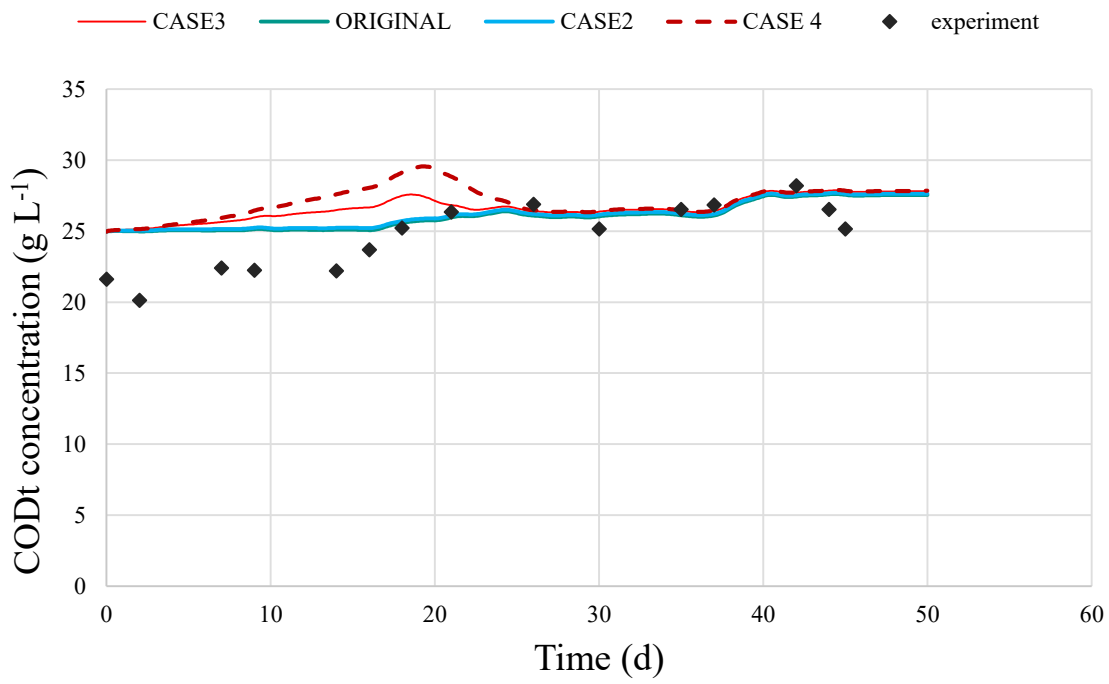

Figure 4-18: Total COD for a different case with pure hydrogen. Case 2(kLa 24), Case 3(kLa 240) and Case 4(kLa 480).

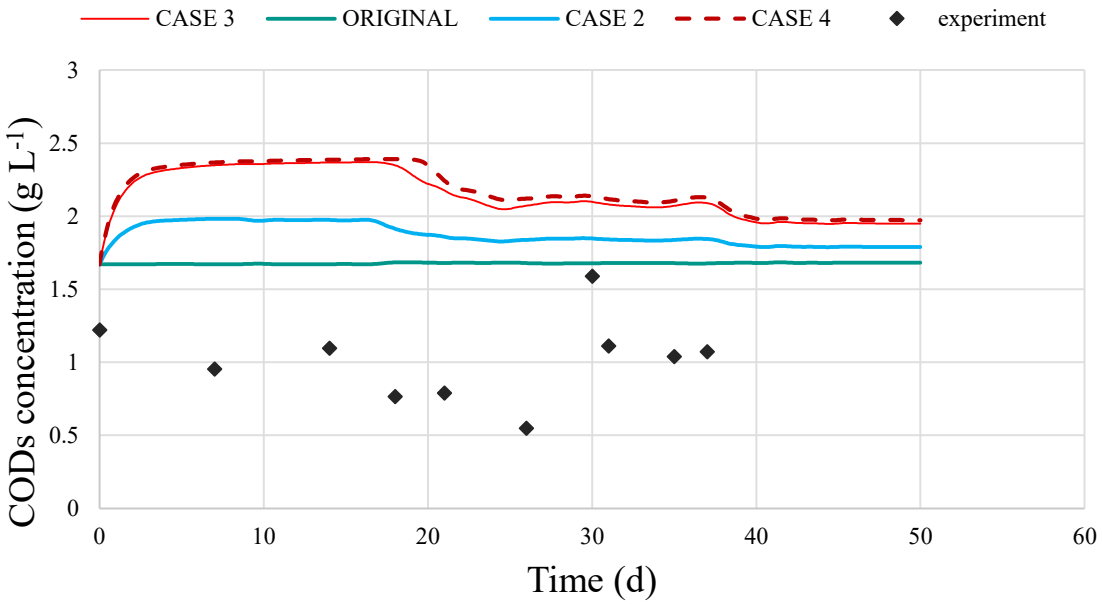

Figure 4-19: soluble COD for a different case with pure hydrogen. Case 2(kLa 24), Case 3(kLa 240) and Case 4(kLa 480).

Figure 4.18 and figure 4.19 shows the total COD concentration and soluble Cod concentration for the different case including original simulation results. With the addition of hydrogen to the reactor, total COD doesn't change much while soluble COD reflects the precise impact of hydrogen addition. Soluble COD has significant increase with higher kLa values. Case 4 and case 3 increases up to 2.4 $g.L^{-1}$ and follow the same trend for about day20.

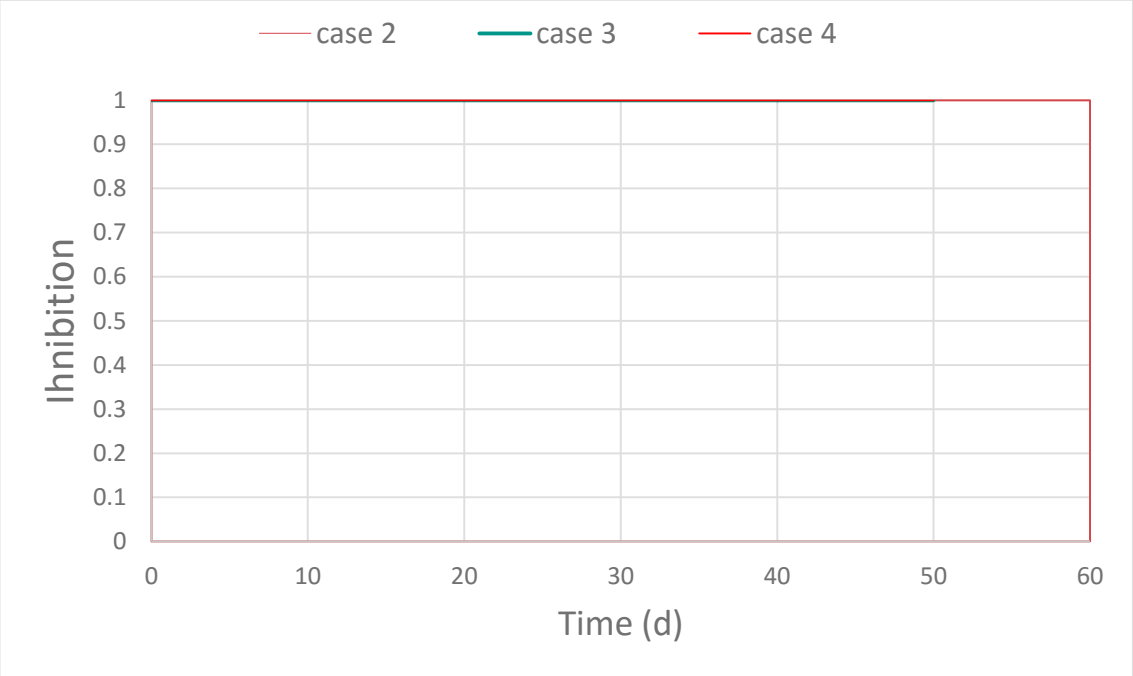

Figure 4-20: Inhibition of pH_ac for different kLa. Case 2(kLa 24), Case 3(kLa 240) and Case 4(kLa 480).

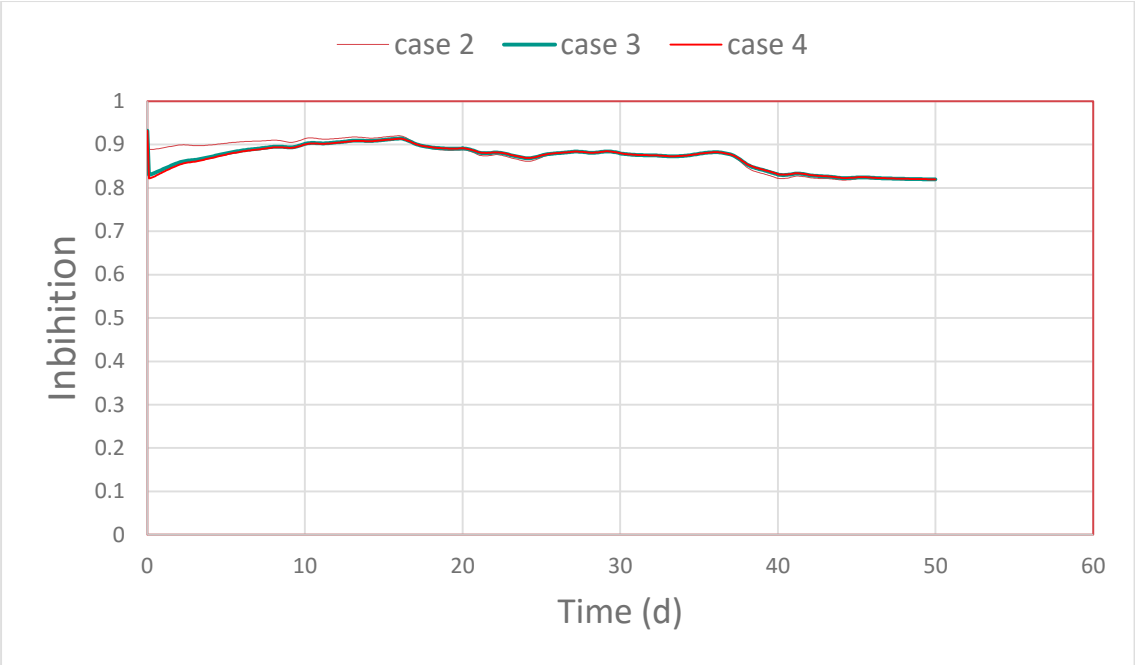

Figure 4-21: Inhibition of h2_co_ac for different kLa. Case 2(kLa 24), Case 3(kLa 240) and Case 4(kLa 480).

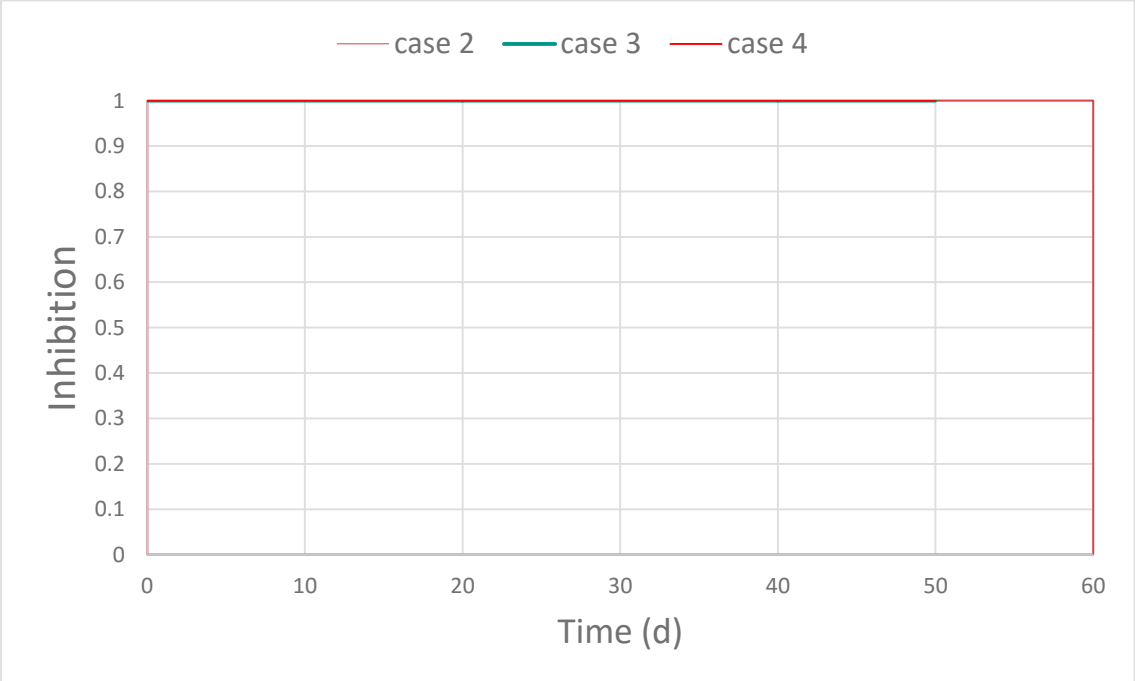

Figure 4-22: Inhibition of pH_co_ac for different kLa. Case 2(kLa 24), Case 3(kLa 240) and Case 4(kLa 480).

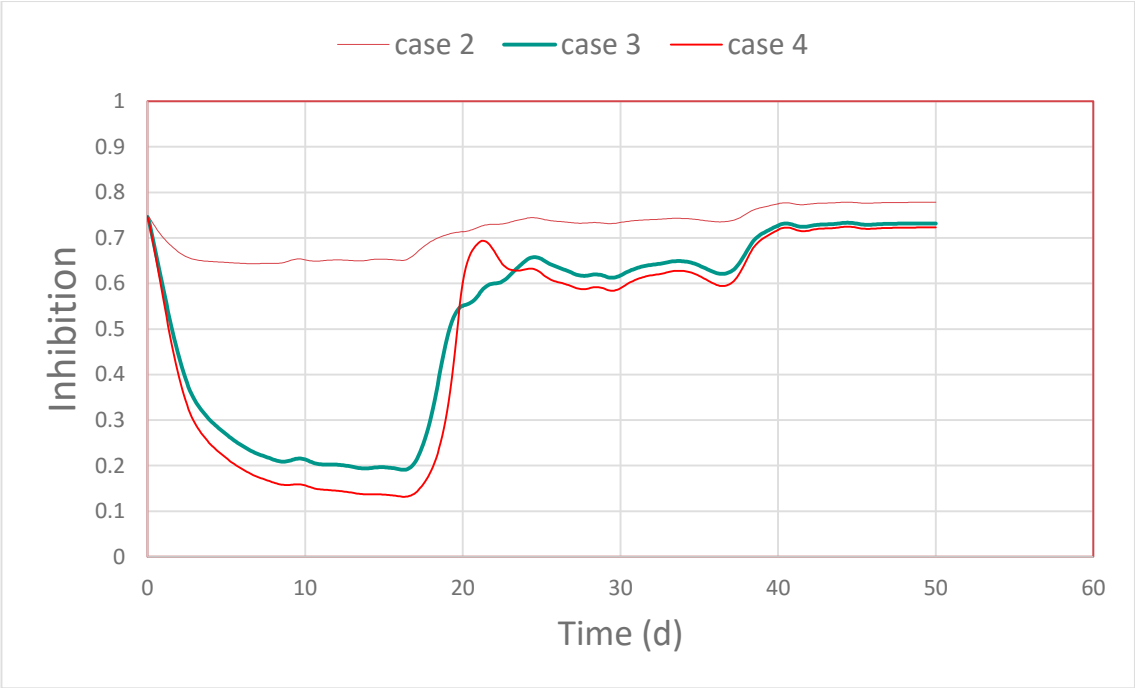

Figure 4-23: Inhibition of NH_3_ac for different kLa. Case 2(kLa 24), Case 3(kLa 240) and Case 4(kLa 480).

From figure 4.20 to figure 4.23 shows the inhibition of methane production inside the reactor. The addition of hydrogen shows some inhibition. In all case, the value of inhibition is either 1 or less than 1.

4.2.1.1 Limitation on H_2 load

This shows how much H_2 is added to the reactor for not to get the failure of AD process. This can be described by the ratio load of H_2 to the reactor and load of feed.

$$\frac{Load\ of\ H_2}{Load\ of\ Feed}$$

This ratio provides the border line which the reactor can handle.

Load of feed calculation:

A load of feed is the input which includes amino acid, fatty acid, sugar and composite organic material (such as dead biomass). The unit of feed is Kg COD.m^{-3}. All the input with values is given in Table 7.

Table 4-2: an input for a load of feed calculation with values.

Input	Values(Kg COD.m^{-3})
input_S_aa_in	4.2
input_S_fa_in	6.3
input_S_su_in	2.8
input_X_c_in	10
Total	23.3

Now for calculation of feed the values, 16 days of input_Qin_dyn is taken, and total values of feed multiply an average of this.

Table 4-3: Values of input_Qin_dyn for 16 days and its average for feed calculation.

No. of days	Values (m^3.day^{-1})
0	1.59
1	1.49
2	1.41
3	1.69
4	1.66
5	1.58
6	1.56
7	1.62
8	1.57
9	1.99
10	1.38
11	1.75
12	1.64
13	1.54
14	1.79
15	1.6
16	1.52
Average	1.61

So,

$$Feed = 23{,}3\frac{\text{Kg COD}}{m^3} * 1{,}61\frac{m^3}{day} = 37{,}5\frac{\text{Kg COD}}{day}$$

A load of hydrogen can be calculated from the figure 5.1.

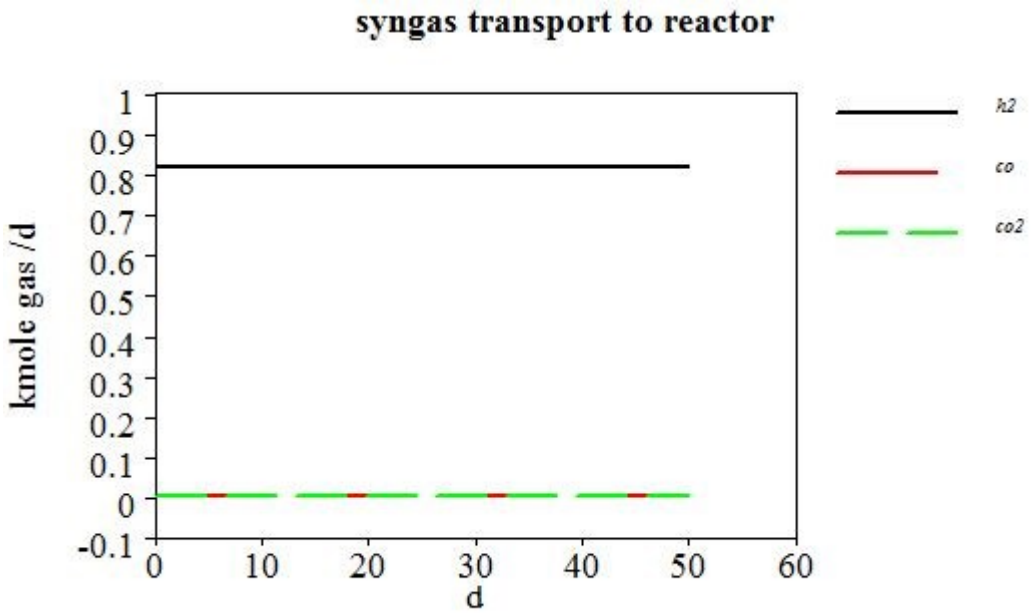

Figure 4-24: Amount of hydrogen diffuses to the reactor at kLa values 240 day^{-1}.

Now from figure 5.1, hydrogen gas transported into the reactor at kLa values 240 day^{-1} is 0.82 kmole.day^{-1}.

$$Load\ of\ H_2 = 0.82\frac{\text{Kmole}}{day} = 820\frac{\text{mole}}{day} = 820 * 2\frac{\text{gram}}{mole.} = 1640\frac{\text{gram}}{day}$$

$$= 1640\frac{\text{gram}}{day} * 8\frac{\text{gramCOD}}{gram} = 13120\frac{\text{gramCOD}}{day} = 13.12\frac{\text{KgCOD}}{day}$$

Now at kLa values of 240 day^{-1}, load to feed ratio is:

$$\frac{Load\ of\ H_2}{Load\ of\ Feed} = \frac{13.12}{37.5} = 0.35$$

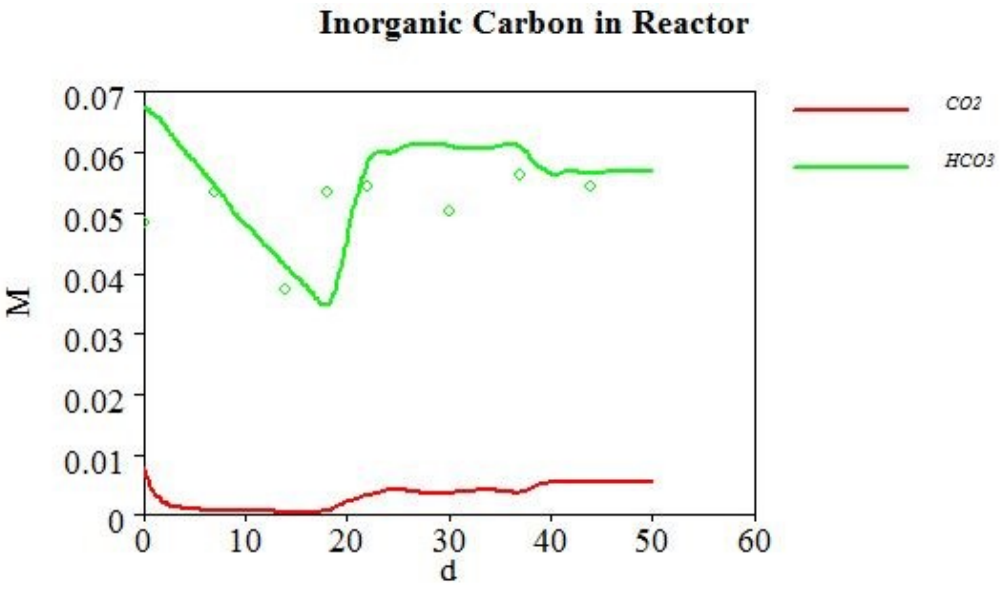

Figure 4-25: Inorganic carbon in the reactor at kLa values 240 day^{-1} for pure H_2.

4.2.2 Simulation results with 86 % H_2, 7 % CO and 7 % CO_2.

The simulated final results with syngas composition of 86 % H_2, 7 % CO and 7 % CO_2 at three different kLa values is illustrated in below figures from 4.26to 4.42.

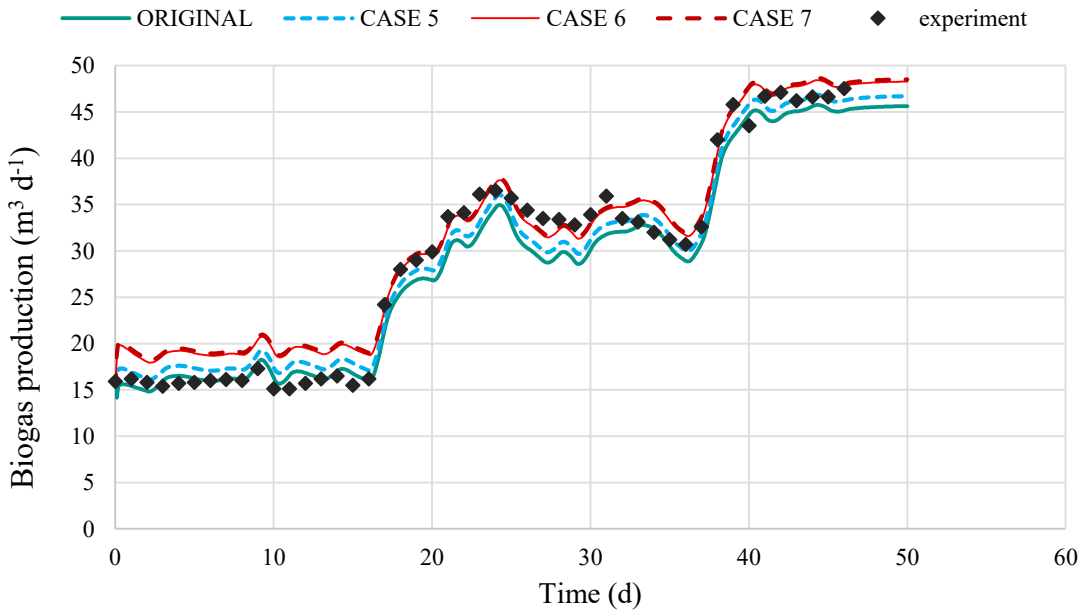

Figure 4-26: Biogas production rate at various kLa with syngas composition of 86 % H_2, 7 % CO and 7 % CO_2.Case 5(kLa 24), Case 6(kLa 240) and Case 7(kLa 480).

The simulation results for cases 5, 6 and 7 with H_2-rich syngas composition are shown in figure 4.26. In this figure, biogas production rate is presented for 50 days of reactor operation. The black dotted line is the experimental results which are around16 $m^3.day^{-1}$in the beginning and reaches to 47 $m^3.day^{-1}$ at the end. The original is a simulation result without syngas. Case 5, case 6, and case 7 are the results obtained after addition of syngas at three different kLa values. In the beginning, all three cases produce biogas between ranges of (15-20) $m^3.day^{-1}$. After day16, biogas production rate is rapid and reaches 37 $m^3.day^{-1}$. And finally, it shows the similar trend up to 35 days and again after that production rate increases and reaches above 45 $m^3.day^{-1}$. From the figure it is clear that case 7 produce more than case 6 followed by case 5.

The methane production rate with different kLa values is shown in figure 4.27. The impact of kLa is clearly illustrated for various cases in the graph. Methane production rate increases with increasing kLa values. Case7 produces around 35 $m^3.day^{-1}$, slightly more than case 6 followed by case 5.

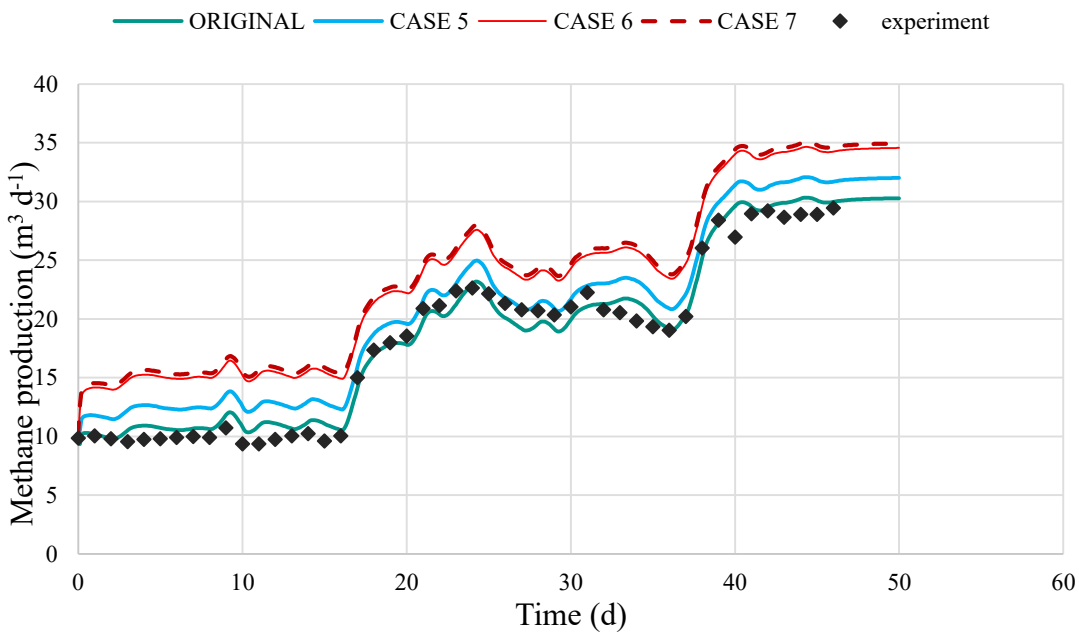

Figure 4-27: methane gas production rate at different kLa with syngas composition of 86 % H_2, 7 % CO and 7 % CO_2. Case 5(kLa 24), Case 6(kLa 240) and Case 7(kLa 480).

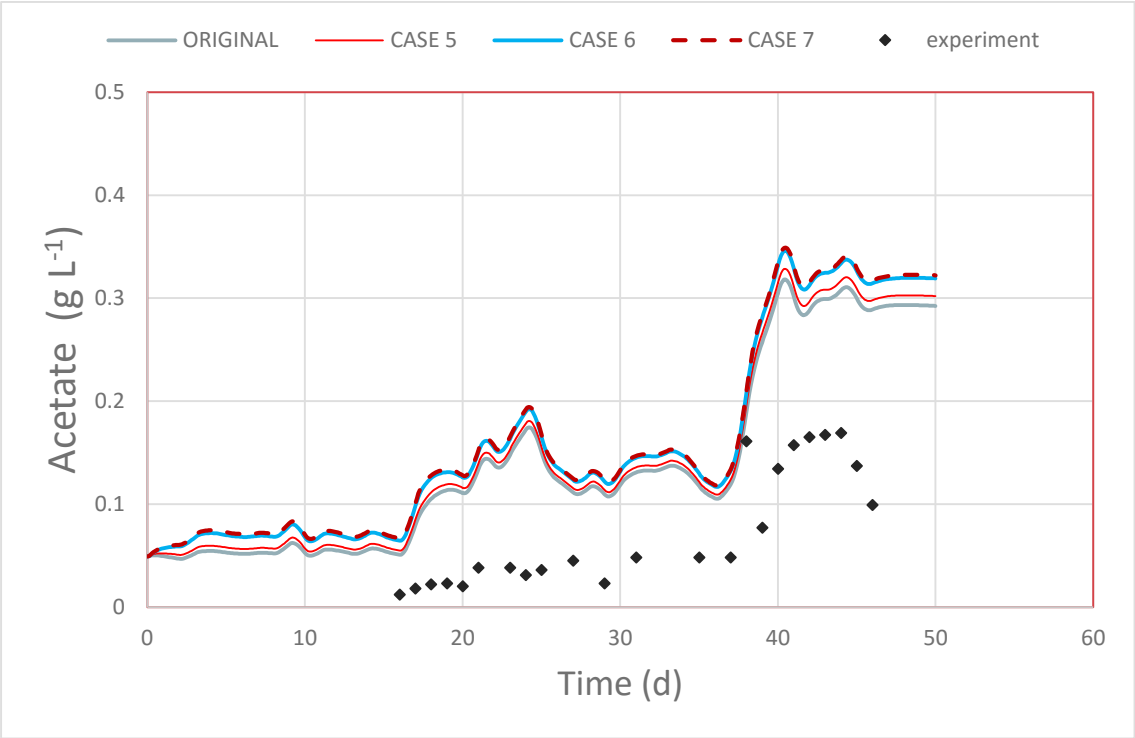

Figure 4-28: Acetate consumption rate at different kLa with syngas composition of 86 % H_2, 7 % CO and 7 % CO_2. Case 5(kLa 24), Case 6(kLa 240) and Case 7(kLa 480).

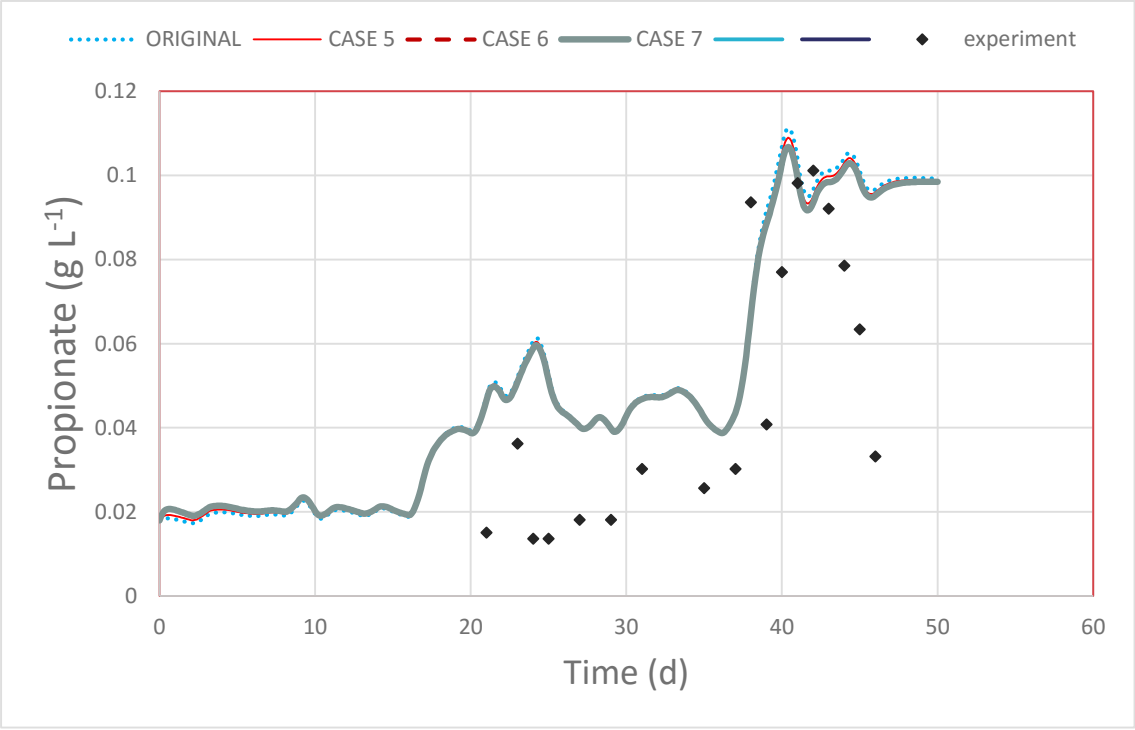

Figure 4-29: propionate consumption rate at different kLa with syngas composition of 86 % H_2, 7 % CO and 7 % CO_2. Case 5(kLa 24), Case 6(kLa 240) and Case 7(kLa 480).

Figure 4.28 and figure 4.29 represents the acetate and propionate consumption rate in the reactor. For each case, the concentration is similar to the original. Case 7 and case 6 shows little higher acetate concentration than case 5 while no any significant changes in propionate concentration.

Figure 4.30 shows the detected percentage of methane in produced biogas. First 16 days, the methane concentration is higher with high kLa value of 480 where it reaches around 81 %. After day16, it starts to decrease and follow the usual trend. This figure clearly tells that the addition of syngas enhances the methane concentration. Case 7 shows a higher percentage than case 6 followed by case 5.

On the other hand, carbon dioxide (CO_2) concentration detected followed the similar behaviour but in opposite way as present in figure 4.31. With the increment in kLa values, the CO_2 decreases. The percentage of CO_2 falls more in case 7 which is more than case 6 and case5 respectively.

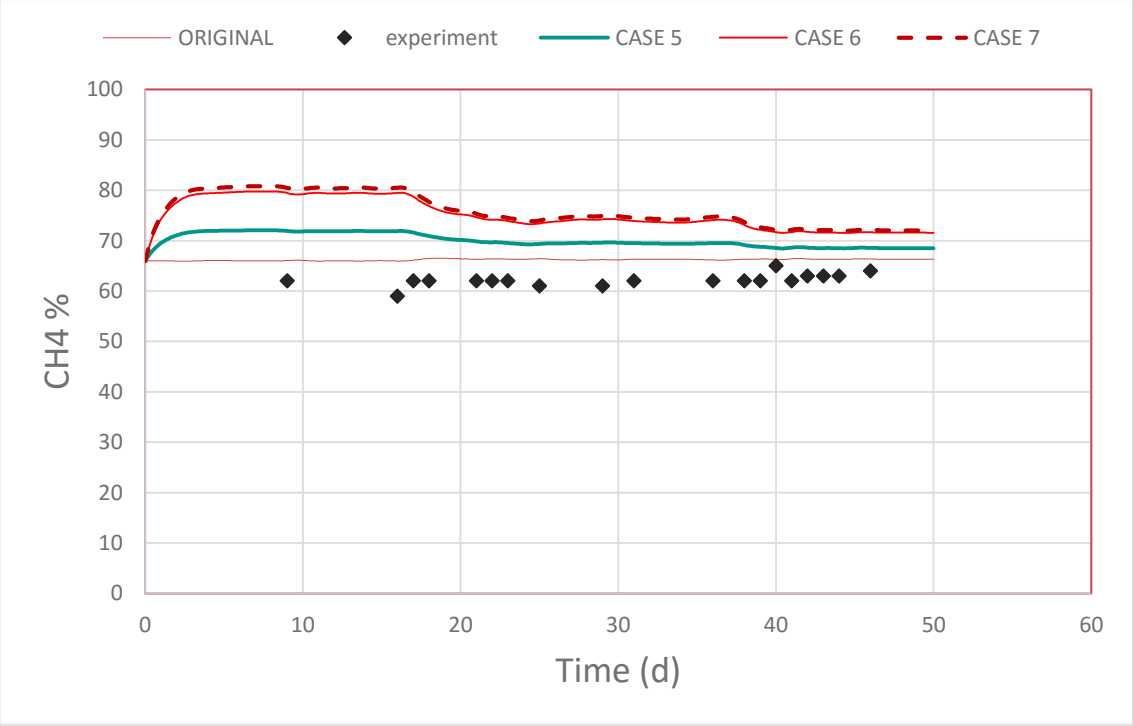

Figure 4-30: percentage of methane in headspace at different kLa with syngas composition of 86 % H_2, 7 % CO and 7 % CO_2. Case 5(kLa 24), Case 6(kLa 240) and Case 7(kLa 480).

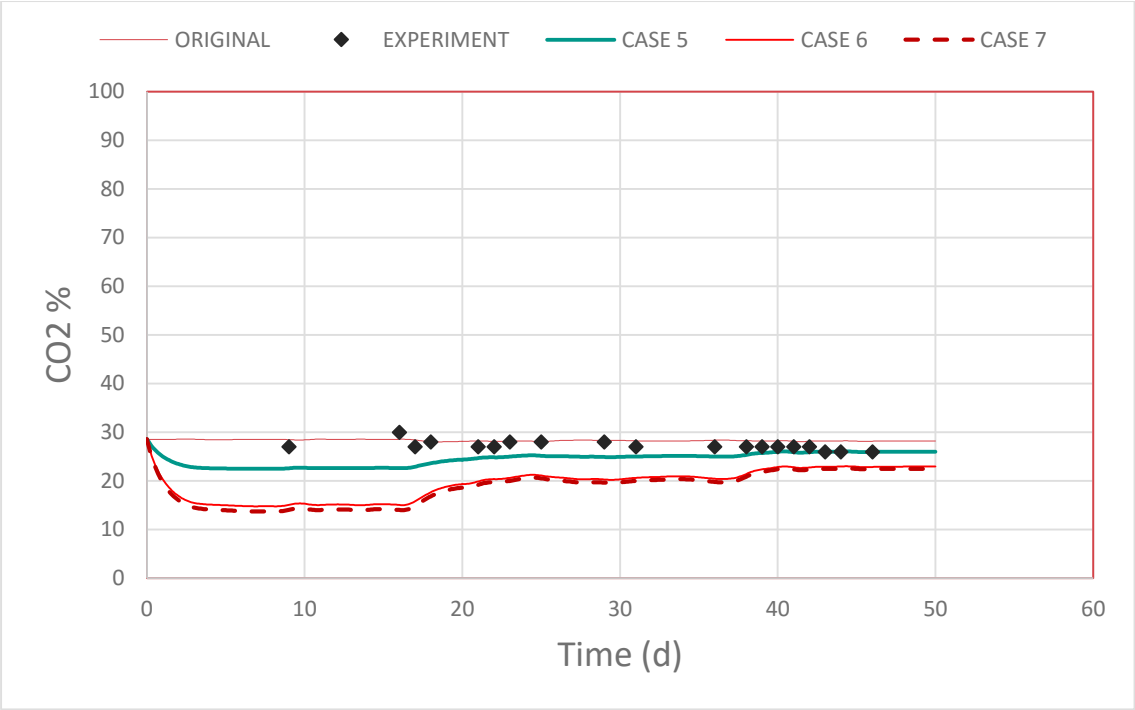

Figure 4-31: percentage of CO_2 in headspace at different kLa with syngas composition of 86 % H_2, 7 % CO and 7 % CO_2. Case 5(kLa 24), Case 6(kLa 240) and Case 7(kLa 480).

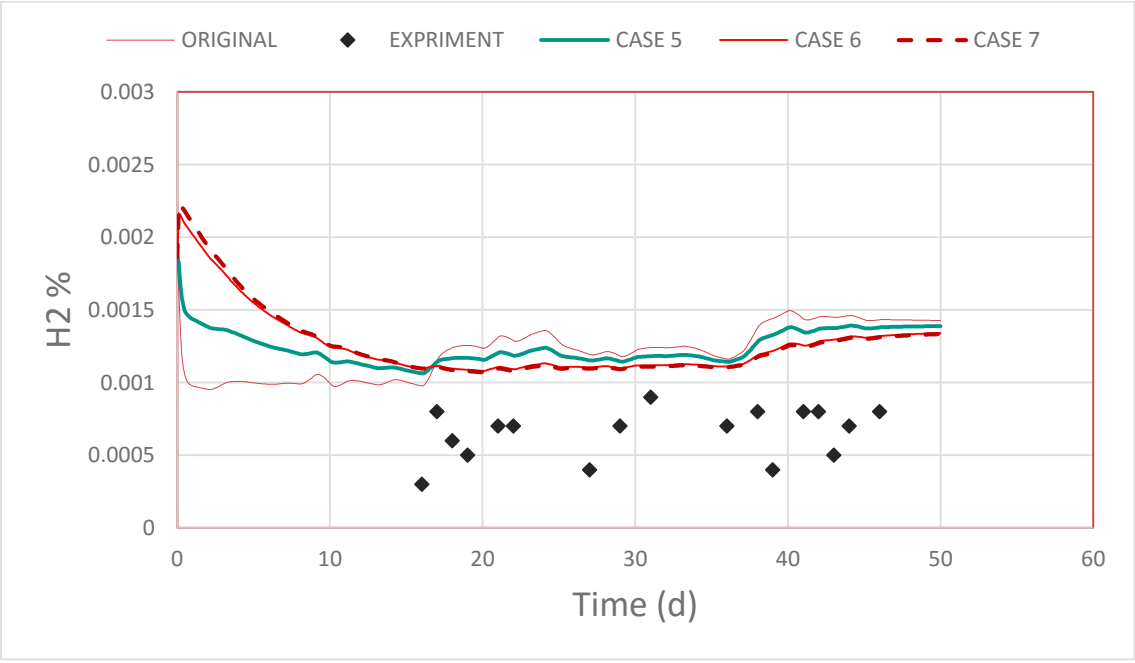

Figure 4-32: percentage of H_2 in headspace at different kLa with syngas composition of 86 % H_2, 7 % CO and 7 % CO_2. Case 5(kLa 24), Case 6(kLa 240) and Case 7(kLa 480).

The percentage of hydrogen in biogas composition is illustrated in figure 4.32. The hydrogen is higher up to day16 days, but its concentration starts to decrease after day16. Again case 7 reflects higher percentage than case 6 followed by case 5.

Figure 4.33 represents the pH value inside the reactor. The pH values of original simulation are similar to the experimental values which are below 7.5. However, the addition of syngas causes rises in pH since syngas contains more hydrogen. Case 7 and case 6 represents higher diffusion rate of hydrogen into the rector through the membrane. The pH of the bulk liquid inside reactor becomes higher with high kLa values and reaches around 7.5. First, 16 days pH increases in a rapid way up to 7.6 and after that, it falls back quickly and stabilises to normal pH values. Also from the figure it is clear that case 7 reaches at maximum than case 6 followed by case 5.

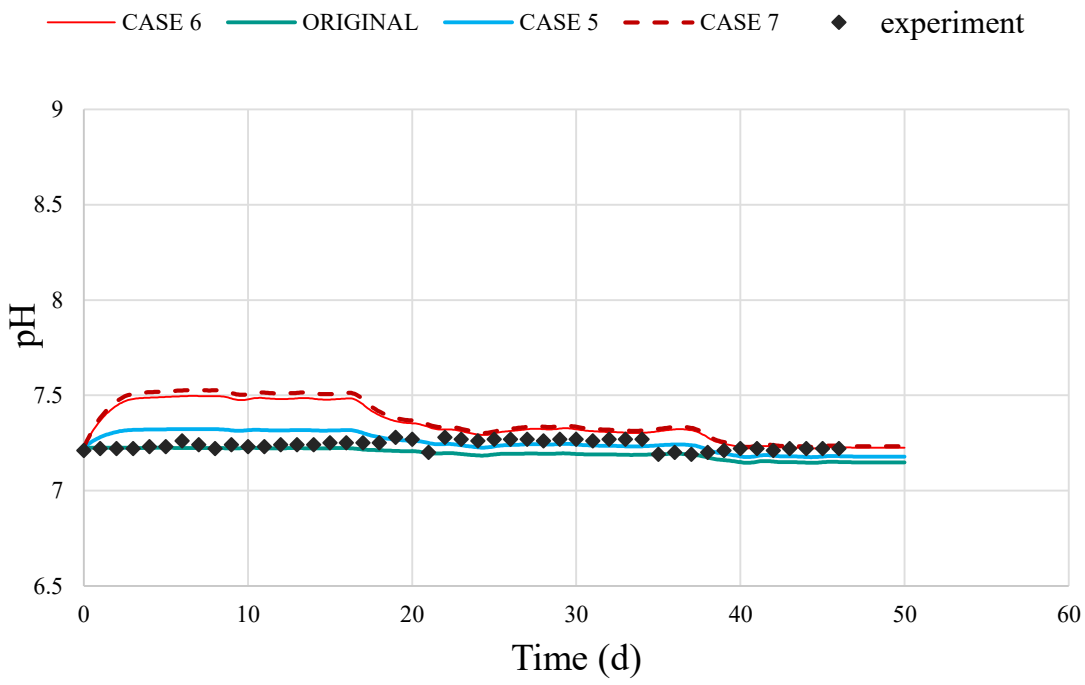

Figure 4-33: pH of bulk reactor volume with syngas composition of 86 % H_2, 7 % CO and 7 % CO_2 at different kLa. Case 5(kLa 24), Case 6(kLa 240) and Case 7(kLa 480).

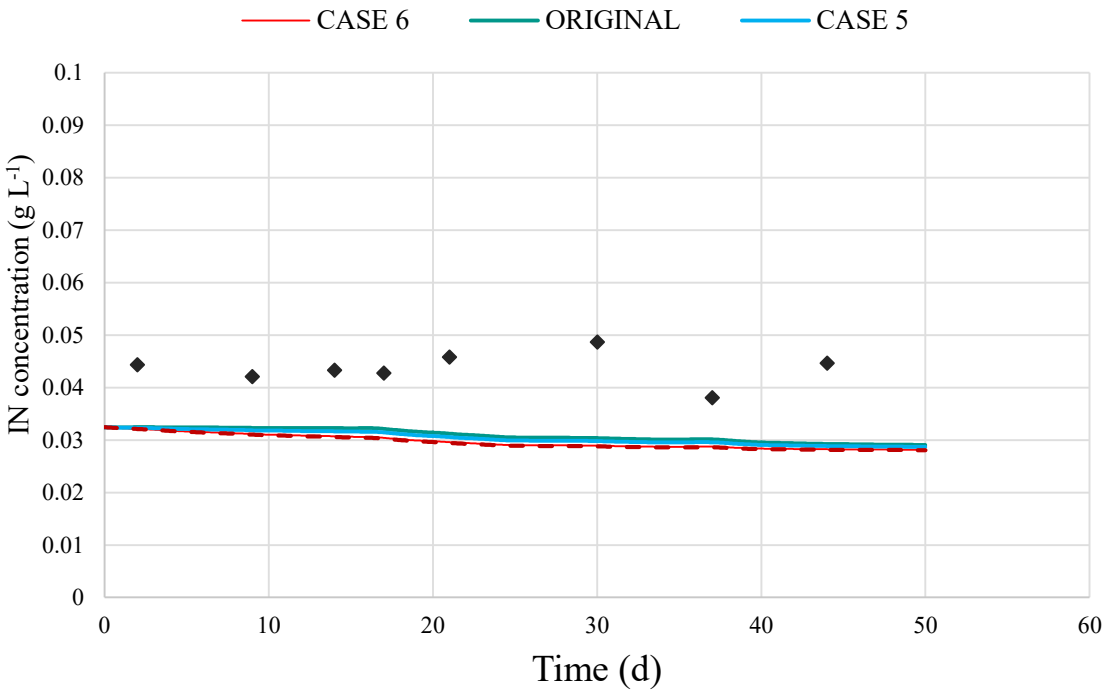

Figure 4-34: Total nitrogen concentration for three different cases with syngas composition of 86 % H_2, 7 % CO and 7 % CO_2 at different kLa. Case 5(kLa 24), Case 6(kLa 240) and Case 7(kLa 480).

The total nitrogen concentration is almost equal to the original values which are in the range between (0.02-0.03) g.L-1 as shown in figure 4.34. The graph also tells us that nitrogen concentration inside the reactor doesn't change much with the addition of syngas.

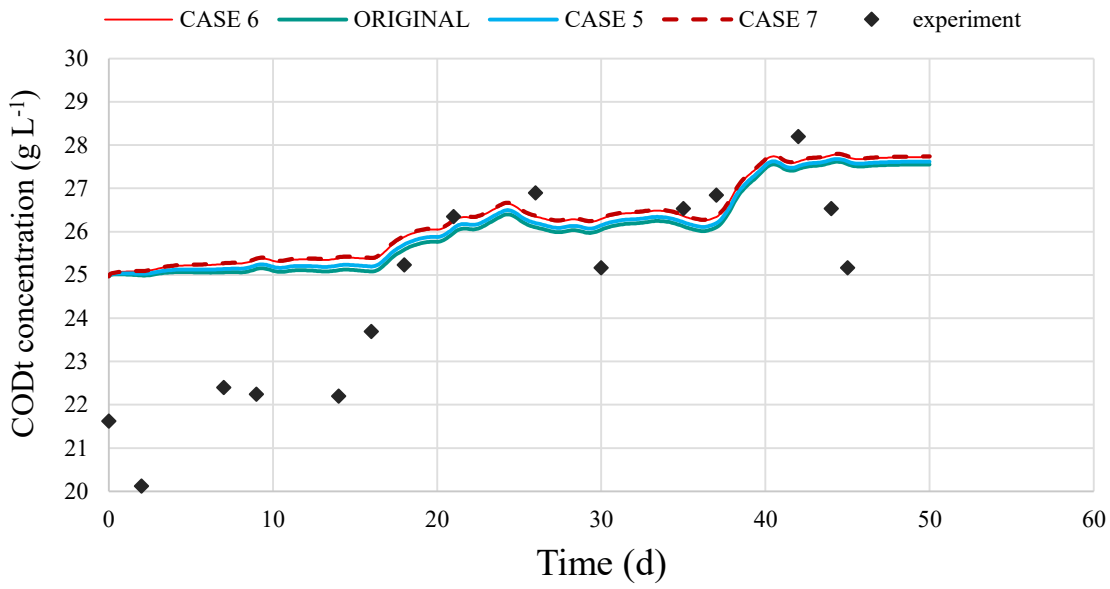

Figure 4-35: Total COD for a different case with syngas composition of 86 % H_2, 7 % CO and 7 % CO_2. Case 5(kLa 24), Case 6(kLa 240) and Case 7(kLa 480).

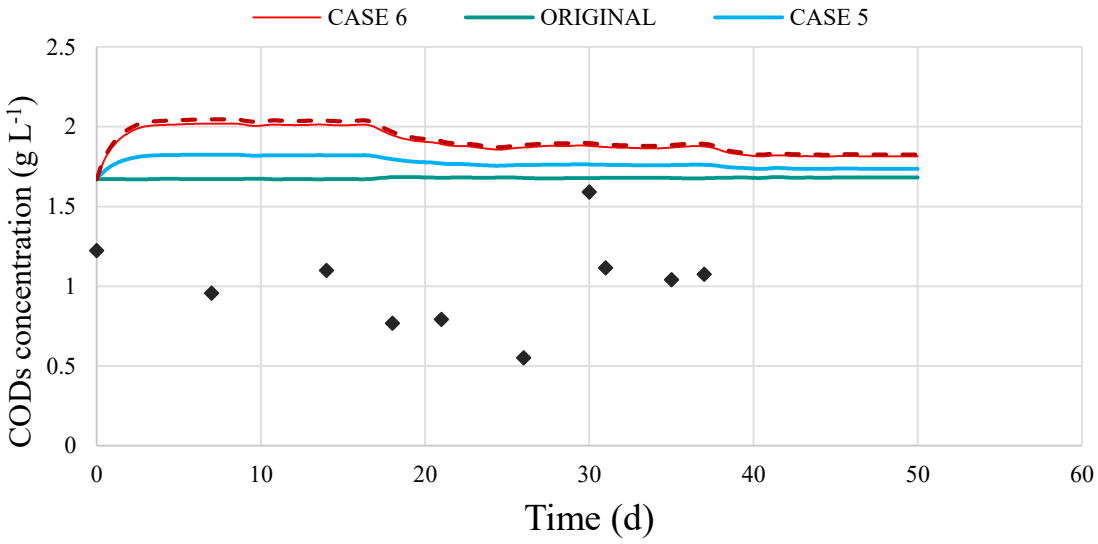

Figure 4-36: Soluble COD for a different case with syngas composition of 86 % H_2, 7 % CO and 7 % CO_2. Case 5(kLa 24), Case 6(kLa 240) and Case 7(kLa 480).

Figure 4.35 and figure 4.36 shows the total COD concentration and soluble COD concentration for the different case including original simulation results. With the addition of syngas to the reactor, total COD doesn't change much while soluble COD reflects the clear impact of syngas addition.

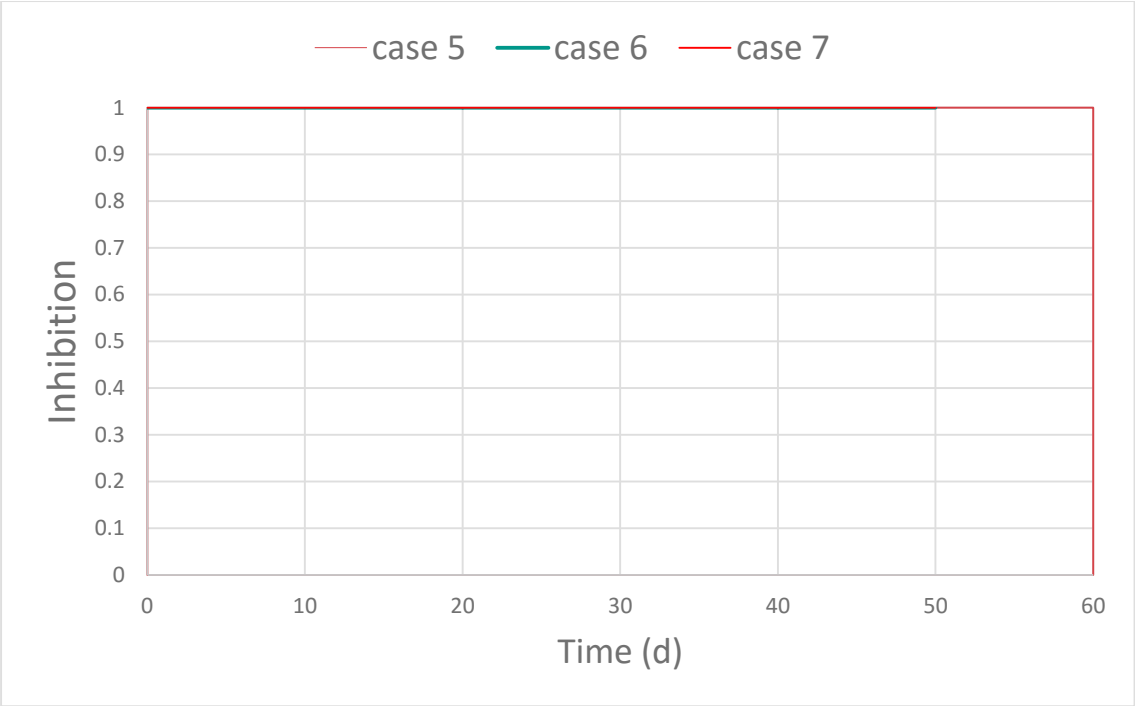

Figure 4-37: Inhibition of pH_ac for different kLa with syngas composition of 86 % H_2, 7 % CO and 7 % CO_2. Case 5(kLa 24), Case 6(kLa 240) and Case 7(kLa 480).

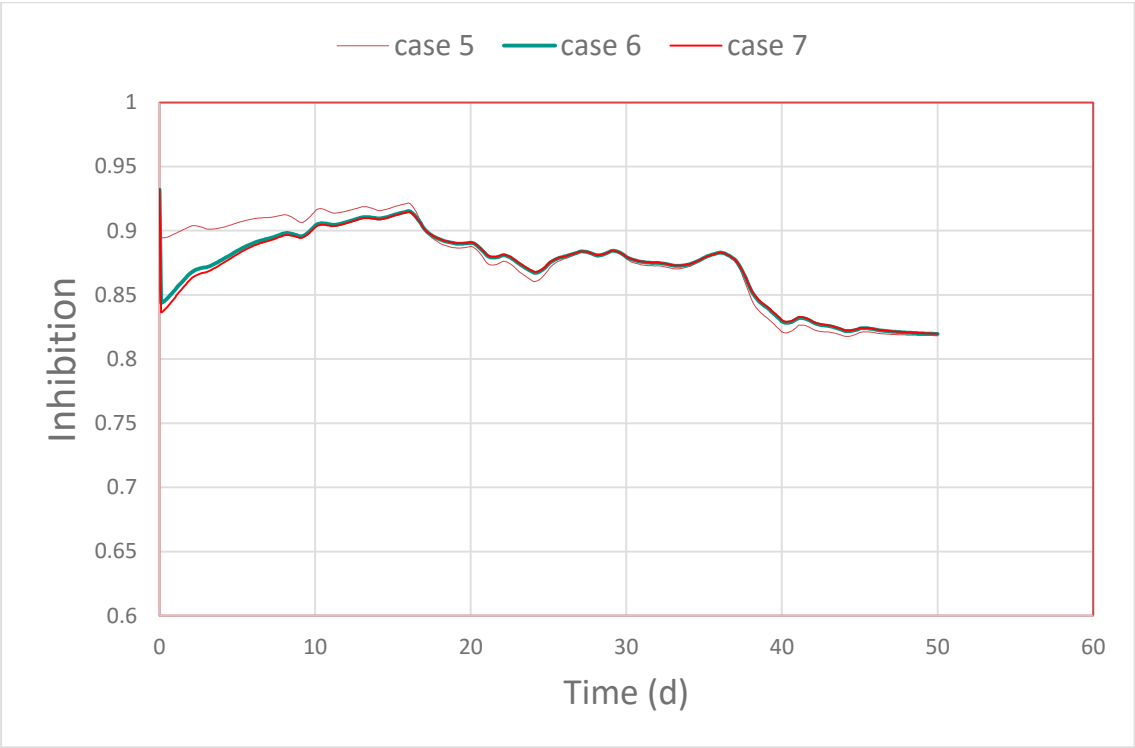

Figure 4-38: Inhibition of h2_co_ac for different kLa with syngas composition of 86 % H_2, 7 % CO and 7 % CO_2. Case 5(kLa 24), Case 6(kLa 240) and Case 7(kLa 480).

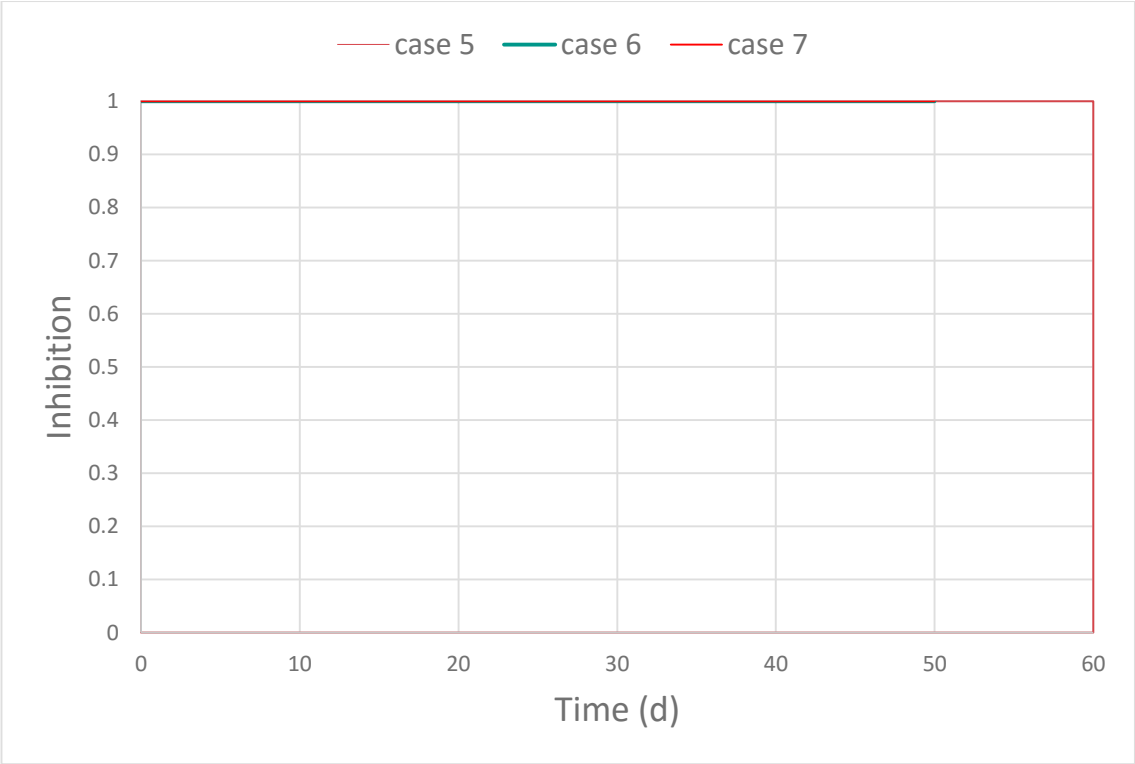

Figure 4-39: Inhibition of pH_co_ac for different kLa with syngas composition of 86 % H_2, 7 % CO and 7 % CO_2. Case 5(kLa 24), Case 6(kLa 240) and Case 7(kLa 480).

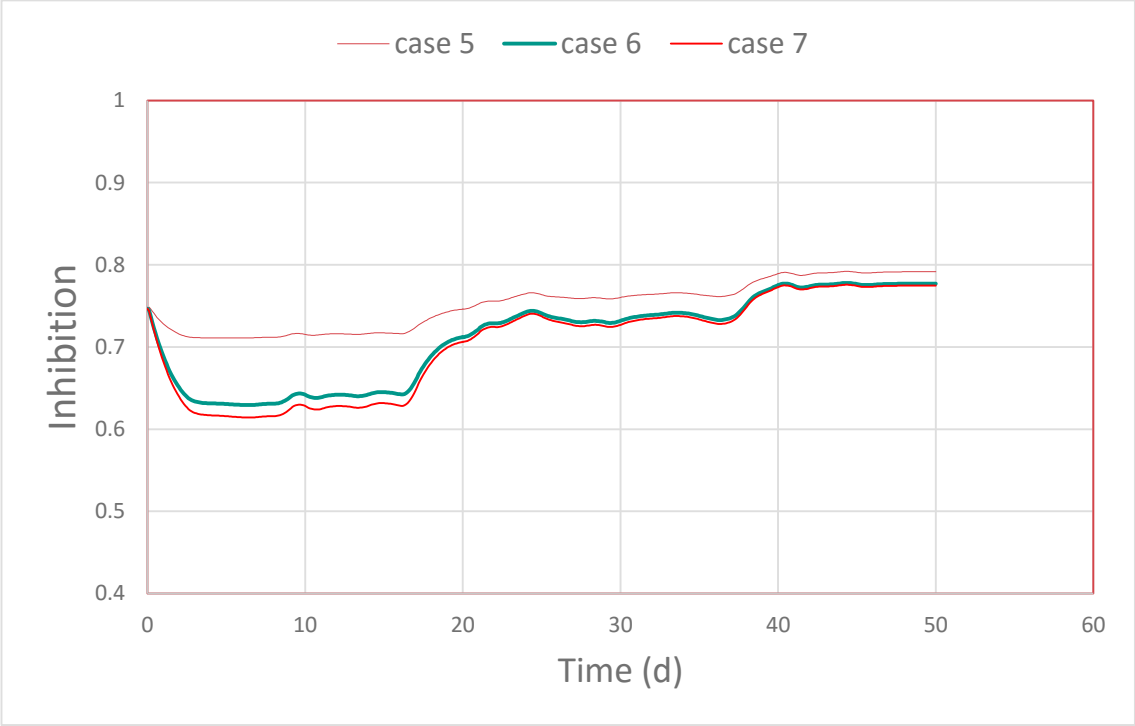

Figure 4-40: Inhibition of NH_3_ac for different kLa with syngas composition of 86 % H_2, 7 % CO and 7 % CO_2. Case 5(kLa 24), Case 6(kLa 240) and Case 7(kLa 480).

Figure 4.37 and figure 4.40 shows the inhibition inside the reactor. In all case, the value of inhibition is either 1 or less than 0.9.

4.2.2.1 Load of H_2 calculation for H_2-rich syngas (composition of 86 % H_2, 7 % CO and 7 % CO_2.)

Load of hydrogen can be calculated from the figure 5.2.

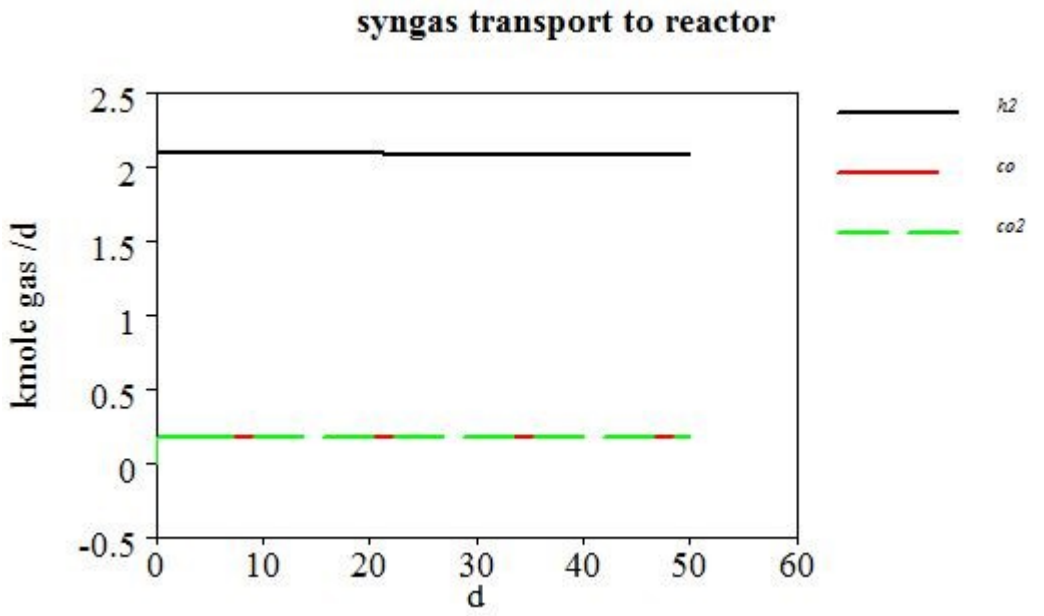

Figure 4-41: Amount of hydrogen diffuses to the reactor at kLa values 480 day^{-1}and inputM_gas_in of 81 m^3.day^{-1}.

Now from figure 5.2, hydrogen gas diffused into the reactor at kLa values 480day^{-1} is 2.1 kmole.day^{-1}.

$$Load\ of\ H_2 = 2.1\frac{\text{Kmole}}{day} = 2100\frac{\text{mole}}{day} = 2100 * 2\frac{\text{gram}}{mole} = 4200\frac{\text{gram}}{mole}$$
$$= 4200 * 8\frac{\text{gramCOD}}{day} = 33600\frac{\text{gramCOD}}{day} = 33.6\frac{\text{KgCOD}}{day}$$

Load of Feed is same for all case which is calculated earlier and the value is:

$$Feed = 23{,}3\frac{\text{Kg COD}}{m^3} * 1{,}61\frac{m^3}{day} = 37{,}5\frac{\text{Kg COD}}{day}$$

Now at kLa values of 480 day^{-1} and inputM_gas_in of 80 m^3.day^{-1}, load to feed ratio is:

$$\frac{Load\ of\ H_2}{Load\ of\ Feed} = \frac{33.6}{37.5} = 0.89$$

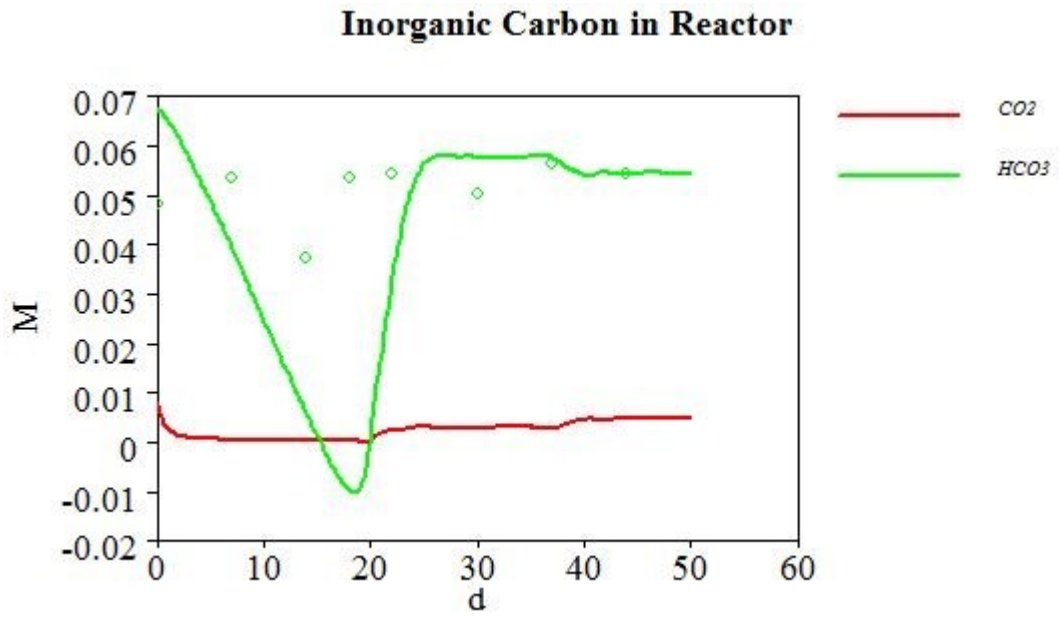

Figure 4-42: Inorganic carbon in the reactor at kLa values 480 day^{-1} for syngas composition of 86 % H_2, 7 % CO and 7 % CO_2.

Figure 4.42 is the inorganic carbon in the reactor for borderline (threshold limit).

So from calculation, $33.6\frac{\mathrm{KgCOD}}{day}$ amount of hydrogen gas shows failure of reactor. This is the threshold limit. In case of kLa 240day^{-1} the inputM_gas_in of 117 m^3.day^{-1} is the threshold limit. Further increment can cause the failure of process.

4.2.3 Simulation results with 44.4 % H_2, 33.3 % CO and 22.2% CO_2

The simulated final results with third syngas composition of 44.4 % H_2, 33.3 % CO and 22.2% CO_2 at three different kLa values is illustrated in below figures from 4.43 to 4.57.

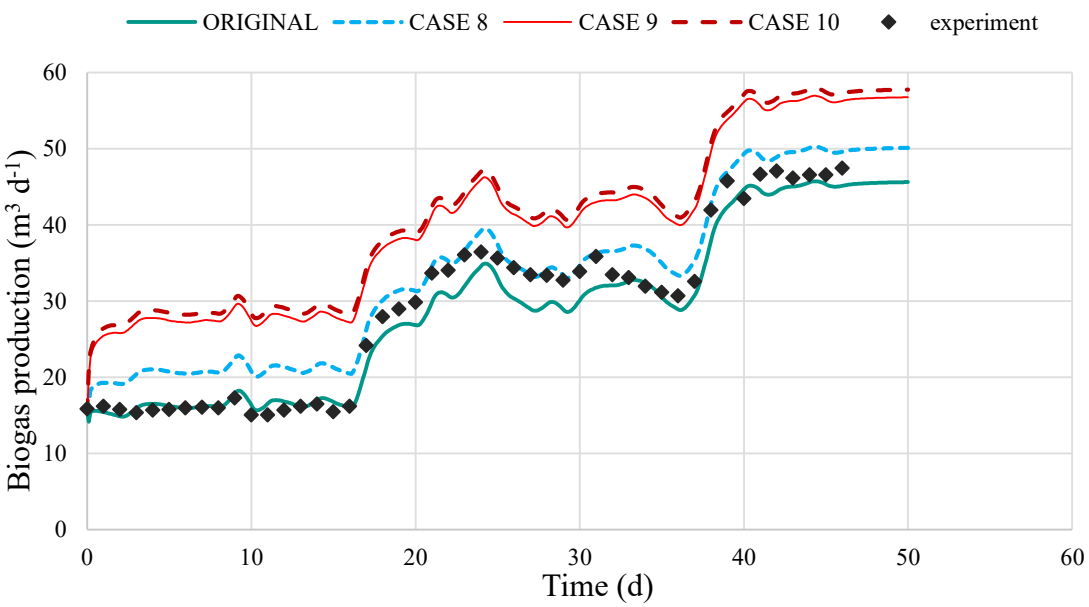

Figure 4-43: Biogas production rate at different kLa with syngas composition of 44.4 % H_2, 33.3 % CO and 22.2 % CO_2. Case 8(kLa 24), Case 9(kLa 240) and Case 10(kLa 480).

The simulation results for cases 8, 9 and 10 with syngas composition of 44.4 % H_2, 33.3 % CO and 22.2% CO_2 are shown in figure 4.43. The black dotted line is the experimental results which are around16 $m^3.day^{-1}$ up to day16 and reaches to 47 $m^3.day^{-1}$ at the end. The original is a simulation result without syngas. Case 8, case 9, and case 10 are the results obtained after addition of syngas composition of 44.4 % H_2, 33.3 % CO and 22.2% CO_2 at three different kLa values. At the beginning, all three cases produce biogas between ranges of (15-30) $m^3.day^{-1}$. And final production rate increases and reaches above up to 58 m3.day^{-1}. From the figure it is clear that case 10 produce more than case 9 followed by case 5.

The methane production rate with different kLa values is shown in figure 4.44. The impact of kLa is clearly illustrated for various cases in the graph. Methane production rate increases with increasing kLa values. Case10 produces more methane per day than case 9 followed by case 8. The final production at day 50 is around 33 $m^3.day^{-1}$.

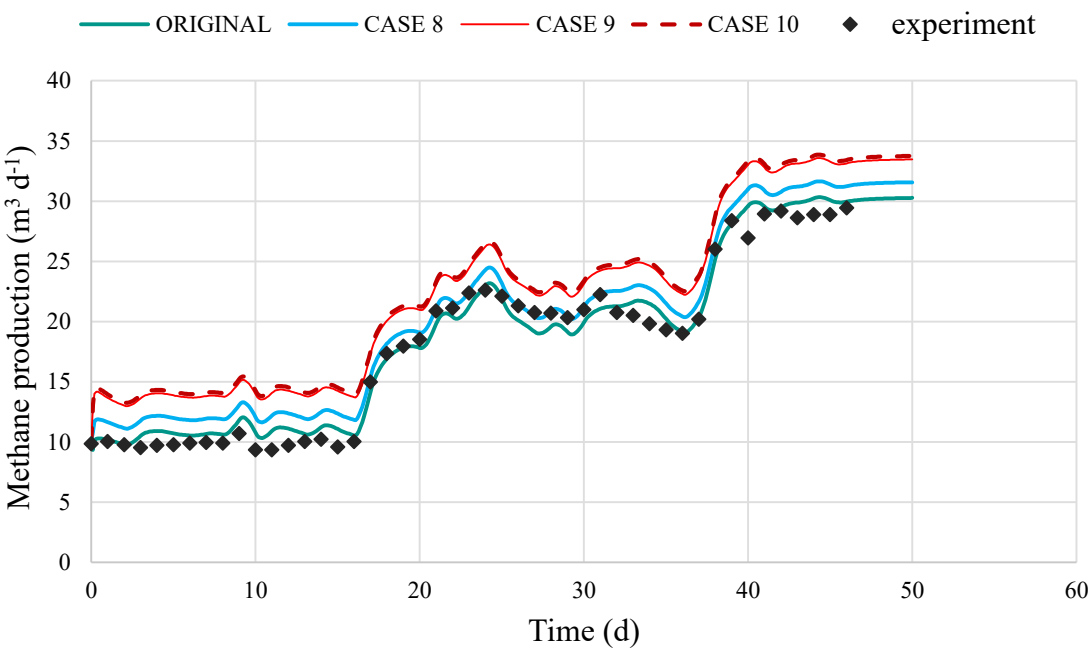

Figure 4-44: methane gas production rate at different kLa with syngas composition of 44.4 % H_2, 33.3 % CO and 22.2 % CO_2. Case 8(kLa 24), Case 9(kLa 240) and Case 10(kLa 480).

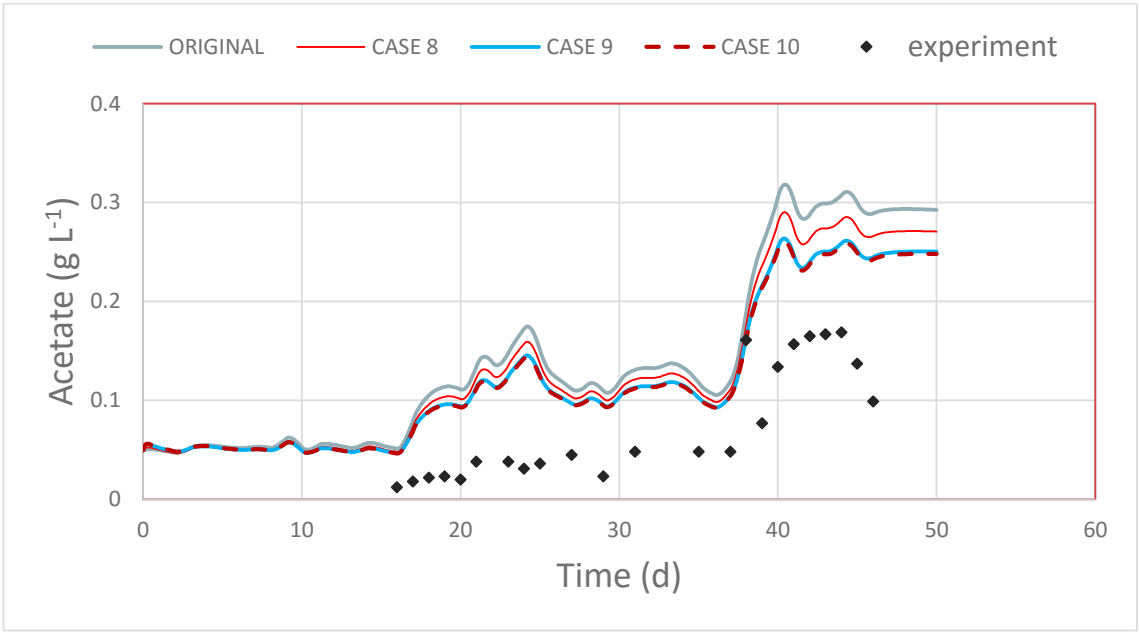

Figure 4-45: Acetate consumption rate at different kLa with syngas composition of 44.4 % H_2, 33.3% CO and 22.2 % CO_2. Case 8(kLa 24), Case 9(kLa 240) and Case 10(kLa 480).

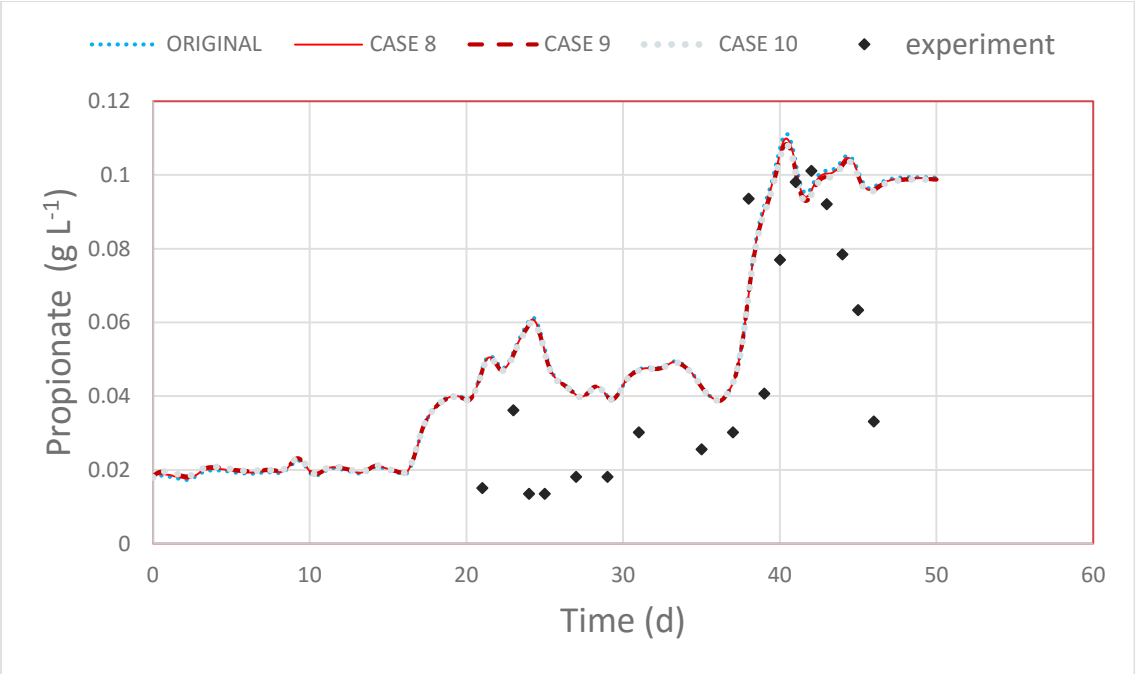

Figure 4-46: propionate consumption rate at different kLa with syngas composition of 44.4 % H_2, 33.3% CO and 22.2 % CO_2. Case 8(kLa 24), Case 9(kLa 240) and Case 10(kLa 480).

Figure 4.45 and figure 4.46 represents the acetate and propionate consumption rate in the reactor. Case 10 and case 9 shows little higher acetate concentration than case 8 after day 40, while no any significant changes in propionate concentration.

Figure 4.47 shows the detected percentage of methane in produced biogas. First 16 days, the methane concentration decreases with increase in kLa and it reaches around 51 % at kLa 480. After day16, it starts to increase but remains less than original throughout the whole period. Case 10 shows lower percentage than case 9 followed by case 8.

On the other hand, carbon dioxide (CO_2) concentration detected followed the similar behaviour but in opposite way as present in figure 4.49. With the increase in kLa values, the CO_2 increases. The percentage of CO_2 increment is more in case 10 than case 9 and case 8 respectively.

The percentage of hydrogen in biogas composition is illustrated in figure 4.48. The hydrogen is higher during up to day16 but its concentration starts to decrease after day16. Again case 10 reflects lower percentage than case 9 followed by case 8.

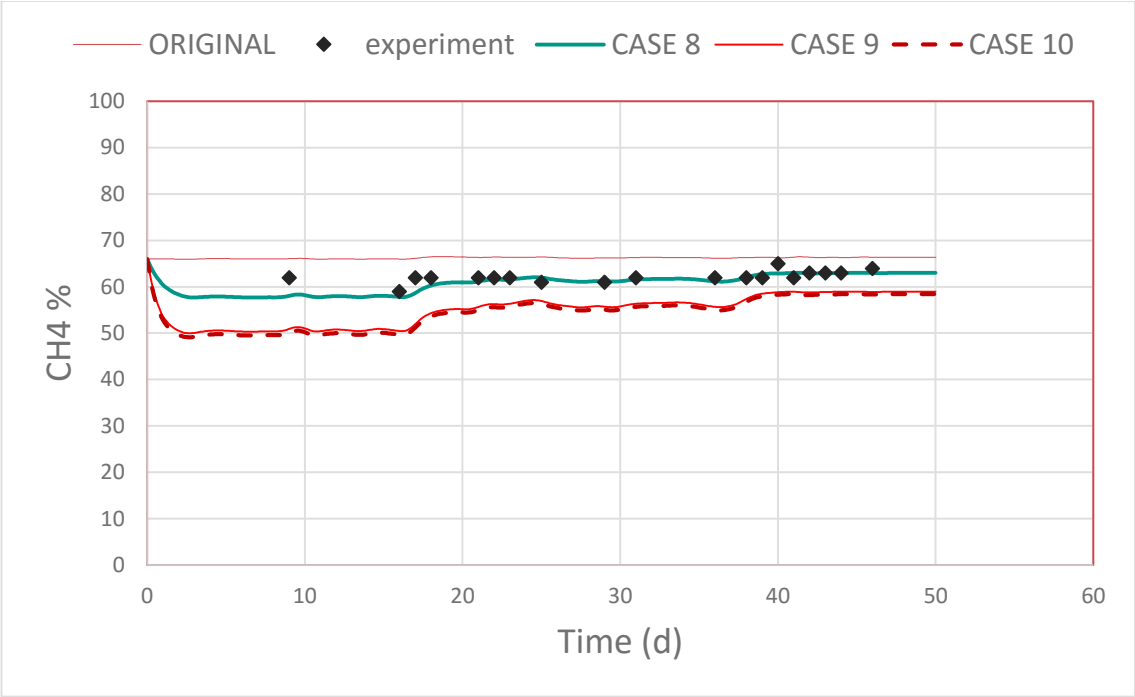

Figure 4-47: percentage of methane in headspace at different kLa with syngas composition of 44.4 % H_2, 33.3% CO and 22.2 % CO_2. Case 8(kLa 24), Case 9(kLa 240) and Case 10(kLa 480).

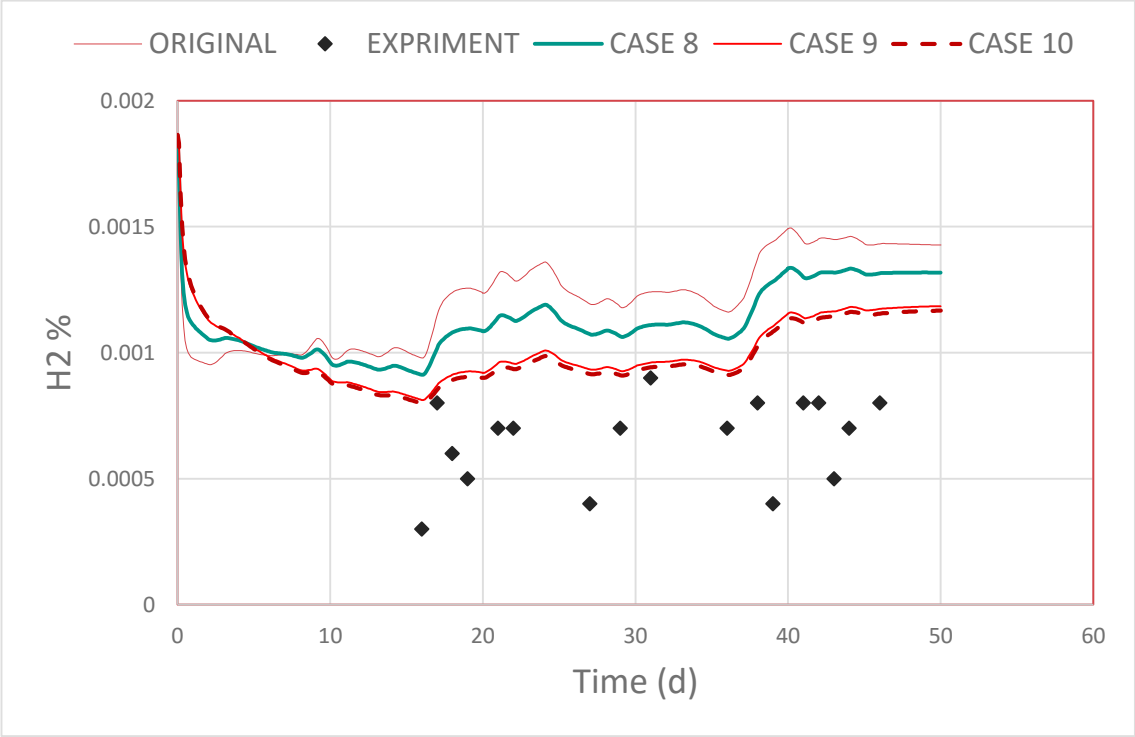

Figure 4-48: percentage of H_2 in headspace at different kLa with syngas composition of 44.4 % H_2, 33.3% CO and 22.2 % CO_2. Case 8(kLa 24), Case 9(kLa 240) and Case 10(kLa 480).

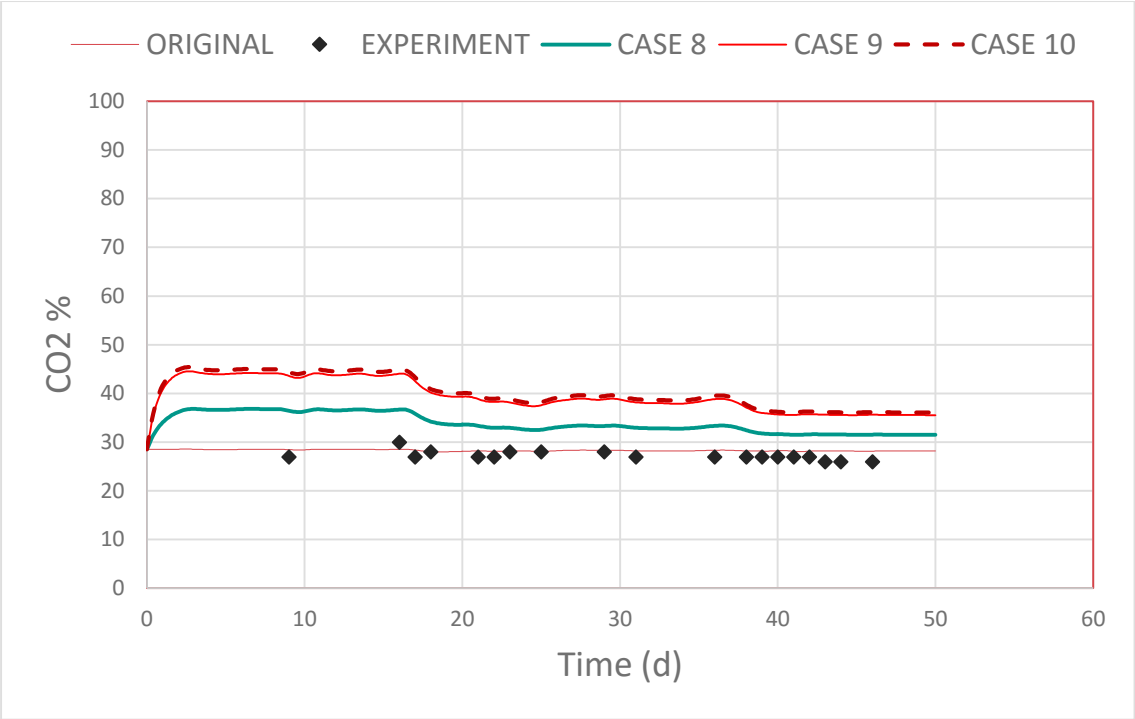

Figure 4-49: percentage of CO_2 in headspace at different kLa with syngas composition of 44.4 % H_2, 33.3% CO and 22.2 % CO_2. Case 8(kLa 24), Case 9(kLa 240) and Case 10(kLa 480).

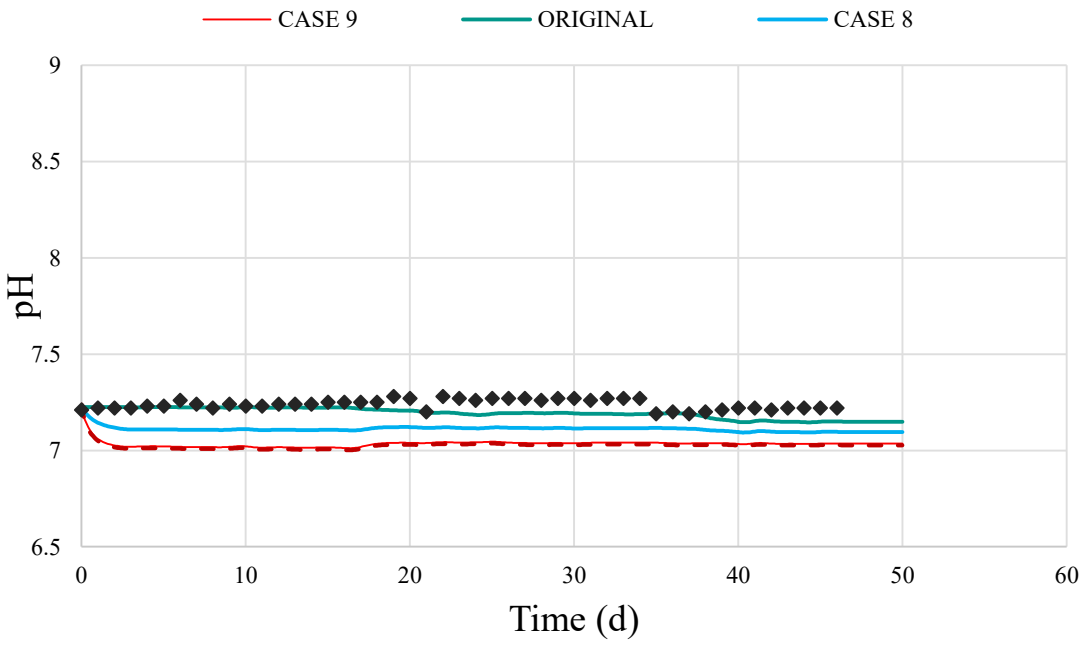

Figure 4-50: pH of bulk reactor volume with syngas composition of 44.4 % H_2, 33.3% CO and 22.2 % CO_2 at different kLa. Case 8(kLa 24), Case 9(kLa 240) and Case 10(kLa 480).

Figure 4.50 represents the pH value inside the reactor. The pH values of original simulation are similar with the experimental values which are around 7.2. However, the addition of syngas composition of 44.4 % H_2, 33.3 % CO and 22.2% CO_2 causes a decrease in pH.

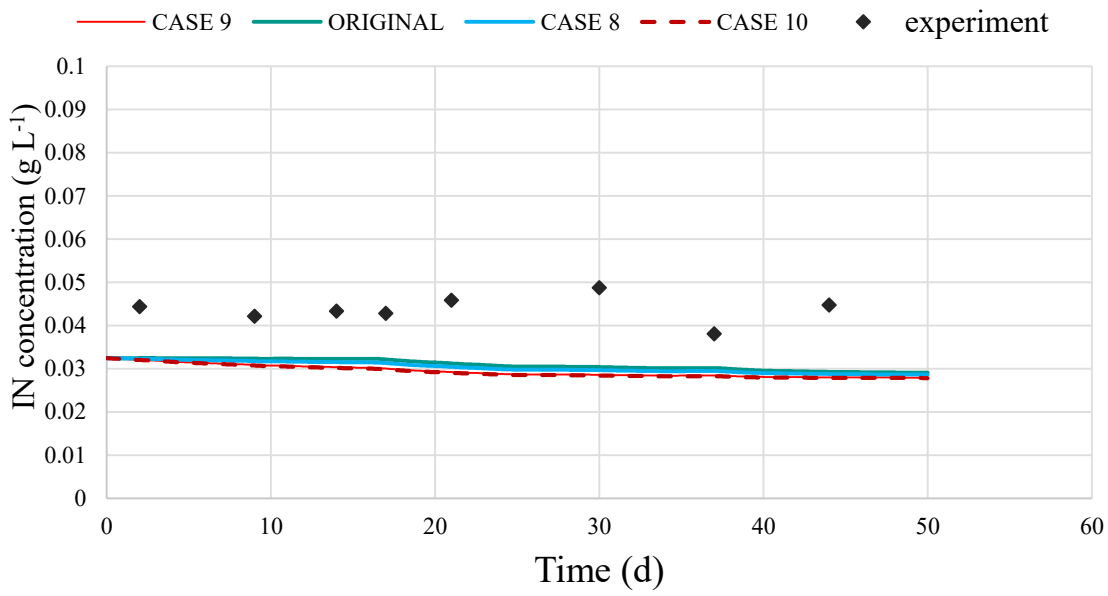

Figure 4-51: Total nitrogen concentration for three different cases with syngas composition of 44.4 % H_2, 33.3% CO and 22.2 % CO_2 at various kLa. Case 8(kLa 24), Case 9(kLa 240) and Case 10(kLa 480).

The total nitrogen concentration is almost equal to the original values which are in the range between (0.02-0.03) g.L-1 as shown in figure 4.51. The graph also tells us that nitrogen concentration inside the reactor doesn't change much with the addition of syngas consists of 44.4 % H_2, 33.3% CO and 22.2 % CO_2.

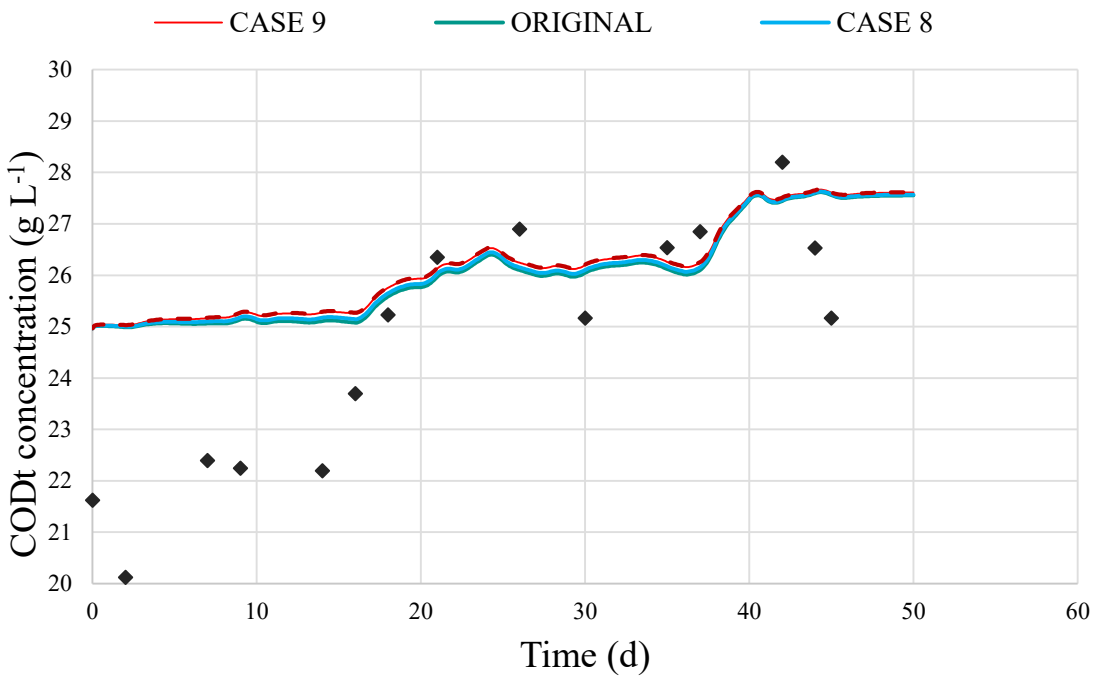

Figure 4-52: Total COD for different case with syngas composition of 44.4 % H_2, 33.3% CO and 22.2 % CO_2. Case 8(kLa 24), Case 9(kLa 240) and Case 10(kLa 480).

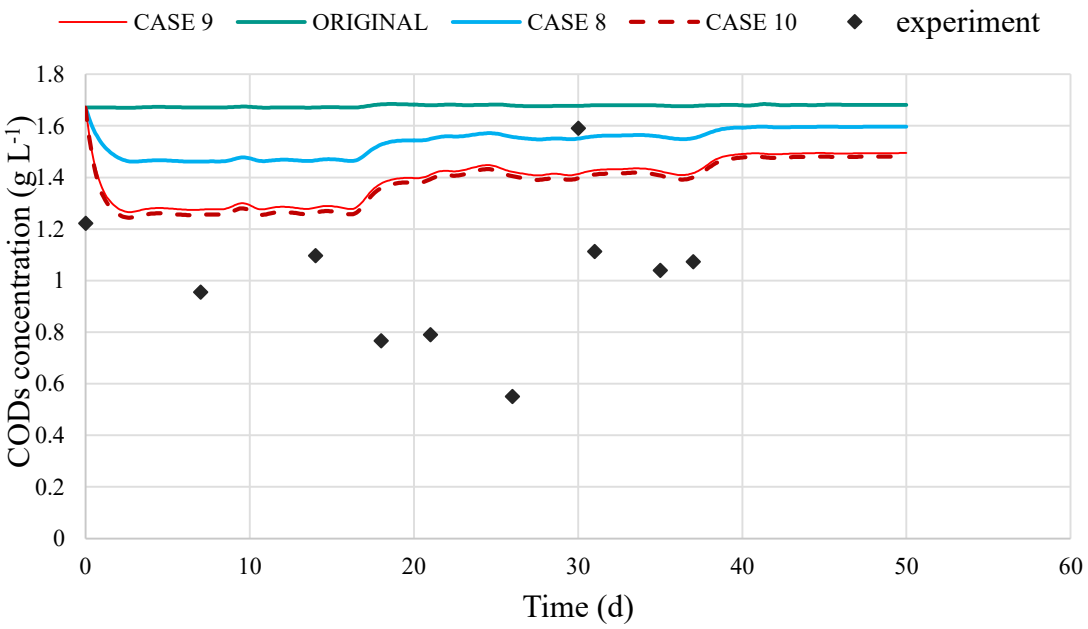

Figure 4-53: Soluble COD for a different case with syngas composition of 44.4 % H_2, 33.3% CO and 22.2 % CO_2. Case 8(kLa 24), Case 9(kLa 240) and Case 10(kLa 480).

Figure 4.52 and figure 4.53 shows the total COD concentration and soluble COD concentration for the different case including original simulation results. With the addition of syngas to the reactor, total COD doesn't change much while soluble COD reflects the clear impact of syngas addition. Soluble COD shows a significant decrease in higher kLa values. Case 9 and case 10 reduces up to 1.3 $g.L^{-1}$ and follow the same trend for about 18 days.

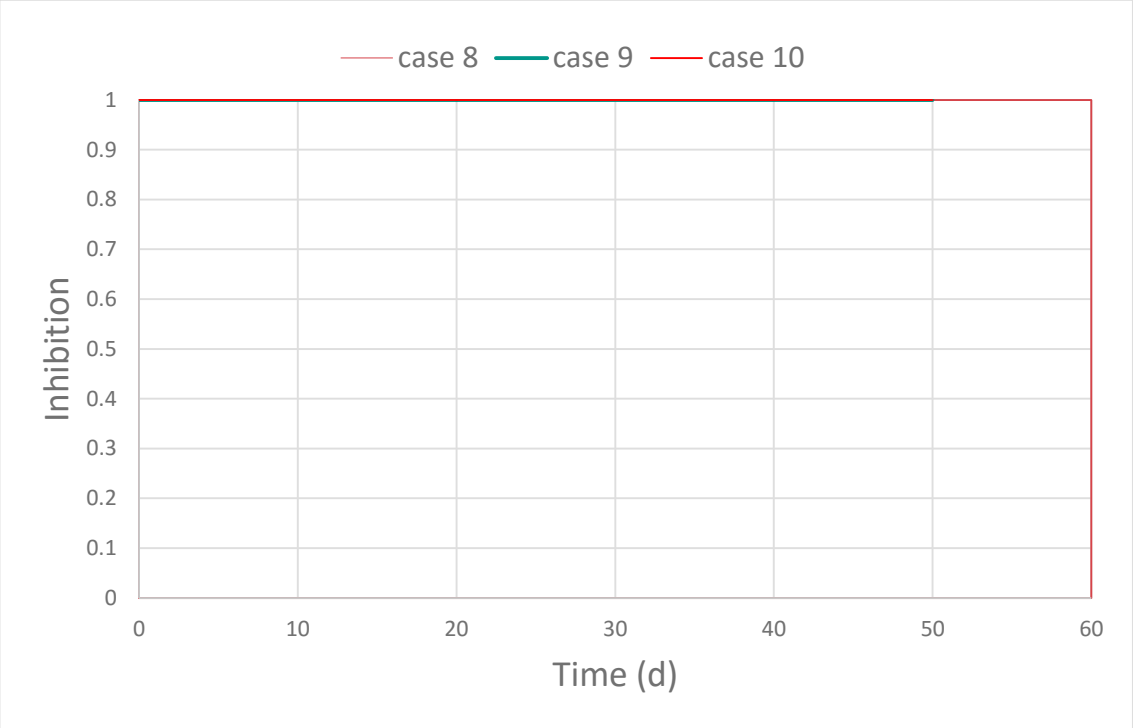

Figure 4-54: Inhibition of pH_ac for different kLa with syngas composition of 44.4 % H_2, 33.3 % CO and 22.2 % CO_2. Case 8(kLa 24), Case 9(kLa 240) and Case 10(kLa 480).

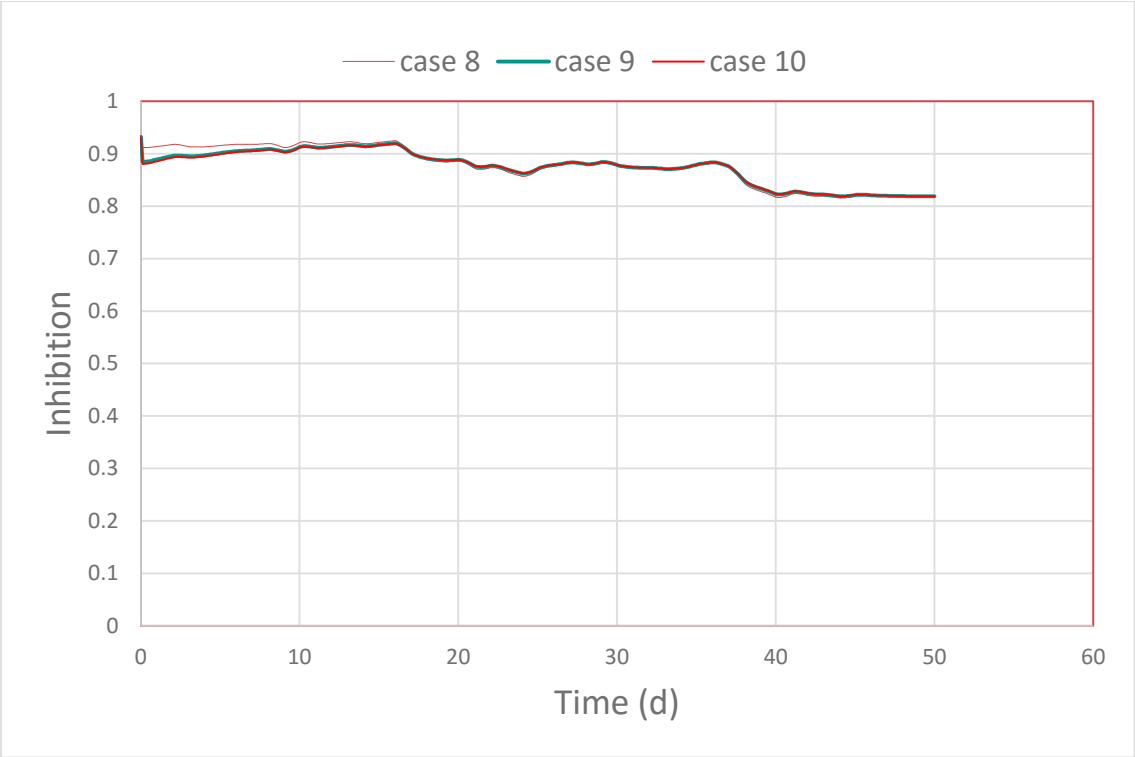

Figure 4-55: Inhibition of h2_co_ac for different kLa with syngas composition of 44.4 % H_2, 33.3 % CO and 22.2 % CO_2. Case 8(kLa 24), Case 9(kLa 240) and Case 10(kLa 480).

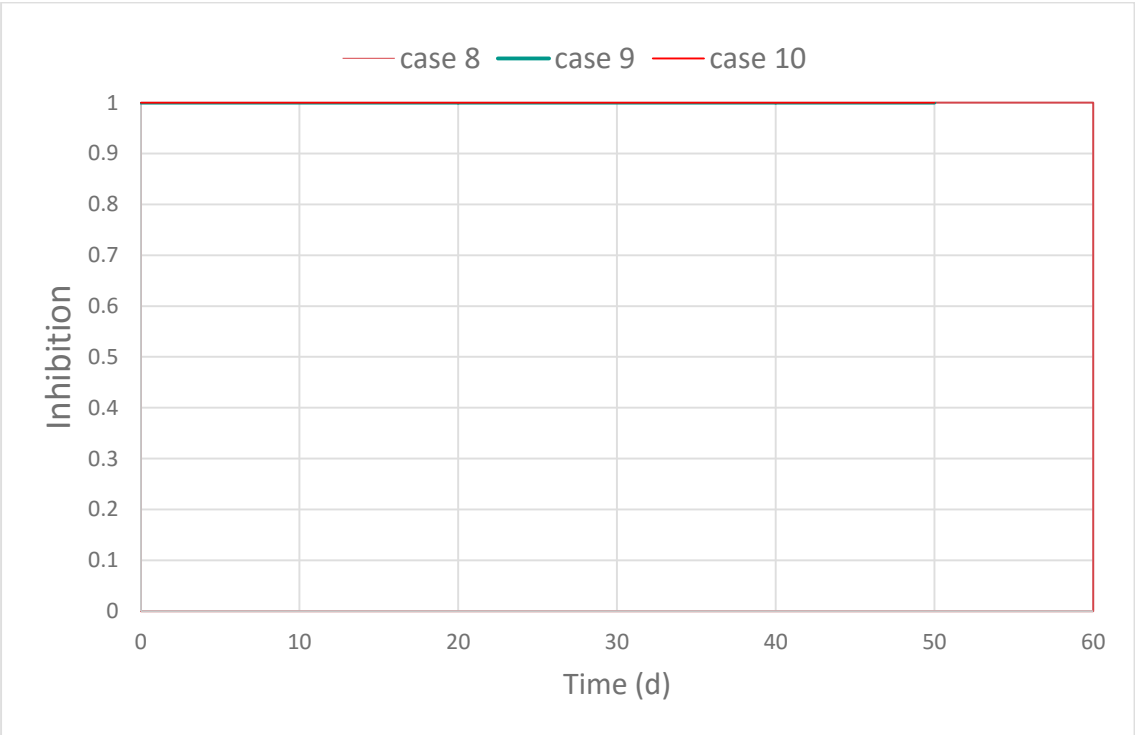

Figure 4-56: Inhibition of pH_co_ac for different kLa with syngas composition of 44.4 % H_2, 33.3 % CO and 22.2 % CO_2. Case 8(kLa 24), Case 9(kLa 240) and Case 10(kLa 480).

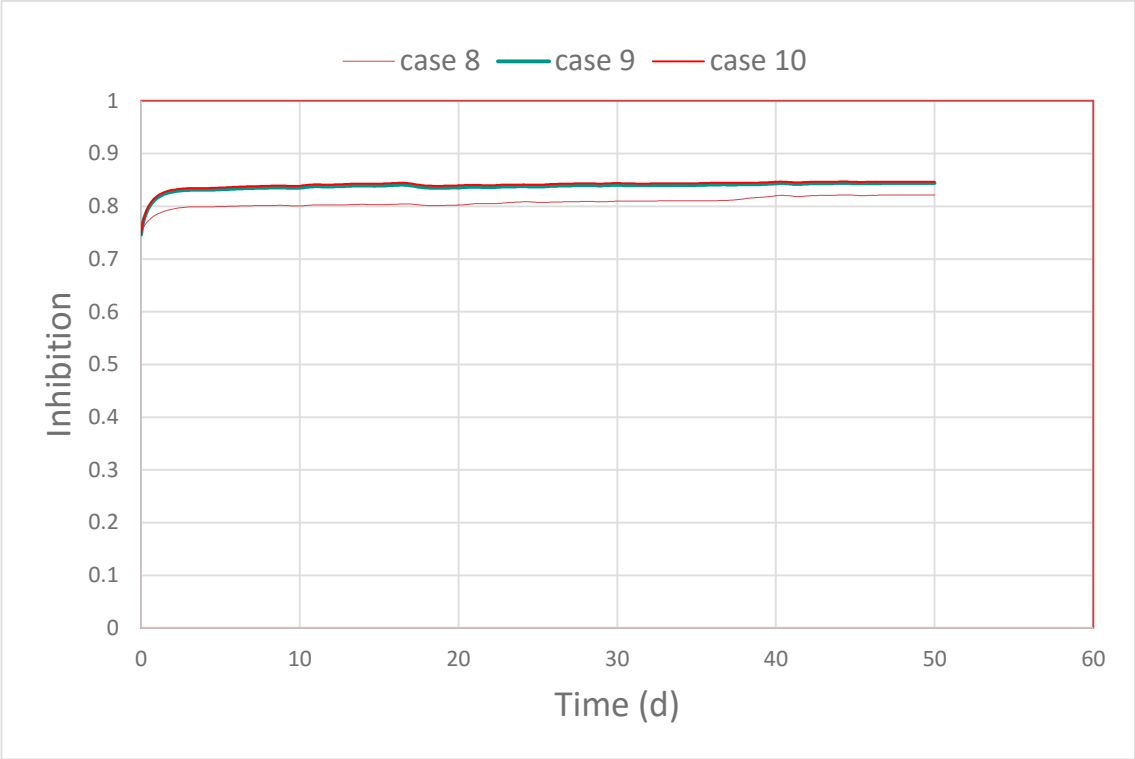

Figure 4-57: Inhibition of NH_3_ac for different kLa with syngas composition of 44.4 % H_2, 33.3 % CO and 22.2 % CO_2. Case 8(kLa 24), Case 9(kLa 240) and Case 10(kLa 480).

Figure 4.54 and figure 4.57 shows the. The addition of syngas shows inhibition. In all case, the value of inhibition is either 1 or less than 0.9.

5 Discussion

5.1 Experiment

The experimental results don't show any significant difference between both reactors. The experimental work is considered as start-up phase since both reactors show no difference within this 20 days of the experiment And the $\frac{Load\ of\ H_2}{Load\ of\ Feed}$ ratio for the reactor A is 0.08, which represents a very low value. This value also explains the lack of a significant difference between both reactors. When we compare this value with the simulation value (0.35 is the limit calculated in section 4.2.1.1.), it should be higher than 0.08 and closer to 0.25 or 0.30 to see the difference.

This work functioned well as a start-up phase since H_2 did not go directly through the reactor and into the headspace that means that the hydrogenotrophic methanogens had time to establish. Further work on this experiment should be done where the load of H_2 should be increased.

5.2 Modelling and simulation

The main objective of this simulation is to investigate the effect of pure hydrogen addition and syngas addition into the ADM1 model. The input to the reactor is fixed at 25 $m3.day^{-1}$, and the gas-liquid mass transfer rate (kLa) is varied from a minimum value (24 day^{-1}) to maximum value (480 day^{-1}).

In the case of pure hydrogen, the biogas production rate (figure 4.9) is not increased significantly except on minor changes on transient phases (between 20-25 days) but methane production rate (figure 4.10) affected clearly by different levels of hydrogen introduced by various kLa. With the increase in kLa methane production increases. The simulation results show that the methane production rate (figure 4.10, case 4) is around 14$m^3.day^{-1}$), which is 4$m^3.day^{-1}$ more than experimental value, i.e.,10 $m^3.day^{-1}$(figure 4.10, experimental). So one can conclude that the methane production rate increases up to 40% by addition of pure hydrogen.

The influence of pure hydrogen addition in AD process enhance the hydrogenotrophic methanogenesis process and increase production of methane. (R4-1)

$$4H_2 + CO_2 \rightarrow CH_4 + 2H_2O \qquad \text{(R4-1)}$$

$$CO_2 + H_2O \leftrightarrow H_2CO_3 \leftrightarrow H^+ + HCO_3^- \quad \text{(R4-2)}$$

$$HCO_3^- \leftrightarrow H^+ + CO_3^- \quad \text{(R4-3)}$$

Reaction R4-2 and R4-3 are the equilibrium reaction between CO_2 and H_2CO_3. Hydrogen uses more CO_2, which disturbs the equilibrium. To preserve the equilibrium, the surplus of CO_2 was then provided by H_2CO_3, which indicates loose of more H^+ ion into the reactor, causes pH inside the reactor goes up as shown in figure 4.16. Also, pH is higher up to day16 due to less load of feed (figure 3.3) which results in less hydraulic retention time (HRT) but after day17, HRT increases due to increase in feed and pH stabilizes.

Figure 4.10 shows higher methane production after day 16. The production of methane increases because of inhibition reduction and the acetate concentration falls as illustrated in figure 4.4. In figure 4.4, during the day (0-16), the acetate concentration increase with higher kLa values. With kLa 24, the concentration is ok, but as the value increases at 240 and 480, the concentration is continuously increasing. The high acetate concentration can be explained by high H_2 load to feed load ratio; it leads to high pH and high concentration of NH_3 which inhibits the process of acetoclastic methanogenesis. The biomass responsible for methane production from acetate belongs from the archaeal group (methanogens) which is inhibited by NH_3 which means slow down the conversion of acetate to methane process.

The main reason for high inhibition is due to more NH_3 present in the reactor which can be explained by the reaction R4-4.

$$NH_4 \leftrightarrow H^+ + \mathrm{N}H_3 \quad \text{(R4-4)}$$

Since pH goes up, H^+ ion from reaction R4-4 is removed which produce more NH_3 into the reactor. The case with kLa 240 and 480 shows higher inhibition than kLa 24.

Propionate concentration is similar in all case, which means degradation unaffected of H_2 or syngas addition.

Load of feed increased after day 16, which means the ratio of $\frac{Load\ of\ H_2}{Load\ of\ Feed}$ is higher before day16. So, there is higher possibilities of failure before day16 than afterwards. After day16 the load of feed was increased which increase the amount of CO_2 into the reactor since, feed contains CO_2. Around 0.35 is the threshold limit a reactor can handle. This is the number which leads to the failure if feed is not added after 16 days. Also for the theoretical border line (threshold limit), pH (figure4.16) seems to stabilise at 8.5 but Inorganic Carbon (IC) graph (figure 4.25) seems to go down, so it cannot be saved by

adding feed after day16, failure is certain. Lie Xi and Irini Angelidaki[64], they show through experiment that pH 9 is the failure and based on the simulation in this thesis work, the border line is 8.5.

The total COD does not change much, but soluble COD changes with an increase in kLa. Soluble COD contains COD from acetate, COD from propionate, COD from methane and COD from H_2.

$$COD_S = COD_{acetate} + COD_{propionate} + COD_{methane} + COD_{hydrogen}$$

So, soluble COD increases due to acetate, methane, and hydrogen.

In the case of H_2-rich syngas composition (86 % H_2, 7 % CO and 7 % CO_2), biogas production rate and methane production rate increases with increase in kLa than pure H_2; since syngas also contains some CO_2, which shows more favourable condition than pure hydrogen. From the graph(figure 4.33), it is clear that syngas is easier to handle than pure H_2 since the pH values don't rise too high as we observe in the case of pure hydrogen. The methane production rate is around 16$m^3.day^{-1}$(figure 4.27, case 7), which is 6 $m^3.day^{-1}$ more than experimental value i.e10 $m^3.day^{-1}$(figure 4.7, experimental). So from this result, one can say that methane production rate can be increased by 60% by adding H_2-rich syngas. The acetate (figure 4.28) concentration at all three kLa is ok with this composition of syngas because NH_3 does not much inhibit it (figure 40). Similarly, the threshold limit for $\frac{Load\ of\ H_2}{Load\ of\ Feed}$ with H_2-rich syngas composition is around 0.89.

In the case of syngas composition of 44.4 % H_2, 33.3 % CO and 22.2 % CO_2, The biogas production rate, and methane production is more and increases with kLa. But, the produced biogas contains more percentage of CO_2 and less percentage of methane which is due to more amount of CO_2 present in the syngas. The amount of acetate increases more during last days which is due to more inhibition in the last days.

The methane percentage is around 94 % (figure 4.13) with pure H_2, around 81 % (figure 4.30) with H_2-rich syngas (composition of 86 % H_2, 7 % CO and 7 % CO_2) and around 49% (figure 4.47) in 3rd syngas composition (syngas composition of 44.4 % H_2, 33.3 % CO and 22.2 % CO_2). Syngas 3 contains more percentage of CO_2, and this is the reason for less methane in 3rd syngas composition since it depends on the H_2/CO_2 ratio.

6 Conclusion

The simulation shows that it is possible to increase the methane production rate up to 40% by adding pure H_2 and up to 60% by adding H_2-rich syngas. Literature experimental data supports these findings. The following conclusion was reached from a simulation of the various cases investigated.

With pure hydrogen

- In the case of pure hydrogen, The addition of hydrogen can improve CH_4 content in produced biogas. The percentage of CH_4 at the highest kLa (480day^{-1}) is around 94 %.
- kLa 480 represents the maximum limit of $\frac{Load\ of\ H_2}{Load\ of\ Feed}$ ratio of 0.35 (kgCOD hydrogen.day^{-1} / (kgCOD feed.day^{-1}) which was observed during simulation.
- CH_4 production rate increase with kLa but biogas production do not increase much because of the higher percentage of methane in biogas.
- The reactor's pH enhances with the amount of hydrogen added. For example in the simulated case, the pH goes above 8.5 with kLa 480.
- Apparently, there is a borderline which shows how much H_2 is added before the process avoids failure. The simulation show if borderline is crossed, then pH will rise above 8.5 and process become a failure. At borderline, pH seems to stabilise at 8.5, but the Inorganic carbon (IC) is still falling which means the pH concentration on the borderline could even be lower than 8.5.
- Such a borderline is also observed experimentally with failure at ph 9 and not failure at 8.
- The rise in pH increase the NH_3 inhibition because a larger fraction of total NH_4 present as NH_3 (which is a most toxic form of ammonia).
- The addition of hydrogen do not affect the propionate concentration.
- The total COD remains similar with different amount of hydrogen addition, but soluble COD increases with h_2 addition.
- Under the case condition I have simulated, changing H_2 addition can be simulated by both kLa and input (inputM_gas_in) flow rate. Both kLa and input (inputM_gas_in) increase the diffusion of hydrogen. So, it's hard to conclude the exact values of kLa on diffusion.

With syngas composition of 86% H_2, 7% CO and 7% CO_2

- In the case of syngas composition of 86% H_2, 7% CO and 7% CO_2, both biogas production, and methane production increases with increase in kLa.
- The highest level of CH_4 content can achieve in produced biogas with H_2-rich syngas composition is around 81 %.
- It appears that there is easier to avoid failure if we use syngas than pure hydrogen due to the pH problem.
- Syngas show less inhibition of NH_3 than pure hydrogen due to pH.
- The theoretical borderline (threshold limit) with syngas is better than pure H_2. The $\frac{Load\ of\ H_2}{Load\ of\ Feed}$ ratio is 0.89. The higher ratio than pure H_2 due to the simultaneous addition of CO_2 into the reactor.

With Syngas composition of 44.4% H_2, 33.3% CO and22.2% CO_2

- In the case of Syngas composition of 44.4% H_2, 33.3% CO and22.2% CO_2, biogas production is higher than pure H_2 or H_2-rich syngas was added, but methane content in produced biogas is very low. The methane production rate depends on the H_2/CO_2 ratio, and syngas with this composition contains more CO_2 than H_2-rich syngas (syngas composition of 86% H_2, 7% CO and 7% CO_2).
- CH_4 content is lower in every tested case with this composition. It decreases more with an increase in kLa. The highest percentage of CH_4 at kLa 480 is around 49%.

References

1. Luo, G., W. Wang, and I. Angelidaki, *Anaerobic digestion for simultaneous sewage sludge treatment and CO biomethanation: process performance and microbial ecology.* Environmental science & technology, 2013. **47**(18): p. 10685-10693.
2. Batstone, D.J., et al., *Anaerobic digestion model no. 1 (ADM1)*. 2002: IWA publishing.
3. Adekunle, K.F. and J.A. Okolie, *A review of biochemical process of anaerobic digestion.* Advances in Bioscience and Biotechnology, 2015. **6**(03): p. 205.
4. Hoornweg, D. and P. Bhada-Tata, *What a waste: a global review of solid waste management.* 2012.
5. Demirbas, M.F., M. Balat, and H. Balat, *Biowastes-to-biofuels.* Energy Conversion and Management, 2011. **52**(4): p. 1815-1828.
6. Deublein, D. and A. Steinhauser, *Biogas from waste and renewable resources: an introduction*. 2011: John Wiley & Sons.
7. Bergland, W., C. Dinamarca, and R. Bakke, *Efficient biogas production from the liquid fraction of dairy manure.* RE&POJ, 2014. **12**: p. 519-521.
8. Bergland, W., C. Dinamarca, and R. Bakke, *Effects of psychrophilic storage on manures as substrate for anaerobic digestion.* BioMed research international, 2014. **2014**.
9. De Mes, T., et al., *Methane production by anaerobic digestion of wastewater and solid wastes.* Bio-methane & Bio-hydrogen, 2003.
10. Youngsukkasem, S., K. Chandolias, and M.J. Taherzadeh, *Rapid bio-methanation of syngas in a reverse membrane bioreactor: Membrane encased microorganisms.* Bioresource technology, 2015. **178**: p. 334-340.
11. Bridgwater, A.V., *Renewable fuels and chemicals by thermal processing of biomass.* Chemical Engineering Journal, 2003. **91**(2): p. 87-102.
12. S.R. Guiot*, R.C., S. Sancho Navarro**, A. Prudhomme** and M. Filiatrault*, *Anaerobic digestion for bio-upgrading syngas into renewable natural gas (methane)*, in *PROCEEDINGS OF THE 13th WORLD CONGRESS ON ANAEROBIC DIGESTION*. 2013: SANTIAGO DE COMPOSTELA, SPAIN.
13. Guiot, S.R., R. Cimpoia, and G. Carayon, *Potential of wastewater-treating anaerobic granules for biomethanation of synthesis gas.* Environmental science & technology, 2011. **45**(5): p. 2006-2012.
14. Luo, G., et al., *Simultaneous hydrogen utilization and in situ biogas upgrading in an anaerobic reactor.* Biotechnology and bioengineering, 2012. **109**(4): p. 1088-1094.
15. Luo, G. and I. Angelidaki, *Integrated biogas upgrading and hydrogen utilization in an anaerobic reactor containing enriched hydrogenotrophic methanogenic culture.* Biotechnology and bioengineering, 2012. **109**(11): p. 2729-2736.
16. Future, C.E. *Advantages and Disadvantages of Biogas.* 2016; Available from: http://www.conserve-energy-future.com/advantages-and-disadvantages-of-biogas.php.
17. Agblevor, F.A., *Feedstocks for Gasification*. 2007, Virginia Polytechnic Institute and State University.

18. Wikipedia. *Energy content of biofuel*. 2016; Available from: https://en.wikipedia.org/wiki/Energy_content_of_biofuel.
19. Boucher, O., et al., *The indirect global warming potential and global temperature change potential due to methane oxidation.* Environmental Research Letters, 2009. **4**(4): p. 044007.
20. Luo, G. and I. Angelidaki, *Co-digestion of manure and whey for in situ biogas upgrading by the addition of H2: process performance and microbial insights.* Applied microbiology and biotechnology, 2013. **97**(3): p. 1373-1381.
21. Osorio, F. and J. Torres, *Biogas purification from anaerobic digestion in a wastewater treatment plant for biofuel production.* Renewable energy, 2009. **34**(10): p. 2164-2171.
22. Mohan, S. and B. Bindhu, *Effect of phase separation on anaerobic digestion of kitchen waste.* Journal of Environmental Engineering and Science, 2008. **7**(2): p. 91-103.
23. Yu, L., et al., *Mathematical modeling in anaerobic digestion (AD).* Journal of Bioremediation & Biodegradation, 2013. **2014**.
24. Aslanzadeh, S., *Pretreatment of cellulosic waste and high rate biogas production.* 2014.
25. Amaya, O.M., M.T.C. Barragán, and F.J.A. Tapia, *Microbial Biomass in Batch and Continuous System.* Biomass Now–Sustainable Growth and Use, 2013.
26. Al Seadi, T., et al., *Biogas Handbook.–University of Southern Denmark Esbjerg*. 2008, ISBN 978-87-992962-0-0.
27. Gerardi, M.H., *The microbiology of anaerobic digesters*. 2003: John Wiley & Sons.
28. Schnurer, A. and A. Jarvis, *Microbiological handbook for biogas plants.* Swedish Waste Management U, 2010. **2009**: p. 1-74.
29. Sreekrishnan, T., S. Kohli, and V. Rana, *Enhancement of biogas production from solid substrates using different techniques—a review.* Bioresource technology, 2004. **95**(1): p. 1-10.
30. Pisutpaisal, N. and U. Sirisukpoca, *Development of Rapid Chemical Oxygen Demand Analysis Using Ozone as Oxidizing Agent.* Energy Procedia, 2014. **50**: p. 711-718.
31. Wang, Q., et al., *Degradation of volatile fatty acids in highly efficient anaerobic digestion.* Biomass and Bioenergy, 1999. **16**(6): p. 407-416.
32. Lyseng, B.C., et al., *Biogas reactor modelling with ADM1.* 2013.
33. Parker, W.J., *Application of the ADM1 model to advanced anaerobic digestion.* Bioresource technology, 2005. **96**(16): p. 1832-1842.
34. Osburn, L. and J. Osburn, *Biomass resources for energy and industry.* Website www. ratical. org/renewables, 1993.
35. Zeng, J., et al., *Lignocellulosic biomass as a carbohydrate source for lipid production by Mortierella isabellina.* Bioresource technology, 2013. **128**: p. 385-391.
36. D'Alessio, L. and M. Paolucci, *Energetic aspects of the syngas production by solar energy: reforming of methane and carbon gasification.* Solar & wind technology, 1989. **6**(2): p. 101-104.
37. E4Tech, *Review of Technologies for Gasification of Biomass and Wastes, NNFCC 09-008 - See more at: http://www.nnfcc.co.uk/tools/review-of-technologies-for-*

gasification-of-biomass-and-wastes-nnfcc-09-008#sthash.2Hdnxm3m.dpuf. 2009.
38. Pfeifer, C., B. Puchner, and H. Hofbauer, *Comparison of dual fluidized bed steam gasification of biomass with and without selective transport of CO 2.* Chemical Engineering Science, 2009. **64**(23): p. 5073-5083.
39. Aho, A., et al., *Chemical energy storage*. 2013: Walter de Gruyter.
40. McKendry, P., *Energy production from biomass (part 3): gasification technologies.* Bioresource technology, 2002. **83**(1): p. 55-63.
41. Newsome, D.S., *The water-gas shift reaction.* Catalysis Reviews Science and Engineering, 1980. **21**(2): p. 275-318.
42. Phillips, J.R., E.C. Clausen, and J.L. Gaddy, *Synthesis gas as substrate for the biological production of fuels and chemicals.* Applied biochemistry and biotechnology, 1994. **45**(1): p. 145-157.
43. Puig-Arnavat, M., J.C. Bruno, and A. Coronas, *Review and analysis of biomass gasification models.* Renewable and Sustainable Energy Reviews, 2010. **14**(9): p. 2841-2851.
44. Munasinghe, P.C. and S.K. Khanal, *Biomass-derived syngas fermentation into biofuels: opportunities and challenges.* Bioresource technology, 2010. **101**(13): p. 5013-5022.
45. Worden, R., M. Bredwell, and A. Grethlein. *Engineering issues in synthesis-gas fermentations*. in *ACS Symposium Series*. 1997. ACS Publications.
46. Abubackar, H.N., M.C. Veiga, and C. Kennes, *Biological conversion of carbon monoxide: rich syngas or waste gases to bioethanol.* Biofuels, Bioproducts and Biorefining, 2011. **5**(1): p. 93-114.
47. Thauer, R.K., *Biochemistry of methanogenesis: a tribute to Marjory Stephenson: 1998 Marjory Stephenson Prize Lecture.* Microbiology, 1998. **144**(9): p. 2377-2406.
48. Daniell, J., M. Köpke, and S.D. Simpson, *Commercial biomass syngas fermentation.* Energies, 2012. **5**(12): p. 5372-5417.
49. Sipma, J., et al., *Carbon monoxide conversion by anaerobic bioreactor sludges.* FEMS microbiology ecology, 2003. **44**(2): p. 271-277.
50. Mörsdorf, G., et al., *Microbial growth on carbon monoxide.* Biodegradation, 1992. **3**(1): p. 61-82.
51. Chynoweth, D.P., *Environmental impact of biomethanogenesis.* Environmental monitoring and assessment, 1996. **42**(1-2): p. 3-18.
52. Daniels, L., et al., *Carbon monoxide oxidation by methanogenic bacteria.* Journal of Bacteriology, 1977. **132**(1): p. 118-126.
53. Wasserfallen, A., et al., *Phylogenetic analysis of 18 thermophilic Methanobacterium isolates supports the proposals to create a new genus, Methanothermobacter gen. nov., and to reclassify several isolates in three species, Methanothermobacter thermautotrophicus comb. nov., Methanothermobacter wolfeii comb. nov., and Methanothermobacter marburgensis sp. nov.* International Journal of Systematic and Evolutionary Microbiology, 2000. **50**(1): p. 43-53.
54. Mazumder, T., N. Nishio, and S. Nagai, *Carbon monoxide conversion to formate byMethanosarcina barkeri.* Biotechnology letters, 1985. **7**(6): p. 377-382.

55. Klasson, K., et al., *Methane production from synthesis gas using a mixed culture ofR. rubrum M. barkeri, and M. formicicum.* Applied Biochemistry and Biotechnology, 1990. **24**(1): p. 317-328.
56. Rother, M. and W.W. Metcalf, *Anaerobic growth of Methanosarcina acetivorans C2A on carbon monoxide: an unusual way of life for a methanogenic archaeon.* Proceedings of the National Academy of Sciences of the United States of America, 2004. **101**(48): p. 16929-16934.
57. Hammel, K.E., et al., *Evidence for a nickel-containing carbon monoxide dehydrogenase in Methanobrevibacter arboriphilicus.* Journal of bacteriology, 1984. **157**(3): p. 975-978.
58. Sokolova, T.G., et al., *Diversity and ecophysiological features of thermophilic carboxydotrophic anaerobes.* FEMS microbiology ecology, 2009. **68**(2): p. 131-141.
59. Oelgeschläger, E. and M. Rother, *Carbon monoxide-dependent energy metabolism in anaerobic bacteria and archaea.* Archives of microbiology, 2008. **190**(3): p. 257-269.
60. Bergland, W.H., et al., *High rate manure supernatant digestion.* water research, 2015. **76**: p. 1-9.
61. Bergland, W.H., *supervisor of this thesis.* 2016.
62. *mass and energy balance in microbial growth, Advanced course in Environmental Biotechnology* 2014, TU Delft.
63. Wenche Bergland*, D.B., Carlos Dinamarca, Rune Bakke, *Considering Culture Adaptations to High Ammonia Concentration in ADM1* in *the 52 nd International Conference of Scandinavian Simulation Society: SIMS*. 2011.
64. Wang, W., et al., *Performance and microbial community analysis of the anaerobic reactor with coke oven gas biomethanation and in situ biogas upgrading.* Bioresource technology, 2013. **146**: p. 234-239.

Annexes

Annex 1: Thesis task description

Telemark University College
Faculty of Technology

FMH606 Master's Thesis

Title: Methane from Syngas by Anaerobic Digestion

TUC supervisors: Wenche Bergland, Rune Bakke and Britt Moldestad

External partner:

Task description:
Evaluate and suggest anaerobic digestion (AD) process design, syngas composition and degradation pathways in an AD reactor.

- Experimental evaluation syngas component effects on the AD reactor performance with different quality of syngas to be used in AD reactor.
- Optimize the overall energy production by evaluate both the AD reactor performance and the syngas production process.
- Evaluate syngas microbial degradation pathways and kinetics, and implement the syngas degradation in the anaerobic digestion model no 1 (ADM1).

The study involves:

- Experiment
- Modelling
- Literature review

Task background:
A new process for transforming syngas to biogas is proposed. It utilizes newly developed farm scale reactors for treatment of manure and biogas production that reduces greenhouse gas emission and produces renewable energy. It is suggested to combine these farm scale reactors with processes for syngas production based on local wood. The produced syngas can be fed to the AD reactor for methane production. This may be an advantageous treatment of the syngas for further use as transport fuel.

Student category: EET and PT students.

Practical arrangements: The work will be carried out at TUC.

Signatures:

Student (date and signature): 5.2.16 Sanjay Shah

Supervisor (date and signature): 5.2.16 Wenche Bergland